Department für Diagnostische Labormedizin
des Universitätsklinikums Tübingen
Institut für Medizinische Virologie und
Epidemiologie der Viruskrankheiten

CD81 is a restriction factor of EBOV trVLP and is downregulated by EBOV GP and VP40

Thesis submitted as requirement to fulfill the degree ,,Doctor of Philosophy" in *Experimental Medicine* (PhD)

at the
Faculty of Medicine
Eberhard Karls Universität
Tübingen

presented by

Hu, Dan

2024

Dean:	Professor Dr. B. Pichler
1st reviewer:	Professor Dr. M. Schindler
2st reviewer:	Professorin Dr. J. Skokowa, Ph.D

Date of oral examination: 19.02.2024

Abbreviations

ADAM17	A disintegrin and metalloprotease 17
ALIX	ALG-2-interacting protein X
APS	Ammonium persulfate
BAG3	BCL2 associated athanogene 3
BDBV	Bundibugyo virus
BOMV	Bombali virus
BSL	Biosafety level
CAPG	Macrophage-capping protein
CHIKV	Chikungunya virus
CIEBOV/TAFV	Cote d'Ivoire ebolavirus/ Taï Forest virus
CRISPR	Clustered regularly interspaced short palindromic repeats
CXCL12	C-X-C motif chemokine 12
CXCR4	C-X-C chemokine receptor type 4
DMEM	Dulbecco’s modified eagle medium
DMSO	Dimethyl sulfoxide
DPP4	Dipeptidyl peptidase 4
DTT	Dithiothreitol
EBOV/ZEBOV	Ebola virus/ Zaire Ebola virus
ESCRT	Endosomal sorting complexes required for transport
EVD	Ebola virus disease
FACS	Fluorescence-activated cell sorting
FCS	Fetal calf serum
HBS	HEPES Buffered Saline
HBV	Hepatitis B virus
HCMV	Human cytomegalovirus
HCV	Hepatitis C virus
HEPES	4-(2-hydroxyethyl)-1-piperazineethanesulfonic acid
HHV	Human herpesvirus
HIV	Human immunodeficiency virus
HLA	Human leukocyte antigen
HPV	Human papillomavirus
HSV	Herpes simplex virus
HTLV-1	Human T-lymphotropic virus type 1
IBV	Infectious bronchitis virus
ICAM-3	Intercellular adhesion molecule 3
IQGAP1	IQ Motif Containing GTPase Activating Protein 1
IRES	Internal ribosome entry site

JAM-A	Junctional adhesion molecule A
KG	Kusabira-green
LAMP3	Lysosome-associated membrane glycoprotein 3
LASV	Lassa virus
LB	Luria-Bertani
LC3	Microtubule-associated protein 1A/1B light chain 3
MARCH8	Membrane-Associated RING-CH Protein 8
MARV	Marburg virus
MERS-CoV	Middle East Respiratory Syndrome Coronavirus
MMP9	Matrix metallopeptidase 9
MOI	Multiplicity of infection
NEAA	Non-essential amino acid
NPC1	Niemann-Pick disease, type C1
PBMC	Peripheral blood mononuclear cell
PBS	Phosphate buffered saline
PE	Phycoerythrin
PEI	Polyethylenimine
PI3K	Phosphoinositide 3-kinase
PMA	Phorbol 12-myristate 13-acetate
PtdSer	Phosphatidylserine
RAVV	Ravn virus
RBBP6	RB binding protein 6, ubiquitin ligase
RBD	Receptor binding domain
REBOV/ RESTV	Reston ebolavirus
RNP	Ribonucleoprotein
SAMHD1	SAM and HD Domain Containing Deoxynucleoside Triphosphate Triphosphohydrolase 1
SEBOV/SUDV	Sudan ebolavirus
SUMO	Small Ubiquitin-like Modifier
TACE	Tumor necrosis factor α-converting enzyme
TAE	Tris Acetate-EDTA
TAM	Tyro3/Dtk, Axl and Mer
TAPA-1	Target of the Antiproliferative Antibody 1
TBS	Tris buffered saline
TEMED	N,N,N’,N’-Tetramethylethylenediamine
Tim1	T-cell Ig and mucin domain 1
TIMP-1	Tissue inhibitor of metalloproteinases 1
TMD	Transmembrane domain

TMPRSS2	Transmembrane protease, serine 2
trVLP	Transcription and replication competent virus like particle
TSG101	Tumor susceptibility gene 101
TSP	Tetraspanin
VSV	Vesicular stomatitis virus
WB	Western blot
WWOX	WW-domain-containing oxidoreductase

Table of Contents

1. Introduction

Ebola virus (EBOV, also known as Zaire EBOV), a member of *Ebolavirus* genus in the *Filoviridae* family, is the causative agent of Ebola virus disease (EVD, formerly Ebola hemorrhagic fever) in humans and nonhuman primates (1, 2). EBOV was firstly discovered in 1976 in Democratic Republic of the Congo (formerly Zaire), caused 28610 cases and 11308 deaths in the largest outbreak in 2014-2016 in West Africa (3). Ebolavirus genus includes five more members, Sudan virus (SUDV), Bundibugyo virus (BDBV), Taï Forest virus (TAFV), Reston virus (RESTV) and Bombali virus (BOMV) (4). Within *Ebolavirus* genus, not only EBOV but also SUDV and BDBV cause lethal diseases to humans (4, 5). There was only one TAFV case in humans reported and shown to be pathogenic but non-lethal (4, 6). RESTV infection in humans was asymptomatic and the pathogenicity of BOMV infection in humans is unknown (4, 7–9). Within *Filoviridae* family, two members of Marburgvirus genus, Marburg virus (MARV) and Ravn virus (RAVV), are also known to cause lethal disease (Marburg virus disease, MVD) to humans (1, 2, 10).

EVD outbreak mainly occurred in Africa, while few cases were confirmed in US and Europe (5). EBOV transmission is mainly through direct contact with body fluids and also via the placenta (11–14). The symptoms of EVD include febrile illness (fever, fatigue and muscle pain), gastrointestinal symptoms (anorexia, vomiting, abdominal pain and diarrhea), bleeding and multiorgan dysfunction (reviewed in (11, 15), (16–19)). A wide range of cell types can be infected by EBOV, including macrophages, dendritic cells, hepatocytes, fibroblasts, endothelial cells, adrenal cortical cells and epithelial cells (reviewed in (20), (21–24)). Macrophages as well as dendritic cells are reported to be early and primary target cells (20–24) . Despite lymphocytes being refractory to productive EBOV infection, lymphopenia is associated with EBOV infection (25–28). So far, four viral vector based vaccines carrying EBOV glycoprotein (GP), Ervebo (rVSVΔG-ZEBOV-GP, US and Europe), Zabdeno/Mvabea (Ad26-ZEBOV/MVA-BN-Filo, Europe), Ad5-EBOV (China) and GamEvac-Combi and-Lyo (rVSV/Ad5-EBOV-GP, Russia), have been licensed for protection from EBOV infection (5, 29–35).

The efficacy of Ervebo in humans was 100% (95% confidence interval, 68.9-100%) (36) while the efficacy of other vaccines in humans is not available. Two monoclonal antibody-based drugs against EBOV glycoprotein, Inmazeb (REGN-EB3, cocktail of three monoclonal antibodies) and Ebanga (mAb114/ansuvimab, single monoclonal antibody), are approved for treatment of EBOV infection (5, 37, 38). In human, Inmazeb reduced the fatality rate from 51.3% to 33.5% and Ebanga reduced the fatality rate from 49.7% to 35.1%. (39).

1.1 EBOV Genome and Structure

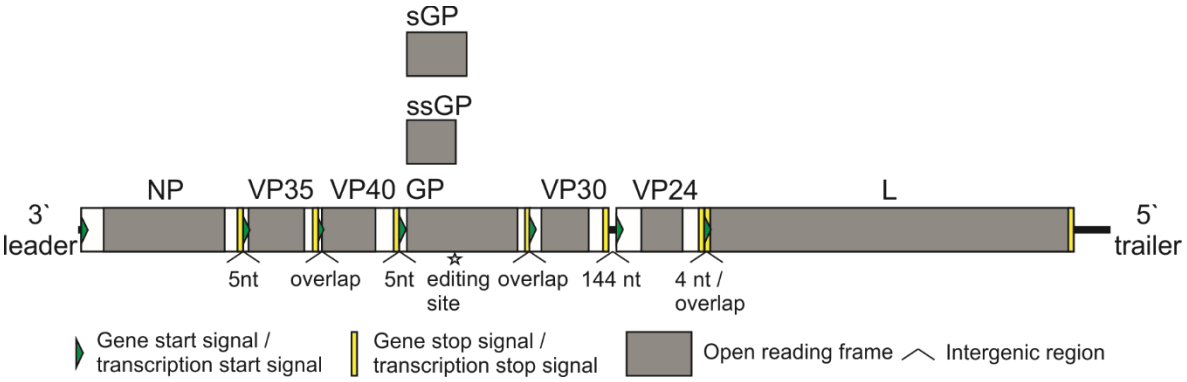

Fig.1 Schematic representation of the EBOV genome. (adapted from (40) and created with CorelDraw).

The EBOV genome is a 19 kb non-segmented negative strand RNA (4). The RNA genome contains nontranscribed 3´ leader and 5´ trailer region and seven genes NP, VP35, VP40, GP, VP30, VP24 and L, and the genes are separated by intergenic region or overlap (4, 40–42). The 3´ leader region (nt 1-55) contains the replication promoter element 1 and forms a stem-loop structure (43). The EBOV replication promoter is bipartie and the promoter element 2, consisted of eight UN5 hexamers, is located within the untranslated region of the NP gene (nt 81-128) (43). The 5´ trailer region (nt 18493-18959, 677 nt) contains the antigenomic replication promoter (terminal 177 nt) (42, 44, 45). The start and end of each gene are conserved transcription start (3′ CU$^{C}/_{A}$CUUCUAAUU) and stop (UAAUUC $(U)_{5/6}$) signal, respectively (46–48). Among the seven genes, GP gene encodes three viral proteins, GP, sGP (secreted GP) and ssGP (second secreted GP). GP is the full-length transmembrane glycoprotein and is produced through transcriptional editing by adding one non-template adenosine (49–51). sGP is

the main product without editing and ssGP is produced by adding two non-template adenosines or rarely deleting one adenosine through transcriptional editing (49–51).

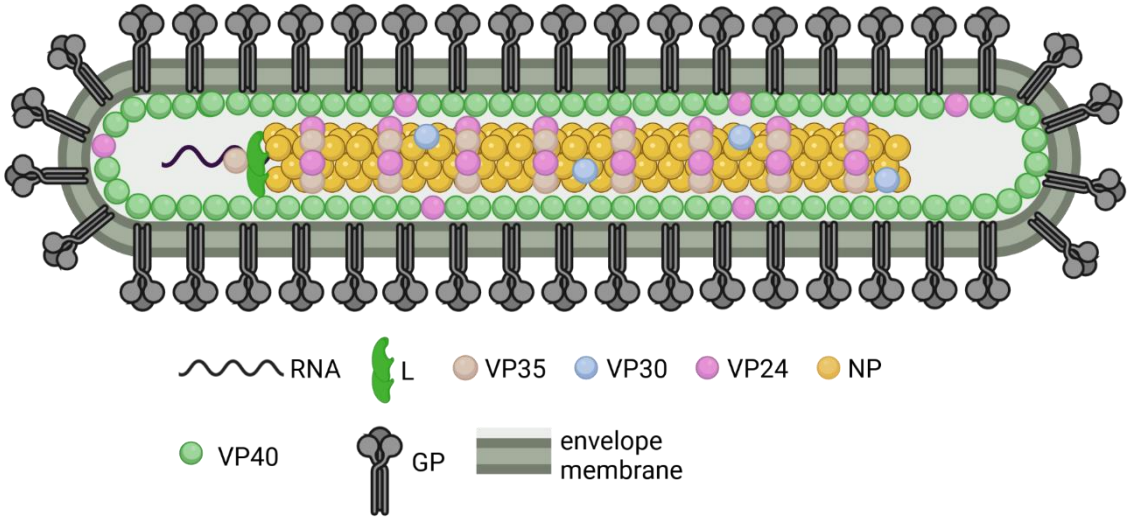

Fig. 2 Schematic representation of the EBOV viral particle structure. (adapted from (47), created with BioRender).

EBOV particles are filamentous with a diameter around 90 nm and mean length of 1028 nm and 1978 nm in two populations (52). The viral particle is enveloped and viral GP is incorporated into the envelope (53). The inner side of the envelope is where the viral matrix localized (47). VP40 is the primary matrix protein efficiently associated with the plasma membrane, and VP24 is recognized as the minor matrix protein slightly associated with the plasma membrane (54–57). The core of the EBOV particle is the nucleocapsid, composed of viral RNA genome, NP (nucleoprotein), L (RNA-dependent RNA polymerase), VP35 (polymerase cofactor), VP30 (transcription factor) and VP24 (47, 58–60). Several studies suggest that NP and the RNA genome form the inner nucleocapsid helix that is rigidified by outer VP24-VP35 bridges (52, 53, 61).

1.2 EBOV life cycle

1.2.1 Entry

EBOV can bind to numerous host receptors, including C-type lectins (DC-SIGN [dendritic cell-specific intercellular adhesion molecule 3-grabbing non-integrin], L-SIGN [liver/lymph node–specific ICAM-3 grabbing nonintegrin, DC-SIGNR],

hMGL [human macrophage galactose- and N-acetylgalactosamine-specific C-type lectin], LSECTin [Liver Sinusoidal Endothelial Cell Lectin] and MBL [mannose-binding lectin]) and phosphatidylserine (PtdSer) receptors (Tim [T-cell immunoglobulin and mucin domain]1,Tim4, Tyro3/Dtk, Axl and Mer [TAM]) (reviewed in (62), (63–71)). Additionally, glycosaminoglycans and ficolin-1 have been identified as EBOV attachment factors (72, 73). The attached viral particles are internalized mainly through macropinocytosis and alternatively via clathrin mediated endocytosis depending in a cell type specific manner (74–76). Macropinocytosis occurs constitutively in macrophages, dendritic cells and many cancer cells, and can be induced by growth factors in other cells (reviewed in (77), (78–81)). Macropinocytosis is initiated by actin polymerization and membrane ruffling to form the macropinosome, and PI3K signaling is involved in macropinosome formation (77, 81–84). EBOV and EBOV VLP can activate the PI3K/Akt signaling pathway and induce macropinocytosis (76, 85–87). Furthermore, the activation of PI3K/Akt by EBOV or EBOV VLP was shown to be dependent on the receptor tyrosine kinases (86, 87). Among them, HER2 (human epidermal growth factor receptor 2) can interact with EBOV attachment factors, the TAM proteins, while the TAM proteins are dispensable for the activation of Akt1 by EBOV (86).

The internalized EBOV particles are further delivered to the NPC1-positive late endosome-lysosome/endolysosome compartment through the endocytic pathway (75, 88–90). The delivery of EBOV particles to NPC1+ compartments requires PIKfyve kinase, HOPS (homotypic fusion and protein sorting) complex and UVRAG (UV radiation resistance-associated gene), which are involved in endosome maturation process (91, 92). In addition, TPCs (two-pore channels), regulating endosomal trafficking, was found to be involved in EBOV trafficking (93). In the endosomes and lysosomes, viral surface GP is cleaved by cysteine proteases cathepsin B/L and exposes the receptor binding domain (94–96). The cleaved GP subsequently interacts with its receptor NPC1, which promotes viral-host membrane fusion and nucleocapsid release into the cytoplasm (97–99). Additionally, cathepsins and cholesterol-GP interaction were demonstrated to be involved in the fusion (90, 100).

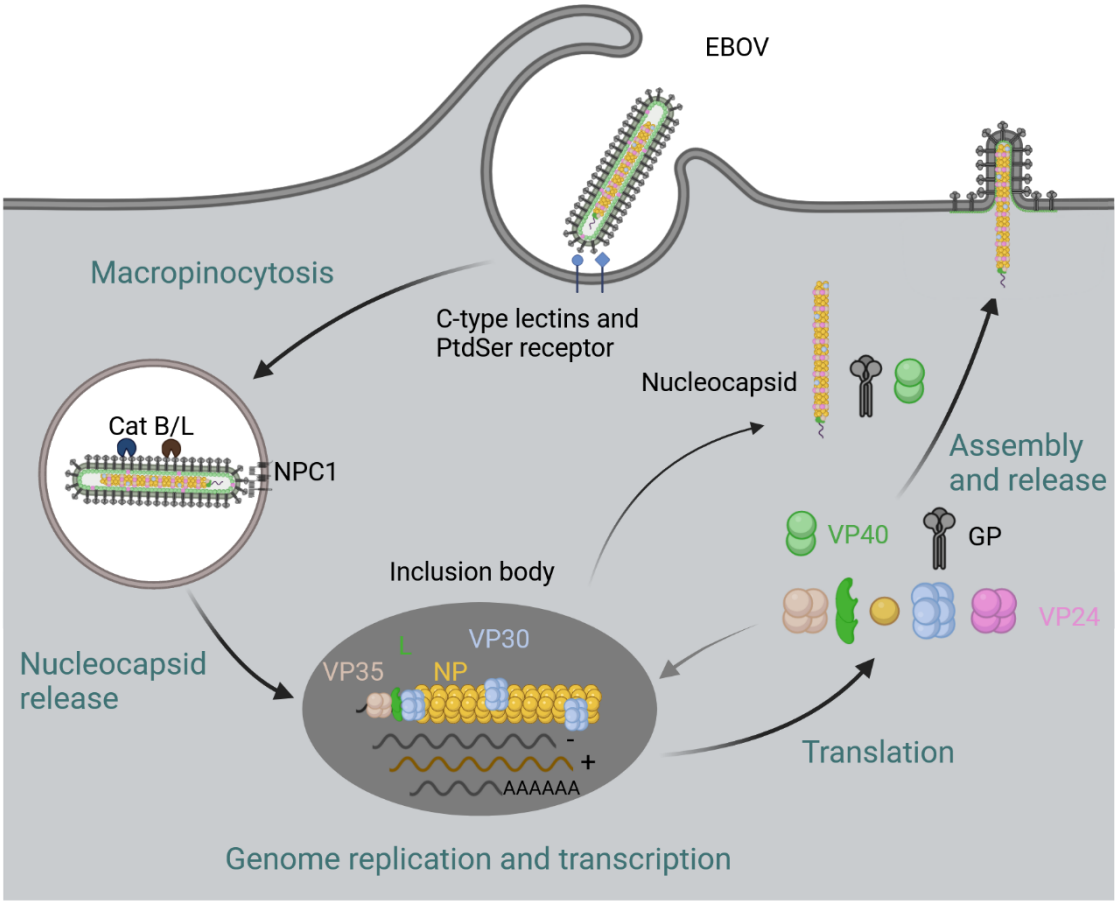

Fig. 3 Schematic representation of EBOV replication cycle. (Adapted from (101), and created with BioRender)

1.2.2 Replication and transcription

In the cytoplasm, the primary transcription is initiated with the nucleocapsid protein NP, L, VP35 and VP30, and dynamic phosphorylation of VP30 was shown to play an essential role in this process (47, 102–104). Newly synthesized NP, VP35, VP30 and L can form the punctate viral inclusion bodies (IBs) in cytoplasm, where viral genome replication and transcription occur (105, 106). NP, VP35 and L are sufficient to support EBOV minigenome replication (103). NP, VP35 and L are also involved in viral transcription, and additionally VP30 is required for transcription initiation and reinitiation (103, 107, 108). VP40 and VP24 also localize to the inclusion bodies and were shown to inhibit viral genome replication and transcription (45, 109–111). The inclusion bodies are liquid organelles and show dynamic features in size and localization during infection (105, 112). The sole expression of NP is sufficient to form the punctate IB distribution in the cytoplasm, and the oligomerization of NP plays an essential role in IB formation

(112, 113). EBOV transcription is thought to occur in a stop-start manner from 3´ to 5´ and generates monocistronic mRNAs for each gene, resulting in gradient amounts of mRNA synthesized from 3´to 5´ (46, 47, 114, 115). The viral mRNAs are 5’ capped and have a polyA tail at 3’ end (107, 114). Within the inclusion bodies, RNA polymerase L can interact with both VP35 and VP30, which are also interaction partners of NP (113, 116–119). In addition to NP, L, VP35 and VP30 form homo-oligomers as well, and homo-oligomerization of NP and VP30 were shown to play essential roles in viral replication and transcription (116, 118, 120–124).

The transition between EBOV genome replication and transcription is regulated by VP30 phosphorylation, which negatively regulates viral transcription and is in favor of genome replication (125, 126). Phosphorylation of VP30 inhibits its interaction with the genome RNA and VP35, and enhances its interaction with NP (126, 127). The RNA binding capacity of VP30 is strongly correlated with the viral transcription activation (127). VP30 is phosphorylated by the host kinase SRPK1 (Serine-Arginine Protein Kinase 1) and dephosphorylated by B56-PP2A phosphatase recruited by NP (128, 129). There are other host proteins involved in viral genome replication and transcription. TOP1 (DNA Topoisomerase 1), STAU 1 (Staufen1), SMYD3 (SET and MYND domain-containing protein 3), CAD (carbamoyl-phosphate synthetase 2, aspartate transcarbamylase, and dihydroorotase), AKIP1 (A kinase interacting protein 1) and CREB1 (cAMP-responsive element-binding protein 1) were found to localize to the IBs and facilitate viral genome replication and transcription (reviewed in(130), (131–135). Host proteins also negatively regulate EBOV replication. Host ubiquitin ligase RBBP6 and NP competitively interact with VP30, and overexpression of RBBP6 was shown to inhibit viral replication and transcription (136). NXF1 (nuclear RNA export factor 1) was identified in the IBs and suggested to be involved in export of the viral mRNA for translation (137, 138). Viral infections can induce translation arrest and stress granules formation (139). In EBOV infected cells, stress granule proteins (eIF4G, eIF3, and PABP) are sequestered within the IBs leading to inefficient stress granules induction (140). Moreover, interferon induction and response are also counteracted by EBOV VP35 and VP24 (141–147).

1.2.3 Assembly and release

The nucleocapsids are assembled in the IBs and transported to the cell periphery in an actin dependent manner (101, 148). There, the incorporation of nucleocapsid into filopodia, the budding sites at the plasma membrane, is facilitated by VP40 (149). Transport and assembly of VP40 involve several host proteins and lipids (reviewed in (150, 151)). The intracellular transport of VP40 to the plasma membrane depends on COPII (coat protein complex II) transport system, and VP40 was identified to interact with COPII coat protein Sec24C (152). The association of VP40 with the plasma membrane leads to VP40 oligomerization, which is dependent on the presence of PtdSer and PI(4,5)P2 (54, 151, 153–155). Besides, membrane binding of VP40 leads to PtdSer clustering and exposure on the outer leaflet of the plasma membrane (154, 156). PtdSer appears on the viral particle surface, which additionally involves Xkr8 (XK-related protein 8) recruited by GP for externalization of PtdSer (157). GP is glycosylated with oligomannosidic N-glycans in the ER (preGPer) and the glycans further mature in the Golgi apparatus (preGP) (158). The fully glycosylated GP is cleaved by furin into two disulfide-linked subunits, GP1 and GP2 (GP1,2) (158, 159). The GP heterodimers can oligomerize to trimers and incorporate into viral particles (160). VP40 alone is able to induce the filamentous virus like particles (VLPs) formation, which can be enhanced by GP and NP (56, 161, 162). Moreover, VP40 mediated budding and release of viral particles involve a set of host proteins, including actin regulatory proteins (IQGAP1, Angiomotin and CAPG), ubiquitin ligases (Nedd4, ITCH, WWP1 and SMURF2) and ESCRT (endosomal sorting complexes required for transport) associated proteins (TSG101, vps4 and ALIX) (reviewed in (163), (164–173)).

1.3 EBOV GP and VP40

1.3.1 GP

EBOV full-length GP is a type 1 transmembrane protein (676 aa, ZEBOV Mayinga-76) containing a signal peptide (1-32 aa) at the N terminus, which plays a role in GP glycosylation and is cleaved in mature GP (160, 174). The remaining region (33-676 aa) is consisted of the extracellular GP1 subunit (33-501 aa) and the transmembrane GP2 subunit (502-676 aa) (158). The GP1 subunit is required

for viral receptor binding and contains the receptor binding domain (RBD, 54-201 aa), the glycan cap (227-310 aa) and the mucin-like domain (313-501 aa) (175–177). The GP2 subunit, including the fusion peptide (FP, 524-539 aa) and the transmembrane domain (TMD, 650-672 aa), is indispensable for viral-host membrane fusion (41, 160, 178, 179). Additionally, the GP2 subunit contains a TACE (tumor necrosis factor α-converting enzyme) shedding site at D637, which results in the release of the GP ectodomain (33-637) from the cell surface (180). EBOV GP is also released in a membrane-bound manner with microvesicles (181, 182).

Apart from the role in viral entry, EBOV GP plays roles in EBOV pathogenicity and immune evasion. Expression of GP leads to cell rounding and detachment, which involves the downregulation of cell surface adhesion molecule integrins (183–185). The downregulation of αV integrin by GP engages dynamin-dependent trafficking and Erk signaling, while the downregulation of β1 integrin is due to steric shielding by GP glycans (185–187). Similarly, MHC class I on the cell surface is masked by GP glycans and CD8 T cell recognition is impeded (187). The ligands of NK cell activation receptor NKG2D and NKp30 are also shielded by the GP ectodomain (SUDV), resulting in impaired NK cell function (188). In addition, EBOV GP is an antagonist of tetherin, an interferon induced antiviral protein known to restrict viruses release (189). EBOV GP can interact with tetherin through the GP2 subunit and interfere with the interaction between tetherin and VP40 (190, 191). Additionally, intact RBD is required for EBOV GP to antagonize tetherin (192). Gustin et al. demonstrated GP mucin domain masks tetherin on the cell surface while is dispensable for tetherin antagonization (191). Other studies indicate GP has no effect on tetherin surface expression or slightly downregulates it (190, 193). This discrepancy could result from the different epitopes recognized by the tetherin antibodies. Moreover, GP and VP40, together with tetherin, can activate NF-κB signaling (194). GP containing microvesicles and shed GP are also known to modulate immune responses (182, 195).

The functional involvement of various GP amino acids has been studied with GP mutants. Mutations in the RBD of GP, F88A, L111A as well as L122A but not

W104A, fail to mediate efficient viral entry and tetherin antagonization (196, 197, 192). Mutations in GP FP, 531A, 532A, 533A, 535A, 536A and 537A but not 528A, show reduced infectivity (179, 196). Mutations in TMD of GP, 670A672A, are deficient in palmitoylation and localizing to lipid rafts while having no effect on infectivity (159, 196, 198, 199).

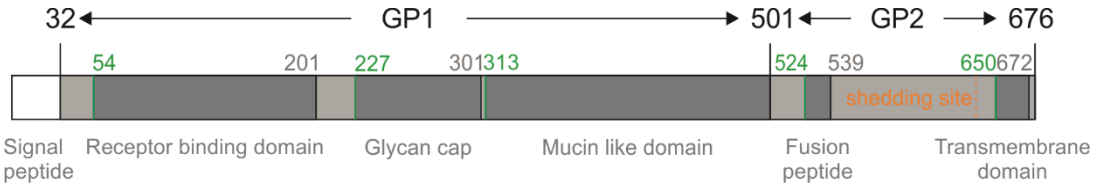

Fig. 4 Schematic representation of EBOV GP domains.

1.3.2 VP40

The EBOV matrix protein VP40 is a membrane and RNA binding protein (326 aa, Mayinga-76) and can oligomerize to dimers, hexamers and octamers (54, 200, 201). VP40 forms dimers in solution and is oligomerized to hexamers when associated with the membrane, which is a key step in virus assembly (153, 200). VP40 octamers, with binding RNA capacity, are essential in the EBOV viral life cycle but not VLP formation (201, 202). Structure studies indicate that VP40 contains two domains, the N terminal domain (44-194 aa) and the C terminal domain (201-321 aa), connected by a flexible loop (195-200 aa) (200, 203). The N terminal disordered region (1-43 aa) contains the late domain (L domain) comprised of PTAP/PSAP (7-10 aa), PPXY (10-13 aa) and YPX(n)L/I (18-26 aa) motifs, which is engaged in recruiting TSG101, ALIX and WW domain containing ubiquitin ligases (Nedd4, ITCH, WWP1 and SMURF2) for budding (163, 165–169, 171, 203). Ubiquitin ligases (Nedd4, ITCH and WWP1) were shown to ubiquitinate VP40 while they have no effect on VP40 stability (166, 167, 204). L domain also recruits WW domain containing proteins (BAG3 and WWOX) negatively regulating virus budding (163, 205–208). Residues essential for dimerization (112T and 117L) and RNA binding (125F and 134R) locate within the N terminal domain (163, 200, 202). Residues required for dimers oligomerization (95W, 160E, 241M and 307I) are distributed in both N- and C-terminal domains (163, 200, 209). Multiple residues identified in the C terminal domain are essential for VP40 plasma membrane localization (163). Bornholdt et

al. and Vecchio et al. demonstrate a basic patch of VP40 (essentially 224KK225 and 274KK275) is important for membrane interaction (163, 200, 210). Residues (303L, 306V and 307I) interacting with Sec24C for VP40 intracellular transport are expectedly required for plasma membrane localization (152). Additionally, mutation or deletion of residues (212KLR214, 309QDCDTCHSP317, 283P and 286P) mainly forming high-molecular-weight oligomers is correlated with impaired membrane localization or association (163, 211, 212). P53 and several hydrophobic residues, I293, L295 and V298, are also important for VP40 localization to the plasma membrane (163, 213, 214). At the C terminal disordered region (322-326 aa), SUMOylation was identified at residue 326 and shown to improve VP40 stability (203, 215). Apart from incorporation into VLPs, VP40 is released into exosomes, which induce apoptosis in the recipient immune cells (216, 217). VP40 was also shown to regulate extracellular vesicle formation and cell cycle (217).

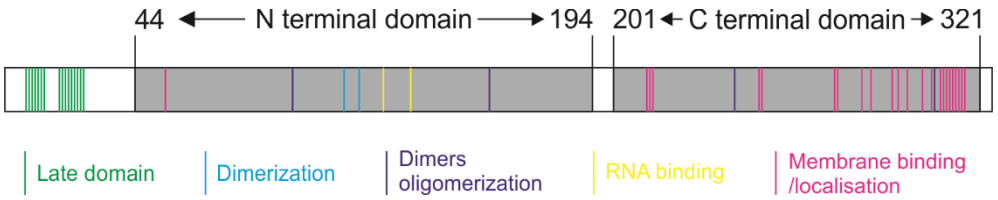

Fig. 5 Schematic representation of **EBOV VP40 domains.**

1.4 Tetraspanins CD81, CD63 and CD9

CD81, CD63 and CD9 belong to the tetraspanin (TSP) superfamily with 33 members in humans, which are four-transmembrane proteins with a small and a large extracellular loop (218, 219). The crystal structures of CD81 and CD9 have been revealed and shown to be similar (220, 221). Tetraspanins were also identified in other organisms, such as zebrafish (*Danio rerio, dr*), fruit fly (*Drosophila melanogaster, dm*), nematode (*C. elegans, ce*) and clawed frogs (*Xenopus tropicalis, xt*) (219). CD81, CD63 and CD9 are ubiquitously expressed in a wide range of cell types and known to form tetraspanin enriched microdomain (TEM) with various host proteins (218, 222). CD81, CD63 and CD9 were found to associate with each other in melanoma cell lines (223). The tetraspanins are

involved in multiple cellular processes and have common and distinct roles in these processes.

1.4.1 CD81

CD81 (TAPA-1) was initially identified as the target of an antiproliferative antibody (5A6) and further observed to engage in cell fusion, adhesion, motility/migration and T cell as well as B cell activation (224–237). Involved in these processes, CD81 has numerous interaction partners associated with various signaling pathways. CD81 was shown to associate with transmembrane integrins (αvβ1/VLA-5, αvβ5, α4β1/VLA-4, α6Aβ1 and α3β1), FGFR (fibroblast growth factor receptor) and JAM-A (junctional adhesion molecule A) regulating cell proliferation, motility, adhesion and integrin dependent particle binding (229, 238–245). Apart from integrins, CD81 interacts with small GTPase Rac and modulates its activation to regulate cell motility/migration (232).

Ig superfamily proteins EWI-2 and EWI-F/FPRP were identified to be the major partners of CD81 and CD9. (246, 247). Accordingly, CD81 was shown to regulate EWI-2 maturation and surface expression (248). EWI-2 and -F were found in complexes containing CD81 and other CD81 associated proteins. EWI-2 is linked to integrin α3β1 by CD81 and CD9 and can modulate cell migration (248). EWI-2 also associates with integrin α4β1 and promotes CD81-α4β1 complex formation (249). Moreover, EWI-2/F and CD81 interact with actin binding ezrin-radixin-moesin (ERM) proteins, and EWI-2 was shown to regulate ERM phosphorylation and cell motility (250). EWI-2 also plays a role in TGF-β signaling through modulating TGF-β receptor complex formation in a CD81 and CD9 dependent manner (251).

Required for proper T cell activation, CD81 is associated with T cell coreceptor CD3, CD4 and CD8, and was shown to control the immune synapse maturation (236, 252). In B cells, CD81 was found to associate with B cell receptor CD19 and is required for CD19 surface expression regulating B cell activation (237, 253–255). Likewise, CD81 was shown to increase αvβ5 surface expression (241). In addition to improving protein surface expression, CD81 promotes associated protein (TfR2) degradation (256). Moreover, CD81 can induce protein

(MT1-MMP) expression on a transcriptional level through the Akt signaling pathway (233). Last, CD81 is present in extracellular microvesicles and exosomes (257, 182, 258). Alix and ESCRT-III are involved in recruiting CD81, as well as CD63 and CD9, to exosomes, and a set of CD81 interaction partners are sorted into exosomes by CD81 (259, 260).

CD81 is involved in the life cycle of several viruses. CD81 is well-known as a coreceptor of HCV for entry (261, 262). HCMV entry into host cells also involves CD81 and two other tetraspanins, CD9 and CD151 (263). Additionally, CD81 is required for influenza virus entry and budding (264) and engaged in different steps of the HIV-1 life cycle. CD81 and CD9 were shown to restrict HIV-1 entry and Env mediated syncytia formation, and CD81 additionally was shown to inhibit HIV-1 transmission through cell to cell fusion (265, 266). On the other hand, CD81 supports HIV-1 reverse transcription (267). Last, HIV-1 is assembled at the tetraspanin enriched domains containing CD81, CD63, CD9, CD82 and CD53, and the infectivity of HIV-1 is negatively regulated by CD81 (268–271). In addition, CD81 is required for HSV-1 and CHIKV genome replication (272, 273).

1.4.2 CD63

CD63, also known as platelet activation marker (Pltgp40) and stage specific melanoma-associated antigen (ME491), is involved in cell fusion, proliferation, adhesion and migration (274, 227, 275, 276). CD63 is a receptor of tissue inhibitor of metalloproteinases 1 (TIMP-1), which can activate the PI3K/Akt/CycD1 signaling pathway to promote cell proliferation in a CD63 dependent manner (275, 277). CD63 is also required for TIMP-1 induced cell adhesion and migration through the β1 integrin signaling (276). Besides, CD63 is involved in VEGFR2 (vascular endothelial growth factor receptor 2) signaling by forming complex with β1 integrin and VEGFR2 (278). CD63 was described as a host factor for several viruses. HPV and Lujo virus involve CD63 in viral entry into host cells (279, 280). CD63 also supports HSV-2 infection (281). CD63 plays a positive role in early and late step of HIV-1 infection, and is involved in viral synapse formation for cell to cell spread (282–284). Moreover, CD63 is engaged in HBV assembly to produce infectious HBV particles (285).

1.4.3 CD9

CD9 (motility-related protein, MRP-1), known to be a key player in egg-sperm fusion, is also a regulator of cell adhesion, migration, proliferation and T cell activation (231, 242, 286–292). CD9 negatively regulates integrin α5β1 mediated cell adhesion by enhancing α5β1-ADAM17 (TACE) interaction (288). Besides, CD9 interacts with ADAM17 and inhibits shedding activity of ADAM17, which attributes to a negative role of CD9 in keratinocyte migration (289). CD9 also regulates E-cadherin/PI3K/Akt signaling and metalloproteinase MMP9 expression via JNK signaling to modulate keratinocyte motility/migration (290, 291). By modulating ADAM17 shedding activity and Erk signaling, CD9 plays a role in HPV16 entry (293). Moreover, CD9 is essential for MERS-CoV entry by scaffolding host receptor DPP4 and protease TMPRSS2 (294). CD9 was also found to support HHV-6A/6B CD46 dependent infection at early stage (295).

1.5 Aims

EBOV is highly pathogenic to humans. To date, highly efficacious vaccine against EBOV has been developed and approved, while treatment licensed for EBOV infection only reduced the case fatality rate to around 30% (36, 39). Numerous host proteins have been identified to be involved in the EBOV life cycle, which are potential targets for antiviral treatment development. Host plasma membrane is the attachment and release site of EBOV and contains various signaling molecules potentially involved in the EBOV life cycle (296). EBOV GP, the only membrane protein, is responsible for viral entry and also known to regulate membrane receptors involved in immune evasion. Our group decided to comprehensively study how EBOV GP modulates host cell plasma membrane receptors and to characterize the role of the modulated receptors in the EBOV life cycle. Julia Nehls, a former PhD student in the lab, analyzed the effect of EBOV GP on 332 plasma membrane receptors expression via a flow-cytometry based screen.

The first goal of this project was to validate the identified modulations from the screen. The modulation of 21 receptors of interest was analyzed in EBOV GP expressing cells, and three receptors CD81, CD63 and CD9 from the same

protein family, tetraspanin superfamily, downregulated by EBOV GP were selected for further investigations. The capability of GP from other filoviruses, EBOV GP subunits and mutants to modulate the TSPs was evaluated as well to determine whether the modulation is conserved among the filoviruses and the GP domains involved in the modulation. The second goal was to study whether the TSPs play a role in EBOV life cycle. EBOV entry, replication and release were investigated in the tetraspanin KO cells with EBOV transcription and replication competent VLP (trVLP) assay. CD81, shown to be involved in EBOV trVLP infection and replication, was further characterized in which stage it plays a role. The third goal was to study CD81 downregulation mechanism by EBOV. Whether other EBOV proteins modulate CD81 expression was determined and the effect of proteasomal and lysosomal protein degradation inhibitor on CD81 downregulation was analyzed. Furthermore, whether CD81 interacts with the EBOV proteins involved in the downregulation was investigated. Last, the effect of a CD81 antibody on trVLP infection was determined to characterize the potential of CD81 to serve as a druggable target for the treatment of EBOV infection.

2. Materials and methods

2.1 Materials

2.1.1 Cells

Table 1 Mammalian cell lines

Name	Description	Source
293T	Human embryonic kidney 293 cells containing SV40 T antigen	AG Schindler
293T control	293T cells stably expressing Cas9	AG Schindler
293T CD81 KO	293T cells stably expressing Cas9 and gRNA targeting CD81 (5'-CATCGGCATTGCTGCCATCG-3')	This project
293T CD81 KO (sorted)	Sorted 293T CD81 KO cells via FACS	This project
293T CD63 KO	293T cells stably expressing Cas9 and gRNA targeting CD63 (5'-GAGGTGGCCGCAGCCATTGC-3')	AG Schindler
293T CD9 KO	293T cells stably expressing Cas9 and gRNA targeting CD9 (5'-GCCCTCACCATGCCGGTCAA-3')	AG Schindler
Huh7.5	Human hepatoma cell line	AG Schindler
Huh7.5 control	Huh7.5 cells stably expressing Cas9	AG Schindler
Huh7.5 CD81 KO	Huh7.5 cells stably expressing Cas9 and gRNA targeting CD81 (5'-CATCGGCATTGCTGCCATCG-3')	AG Schindler
Huh7.5 CD63 KO	Huh7.5 cells stably expressing Cas9 and gRNA targeting CD63 (5'-GAGGTGGCCGCAGCCATTGC-3')	AG Schindler
Huh7.5 CD9 KO	Huh7.5 cells stably expressing Cas9 and gRNA targeting CD9 (5'-GCCCTCACCATGCCGGTCAA-3')	AG Schindler
Hela	Human cervical adenocarcinoma cell line	AG Schindler
Hela control	Hela cells stably expressing Cas9	This project
Hela CD81 KO	Hela cells stably expressing Cas9 and gRNA targeting CD81 (5'-CATCGGCATTGCTGCCATCG-3')	This project
Hela CD63 KO	Hela cells stably expressing Cas9 and gRNA targeting CD63 (5'-GAGGTGGCCGCAGCCATTGC-3')	This project
Hela CD9 KO	Hela cells stably expressing Cas9 and gRNA targeting CD9 (5'-GCCCTCACCATGCCGGTCAA-3')	This project

2.1.2 Plasmids and primers

Table 2 pCG-IRES-GFP plasmids. The plasmids express GFP only or co-express GFP and viral protein via the internal ribosome entry site (IRES).

Name	Protein	Source
pCG-NL43nef 3*-IRES-eGFP	GFP only	(297)
pCG-GPwt-IRES-GFP	EBOV GP and GFP	(182)
pCG-IRES-EGFP SEBOV-GP	SUDV GP and GFP	S. Pöhlmann
pCG-IRES-EGFP REBOV-GP	RESTV GP and GFP	S. Pöhlmann
pCG-IRES-EGFP CIEBOV-GP	TAFV GP and GFP	S. Pöhlmann
pCG-IRES-EGFP MARV-GP	MARV GP and GFP	S. Pöhlmann
pCG-IRES-EGFP Lassa-GP	LASV GP and GFP	S. Pöhlmann
pCG-IRES-EGFP NL4-3 Env	HIV-1 Env and GFP	S. Pöhlmann
pCG-ZEBOV_GP1 -IRES-GFP	EBOV GP1 and GFP	AG Schindler
pCG-ZEBOV_GP2 -IRES-GFP	EBOV GP2 and GFP	AG Schindler
pCG-IRES-EGFP SEBOV-GP1	SUDV GP1 and GFP	S. Pöhlmann
pCG-IRES-EGFP SEBOV-GP2	SUDV GP2 and GFP	S. Pöhlmann
pCG-GP F88A-IRES-GFP	EBOV GP F88A and GFP	(182)
pCG-GP W104A-IRES-GFP	EBOV GP W104A and GFP	(182)
pCG-GP L111A-IRES-GFP	EBOV GP L111A and GFP	(182)
pCG-GP L122A-IRES-GFP	EBOV GP L122A and GFP	(182)
pCG ZEBOV GP 526I 528A-IRES-EGFP	EBOV GP 526I 528A and GFP	S. Pöhlmann
pCG ZEBOV GP 531A 532A 533A-IRES-EGFP	EBOV GP 531A 532A 533A and GFP	S. Pöhlmann
pCG ZEBOV GP 535A 536A 537A-IRES-EGFP	EBOV GP 535A 536A 537A and GFP	S. Pöhlmann
pCG ZEBOV GP 655A 656A-IRES-EGFP	EBOV GP 655A 656A and GFP	S. Pöhlmann
pCG ZEBOV GP 666A 667I 668A-IRES-EGFP	EBOV GP 666A 667I 668A and GFP	S. Pöhlmann
pCG ZEBOV GP 670A 672I-IRES-EGFP	EBOV GP 670A 672I and GFP	S. Pöhlmann
pCG-GP LxxxL-IRES-GFP	EBOV GP LxxxL and GFP	(182)
pCG-IRES-GFP ZLZ GP	EBOV GP replaced with LASV TMD and GFP	(182)
pCG-IRES-GFP GP losh mut	EBOV GP low shedding mutant	AG Schindler
pCG-IRES-GFP GP hish mut	EBOV GP high shedding mutant	AG Schindler
pCG-IRES-GFP GPwt 2014	EBOV GP circulated in 2014 and GFP	AG Schindler

pCG-IRES-GFP GP V82A 2014	EBOV GP V82A circulated in 2014 and GFP	AG Schindler
pCG-L-IRES-GFP	EBOV L and GFP	This project
pCG-NP-IRES-GFP	EBOV NP and GFP	This project
pCG-VP35-IRES-GFP	EBOV VP35 and GFP	This project
pCG-VP30-IRES-GFP	EBOV VP30 and GFP	This project
pCG-VP40-IRES-GFP	EBOV VP40 and GFP	This project
pCG-VP24-IRES-GFP	EBOV VP24 and GFP	This project

Table 3 Plasmids for EBOV trVLP assay

Name	Feature	Source
pCAGGS-NP-v1.1	EBOV NP	T. Hoenen
pCAGGS-VP35-v1.1	EBOV VP35	T. Hoenen
pCAGGS-VP30-v1.1	EBOV VP30	T. Hoenen
pCAGGS-L-v1.1	EBOV L	T. Hoenen
pCAGGS-T7opt	T7 RNA polymerase	T. Hoenen
pT7.1-4cis-vRNA-EBOV GP-nLuc	EBOV 4-cistonic minigenome	T. Hoenen
pT7.1-4cis-vRNA-dGP-nluc	EBOV GP deficient ‘tricistronic’ minigenome	T. Hoenen
pPol II-4cis-vRNA-EBOV GP-GFP	EBOV 4-cistonic minigenome	T. Hoenen
pPol II-4cis-vRNA-dGP-GFP	EBOV GP deficient ‘tricistronic’ minigenome	This project
pCAGGS-Tim1-v1.2	Tim1	T. Hoenen
pCAGGS-MCS	-	S. Pöhlmann
pCAGGS ZEBOV GP wt	EBOV GP	S. Pöhlmann
pVSV-G	VSV G	(297)
pWPI	GFP	(298)
pWPI_BLR	-	(299)
pWPI-hCD81-HAHA-BLR	CD81-HA	(299)
pCAGGS-luc2	Firefly luciferase	T. Hoenen
mCherry-C1	mCherry	J. Schmid
pmtagBFP-C1	BFP	AG Schindler

Table 4 Plasmids for lentivirus pseudotypes production

Name	Feature	Source
pMD2G	VSV G	Addgene #12259
psPAX2	Lentiviral packaging plasmid	Addgene #12260
lentiCRISPRv2	Lentiviral CRISPR/Cas9 expression plasmid	Addgene #52961

lentiCRISPRv2-CD81.2	Lentiviral CRISPR/Cas9 expression plasmid targeting CD81 (5'- CATCGGCATTGCTGCCATCG-3')	AG Schindler
lentiCRISPRv2-CD63_oligo3	Lentiviral CRISPR/Cas9 expression plasmid targeting CD63 (5'- GAGGTGGCCGCAGCCATTGC-3')	AG Schindler
lentiCRISPRv2-CD9_oligo1	Lentiviral CRISPR/Cas9 expression plasmid targeting CD9 (5'- GCCCTCACCATGCCGGTCAA-3')	AG Schinlder
pSIV-vpr-vpx+	Packaging plasmid to produce Vpx-VLP	T. Gramberg
pWPXLd	Lentiviral plasmid expressing GFP	Addgene # 12258

Table 5 Plasmids for Kusabira-green (KG) based BiFC assay.

Name	**Protein (*N*=KGN, *C*=KGC)**	**Source**
phmKGN-MC	***N***	MBL life science
phmKGN-MN	***N***	MBL life science
phmKGC-MN	***C***	MBL life science
pKGN_MC_NP	***N***-EBOV NP	This project
pKGN_MN_NP	EBOV NP-***N***	This project
pKGC_MN_NP	EBOV NP-***C***	This project
pKGN_MC_VP35	***N***-EBOV VP35	This project
pKGN_MN_VP35	EBOV VP35-***N***	This project
pKGC_MN_VP35	EBOV VP35-***C***	This project
pKGN_MN_GP	EBOV GP-***N***	This project
pKGC_MN_GP	EBOV GP-***C***	This project
pKGN_MC_VP40	***N***-EBOV VP40	This project
pKGN_MN_VP40	EBOV VP40-***N***	This project
pKGC_MN_VP40	EBOV VP40-***C***	This project
pKGN_MC_CD81	***N***-CD81	This project
pKGN_MN_CD81	CD81-***N***	This project
pKGC_MN_CD81	CD81-***C***	This project

Table 6 Primers for cloning PCR.

Name	**Sequence (5'-3')**
XbaI-EBOV L fw	gta *TCTAGA* ATGGCTACACAACATACC
EBOV L (*XbaI**) rv	CCATGTTGA *cCTtGA* GTTTCCT
EBOV L (*XbaI**) fw	AGGAAAC *TCaAGg* TCAACATGG
MluI-EBOV L rv	cct *ACGCGT* CTAATCAAACCTGTAGAG

XbaI-EBOV NP fw	gta *TCTAGA* ATGGATTCTCGTCCTCAG
EBOV NP (*XbaI**) rv	GTCCTCG *TCaAGg* TCGAATAGG
EBOV NP (*XbaI**) fw	CCTATTCGA *cCTtGA* CGAGGAC
MluI-EBOV NP rv	cct *ACGCGT* CTACTGATGATGTTGCAG
XbaI-EBOV VP35 fw	gta *TCTAGA* ATGACAACTAGAACAAAG
MluI-EBOV VP35 rv	cct *ACGCGT* CTAAATTTTGAGTCCAAG
XbaI-EBOV VP30 fw	gta *TCTAGA* ATGGAAGCTTCATATGAG
MluI-EBOV VP30 rv	cct *ACGCGT* CTAAGGGGTACCCTCATC
XbaI-EBOV VP40 fw	gta *TCTAGA* ATGAGGCGGGTTATATTG
MluI-EBOV VP40 rv	cct *ACGCGT* TTACTTCTCAATCACAGC
XbaI-EBOV VP24 fw	gta *TCTAGA* ATGGCTAAAGCTACGGGA
MluI-EBOV VP24 rv	cct *ACGCGT* TTAGATAGCAAGAGAGCT
BamHI-EBOV NP fw	gta *GGATCC* ATGGATTCTCGTCCTCAGAAAATC
NotI-stop-EBOV NP rv	cct *GCGGCCGC* CTACTGATGATGTTGCAGGAT
NotI-EBOV NP rv	cct *GCGGCCGC* CTGATGATGTTGCAGGATTGC
BamHI-EBOV VP35 fw	gta *GGATCC* ATGACAACTAGAACAAAGGGC
NotI-stop-EBOV VP35 rv	cct *GCGGCCGC* CTAAATTTTGAGTCCAAGTGT
NotI-EBOV VP35 rv	cct *GCGGCCGC* AATTTTGAGTCCAAGTGTTTT
BamHI-EBOV GP fw	gta *GGATCC* ATGGGCGTTACAGGAATATTG
NotI-EBOV GP rv	cct *GCGGCCGC* AAAGACAAATTTGCATATACA
BamHI-EBOV VP40 fw	gta *GGATCC* ATGAGGCGGGTTATATTGCCT
NotI-stop-EBOV VP40 rv	cct *GCGGCCGC* TTACTTCTCAATCACAGCTGG
NotI-EBOV VP40 rv	cct *GCGGCCGC* CTTCTCAATCACAGCTGGAAG
BamHI-CD81 fw	gta *GGATCC* ATGGGAGTGGAGGGCTGC
NotI-stop-CD81 rv	cct *GCGGCCGC* TTATCAGTACACGGAGCT
NotI-CD81 rv	cct *GCGGCCGC* GTACACGGAGCTGTTCCG

Table 7 Primers for sequencing

Name	**Sequence (5'-3')**	**Reference**
pCG fw	CCATAGAAGACACCGGGACC	This project
IRES rv	CTCACATTGCCAAAAGACG	AG Schindler
EBOV L 704-721 fw	ACGTCTTGATAATGTGCA	This project
EBOV L 1700-1717 fw	CTTATCCGACTCGCAATG	This project
EBOV L 2657-2723 fw	GACAGTTAACACTCGGC	This project
EBOV L 3514-3532 fw	CATATTGTTAGTGCATGGC	This project
EBOV L 4430-4447 fw	GCAATACAATTCTTCGGA	This project
EBOV L 5327-5344 fw	CGTCATCCAATGAGTCAC	This project
EBOV GP 585-604 fw	CTCACACCCCTTGAGAGAGC	AG Schindler

KGN-MC fw	GAGGAGAAGATCACCGCC	This project
MC rv	GCTGCAATAAACAAGTTAACAACAAC	This project
MN fw	CGCCCCATTGACGCAAAT	MBL life science
KGN-MN rv	CTCATGCCCATTGACGGAG	This project
KGC-MN rv	CCAGGATCTCCTTGGCGG	This project

Table 8 Primers for RT-qPCR

Name	**Sequence (3'-5')**	**Reference**
vRNA primer	ATTGAAGATTCAACAACCCTAAAG	Transcription of vRNA (133)
cRNA primer	AATATGAGCCCAGACCTTTCG	Transcription of cRNA (133)
Oligo(dT)12-18	-	Thermo Fisher
hGAPDH fw	TGCACCACCAACTGCTTAGC	(300)
hGAPDH rv	GGCATGGACTGTGGTCATGAG	(300)
Fluc fw	CAGTCGTCGTGCTGGAACAC	(137)
Fluc rv	GTCCAACTTGCCGGTCAGTC	(137)
EBOV VP40 fw	TCCCGGATCATCCCCTCAGGC	(301)
EBOV VP40 rv	GCAGCAGGCAGTGGTTGGGT	(301)

Primers used in this project were synthesized by Metabion.

2.1.3 Antibodies and kits

Table 9 Antibodies. FC= Flow Cytometry, WB= Western Blot

Name	Usage	Dilution	Source
PE anti-human CD357 Antibody	FC	1/50	Biolegend, Cat. # 371203
PE anti-human CD79b Antibody	FC	1/50	Biolegend, Cat. # 341404
PE anti-human HLA-A, B, C Antibody	FC	1/50	Biolegend, Cat. # 311406
PE anti-human CD59 Antibody	FC	1/50	Biolegend, Cat. # 304707
PE anti-human CD257 Antibody	FC	1/50	Biolegend, Cat. # 366505
PE anti-human CD9 Antibody	FC	1/50, 1/100	Biolegend, Cat. # 312105
PE anti-human CD276 Antibody	FC	1/50	Biolegend, Cat. # 331605
PE anti-human CD24 Antibody	FC	1/50	Biolegend, Cat. # 311105
PE anti-human CD81 Antibody (5A6)	FC	1/50, 1/100	Biolegend, Cat. # 349506
CD277 Antibody, anti-human, PE	FC	1/50	Miltenyi Biotec, Cat. # 130-101-805

PE anti-human CD137L Antibody	FC	1/50	Biolegend, Cat. # 311503
PE anti-human CD201 Antibody	FC	1/50	Biolegend, Cat. # 351903
PE anti-human CD146 Antibody	FC	1/50	Biolegend, Cat. # 342003
PE anti-human CD63 Antibody	FC	1/50, 1/100	Biolegend, Cat. # 353003
PE anti-human CD338 Antibody	FC	1/50	Biolegend, Cat. # 332007
PE anti-human CD317 Antibody	FC	1/50	Biolegend, Cat. # 348406
PE anti-human CD116 Antibody	FC	1/50	Biolegend, Cat. # 305908
PE anti-human CD184 Antibody	FC	1/50	Biolegend, Cat. # 306505
PE anti-human CD49c Antibody	FC	1/50	Biolegend, Cat. # 343803
PE Mouse Anti-Human CD107a	FC	1/25	BD Biosciences, Cat. # 555801
CD55 (DAF) Antibody, anti-human	FC	1/100	Miltenyi Biotec, Cat. # 130-101-805
PE Mouse IgG1, κ Isotype Ctrl Antibody	FC	1/20 (sorting)	Biolegend, Cat. # 400113
Mouse anti-EBOV VP40 mAb (3G5)	WB	1/2000, 1/4000	IBT Bioservices, Cat. # 0201-016
Rabbit anti-EBOV GP1	WB	1/2000	(182)
CD81 Antibody (B-11)	WB	1/200	Santa Cruz, Cat. # sc-166029
α-Tubulin Polyclonal Antibody	WB	1/1000	Thermo Fisher, Cat. # PA5-29444
Anti-GAPDH Antibody	WB	1/1000	Biolegend, Cat. # 607902
IRDye 680RD Goat-anti-Mouse IgG	WB	1/15000	LI-COR, Cat. # 926-68070
IRDye 800CW Goat anti-Rabbit IgG	WB	1/15000	LI-COR, Cat. # 926-32211
IRDye 800CW Goat anti-Rat IgG	WB	1/15000	LI-COR, Cat. # 926-32219
Anti-human CD81 Antibody (5A6)	Cell treatment	5 µg/ml, 1 µg/ml	Biolegend, Cat. # 349502
Mouse IgG1, κ Isotype Ctrl Antibody	Cell treatment	5 µg/ml, 1 µg/ml	Biolegend, Cat. # 400102

Table 10 Kits

Name	**Source**
NucleoSpin Gel and PCR cleanup Kit	Macherey-Nagel
GeneJET Plasmid Miniprep System	Thermo Fisher
PureYield Plasmid Midiprep System	Promega
RNeasy Mini Kit	Qiagen
QuantiTect Reverse Transcription kit	Qiagen

Luna Universal qPCR Master Mix	New England Biolabs
Nano-Glo Luciferase Assay System	Promega

2.1.4 Buffers and reagents

Table 11 Buffers

Buffer	Composition
10× HBS	**1**.4 M NaCl, 250 mM HEPES, 14 mM Na_2HPO_4 in H2O
2× HBS	Dilute from 10× HBS, pH7.23
FACS buffer	1% (v/v) FCS in PBS
4% PFA	4% (w/v) PFA in PBS
0.2% Saponin	0.2% (w/v) Saponin in PBS
RIPA lysis buffer	140 mM NaCl, 10 mM Tris-HCl, 1 mM EDTA, 0.5 mM EGTA, 0.1% (w/v) Na-Deoxycholate, 0.1% (w/v) SDS, 1% (v/v) TritonX-100 in H_2O, pH7.4
5× Laemmli	250 mM Tris-HCl, 10% SDS, 10% 2-mercaptoethanol, 7.5% glycerol, 0.05% bromophenol blue in H_2O
10% SDS	10% (w/v) SDS in H_2O
10% APS	10% (w/v) APS in H_2O
Separating gel (15%).	4.6 ml H_2O, 5 ml Tris (1.5 M, pH 8.8), 10 ml Acrylamide (30%), 200 µl SDS (10%), 200 µl APS (10%), 10 µl TEMED
Separating gel (12%)	6.69 ml H_2O, 5 ml Tris (1.5 M, pH 8.8), 8 ml Acrylamide (30%), 200 µl SDS (10%), 200 µl APS (10%), 10 µl TEMED
Stacking gel (5%)	3.02 ml H_2O, 1.25 ml Tris-HCl (0.5 M, pH 6.8), 650 µl Acrylamide (30%), 50 µl SDS (10%), 50 µl APS (10%), 5 µl TEMED
10× SDS-PAGE running buffer (1 L)	30 g Tris base (250 mM), 144 g glycine (1.92 M), pH8.3, 10 g SDS (1%) in H_2O
1× SDS-PAGE running buffer	100 ml 10× SDS-PAGE running buffer, 900 ml H_2O
10x Transfer buffer (1 L)	250 mM Tris base (30.3 g), 1.92 M glycine (144.1 g) in H_2O
1x Transfer buffer (1 L)	100 ml 10x transfer buffer, 700 ml H_2O, 200 ml Methanol
10x TBS (1 L)	78.8 g Tris-HCl (500 mM), 87.66 g NaCl (1.5 M), pH7.5
1x TBS (1 L)	100 ml 10x TBS, 900 ml H_2O
1x TBS-T	0.1% (v/v) Tween 20 in 1x TBS
Luciferase lysis buffer	25 mM glycylglycine (pH 7.8), 15 mM $MgSO_4$, 4 mM EGTA, 10% (v/v) glycerol, 1% (v/v) Triton X-100, 1 mM DTT (before use) in H_2O

Fluc assay buffer	0.1 M KH_2PO_4 /K_2HPO_4 pH 7.8, 15 mM $MgSO_4$, 5 mM ATP in H_2O
50x D-Luciferin	50 mg D-Luciferin in 3.6 ml Fluc assay buffer
Fluc substrate buffer	1× D-Luciferin in Fluc assay buffer
LB (1 L)	20 g LB-Medium (Lennox) in H_2O
LB agar (1 L)	20 g LB-Medium (Lennox), 20g agar in H_2O
P1	50 mM Tris-HCl, pH8.0, 10 mM EDTA, 100 µg/ml RNase A in H_2O
P2	200 mM NaOH, 1 % SDS in H_2O
P3	3 M Potassium acetate in H_2O, pH 5.5
50× TAE (1 L)	241 g Tris Base (2 M), 57.1 ml acetic acid, 50 mM EDTA in H_2O
1×TAE (1 L)	20 ml 50× TAE, 980 ml H_2O

Table 12 Reagents

Name	**Source**
DMEM	Thermo Fisher
RPMI 1640	Thermo Fisher
FCS	Thermo Fisher
Human AB serum	Sigma-Aldrich
Penicillin/streptomycin	Life Technologies
Non-Essential Amino Acids	Life Technologies
Sodium Pyruvate	Life Technologies
MEM vitamins	Sigma-Aldrich
Poly-L-lysine hydrobromide	Sigma-Aldrich
Puromycin	Sigma-Aldrich
PBS	Thermo Fisher
Trypsin	Sigma-Aldrich
Accutase	Sigma-Aldrich
DMSO	Sigma-Aldrich
Ficoll-Paque PLUS	VWR
PEI	Polysciences
jetPRIME	Polyplus
Opti-MEM	Thermo Fisher
DharmaFECT 4 Transfection Reagent	Horizon Discovery Ltd.
ON-TARGETplus Human CD81 siRNA - SMARTPool	Horizon Discovery Ltd.
ON-TARGETplus Non-targeting Control siRNA #2	Horizon Discovery Ltd.
Protease Inhibitor	Sigma-Aldrich
PageRuler Prestained Protein Ladder	Thermo Fisher
Nonfat dried milk powder	AppliChem

Q5 High-Fidelity DNA Polymerase	New England Biolabs
dNTPs	Thermo Fisher
Agarose	Lonza
Ethidium bromide	VWR
GeneRuler 1 kb Plus DNA Ladder	Thermo Fisher
Gel Loading Dye, Purple (6X)	New England Biolabs
FastDigest EcoRI	Thermo Fisher
FastDigest Eco81I	Thermo Fisher
FastDigest XbaI	Thermo Fisher
FastDigest MluI	Thermo Fisher
FastDigest BamHI	Thermo Fisher
FastDigest NotI	Thermo Fisher
FastAP Phosphatase	Thermo Fisher
T4 DNA Ligase	Thermo Fisher
RNase-Free DNase Set	Qiagen
MG132	AdipoGen Life Sciences
Bafilomycin A1	AdipoGen Life Sciences
PMA	Sigma-Aldrich
Dextran, Alexa Fluor 555; 10,000 MW	Thermo Fisher
$CaCl_2$	Merck
NaCl	VWR
HEPES 1 M	Gibco
Na_2HPO_4	Merck
PFA	Roth
Saponin	AppliChem
Tris-HCl	AppliChem
EDTA	Sigma-Aldrich
EGTA	Roth
Na-Deoxycholate	Sigma-Aldrich
SDS	Sigma-Aldrich
TritonX-100	Sigma-Aldrich
2-mercaptoethanol	Sigma-Aldrich
Glycerol	AppliChem
Bromophenol blue	AppliChem
APS	Bio-Rad
Tris base	Sigma-Aldrich
Acrylamide (30%)	AppliChem
TEMED	Roth

glycine	Sigma-Aldrich
Methanol	AppliChem
Tween 20	AppliChem
Glycylglycine	Roth
$MgSO_4$	Roth
DTT	AppliChem
KH_2PO_4	Roth
K_2HPO_4	Roth
ATP	AppliChem
D-Luciferin	PJK Biotech
LB-Medium (Lennox)	Roth
RNase A	Macherey-Nagel
NaOH	Merck
Potassium acetate	Roth
Acetic acid	Merck

2.1.5 Equipment and software

Table 13 Equipment

Name	Company	Usage
NanoDrop	Thermo Fisher	DNA, RNA concentration measurement
MACSquant VYB	Miltenyi Biotec	Flow cytometry
Mini-PROTEAN Tetra Handcast System	Bio-Rad	WB running gel
Mini Trans-Blot Cell System	Bio-Rad	WB transfer
Odyssey Fc Imaging System	LI-COR	WB imaging
Cytation3 Cell Imaging Multi-Mode Reader	BioTek	Luciferase assay
Incucyte S3 Live-Cell Analysis System	Sartorius	Live cell imaging
LightCycler 480 System	Roche	qRT-PCR

Table 14 Software

Name	Company	Usage
Serial Cloner	Serial Basics	Cloning design and sequence alignment
FlowLogic	Inivai	Flow cytometry data analysis
Image Studio	LI-COR	WB image quantification
Incucyte	Sartorius	Microscopy image quantification
Microsoft Office	Microsoft	Calculations and writing
GraphPad Prism 9.4.1	GraphPad	Statistics analysis and create graph

CorelDraw	Corel	Arrange and create figures
BioRender	BioRender	Create Graphs
Zotero	Corporation for Digital Scholarship	Citation and reference

2.2 Methods

2.2.1 Cell culture

The cell lines were cultured with the medium listed in Table 15.

Table 15 Cell culture medium

Medium	**Cells**
DMEM + 10% FCS + 1% P/S	293T, Hela
DMEM + 10% FCS + 1% P/S + 1 µg/ml puromycin	293T and Hela control, CD81 KO, CD63 KO and CD9 KO
DMEM + 10% FCS + 1% NEAA + 1% Sodium Pyruvate + 1% P/S	Huh7.5
DMEM + 10% FCS + 1% NEAA + 1% Sodium Pyruvate + 1% P/S + 1 µg/ml puromycin	Huh7.5 control, CD81 KO, CD63 KO and CD9 KO

Cells maintenance

The cells were cultured at 37 °C with 5% CO_2 and 90% relative humidity, and passaged 2 to 3 times every week. To passage 293T cells, the cells were washed with PBS and suspended with fresh medium by tapping and pipetting, 1/5 to 1/10 cells were transferred to new flask filled with fresh medium. To passage Huh7.5 and Hela cells, the cells were washed with PBS and added with trypsin to detach the cells. After 2-3 minutes incubation at 37 °C, fresh medium was added and the cells were suspended by pipetting, 1/6 to 1/10 cells were transferred to a new flask filled with fresh medium. For cell seeding, medium without puromycin was used. To seed 293T cells in 96-well plates, the plates were coated with 0.01 mg/ml poly-L-lysine for 1 hour at 37°C and washed with PBS twice.

Freezing and thawing cells

To freeze the cells, the suspended cells were centrifuged at 300 g for 5 minutes, and the cells were resuspended with freezing medium (fresh medium+ 10% DMSO) and transferred to cryotubes. The tubes wrapped with tissue papers in

foam box were firstly freezed at -80 °C freezer and transferred to liquid nitrogen. To thaw the cells, the cryotubes were putted in 37 °C water bath. After thawing, the cells were immediately transferred to a flask filled with fresh medium for culture, and the medium was changed to fresh medium next day. Alternatively, the thawed cells were immediately transferred to a 15 ml tube filled with fresh medium and centrifuged at 300 g for 5 minutes to remove the DMSO. The cells were then suspended with fresh medium and transferred to a new flask for culture.

Human primary macrophages preparation

Human primary macrophages were prepared by Georgios Vavouras Syrigos, a PhD student in the group. Firstly, PBMC were isolated from the buffy coats of blood samples (Zentrum für Klinische Transfusionsmedizin, Tübingen) using Ficoll-Paque PLUS. The blood samples were mixed with the same volume of PBS and carefully top layered on 20 ml Ficoll-Paque in a 50 ml tube for centrifugation. The centrifugation was done at 2000 rpm (5810R) for 45 minutes at RT without deceleration. After centrifugation, the PBMC layer was took and transferred to a new tube filled with PBS, and the cells were centrifuged at 300 g for 5 minutes. The cells were washed with PBS for extra two times and suspended in macrophage medium (RPMI + 4% human AB serum + 1% NEAA + 1% Sodium Pyruvate + 1% P/S + 0.4% MEM vitamins). To differentiate into macrophages, 15×10^6 PBMC were transferred to petri dish in macrophage medium and cultured for 5 days, followed by wash with PBS and medium change. The cells were cultured for extra 2 days before use.

2.2.2 Molecular cloning

Polymerase chain reaction

Polymerase chain reaction (PCR) was performed as the manufacture's protocol of Q5 High-Fidelity DNA Polymerase to amplify the insert gene for cloning. The PCR products were analyzed by agarose gel (0.8% or 1% in 1× TAE buffer) electrophoresis (100 V, 30-45 min) and extracted from the gel with NucleoSpin Gel and PCR cleanup Kit.

Overlap extension PCR

Overlap extension PCR was done to mutate the XbaI site within EBOV NP and L gene. The mutation of XbaI site did not change the protein sequence of EBOV NP and L. The overlap extension PCR was designed according to the established protocols (302, 303). As Fig. 6 shown, step1 PCR was done with the standard protocol of Q5 High-Fidelity DNA Polymerase to amplify the two fragments with mutated XbaI site (XbaI*). After agarose gel electrophoresis, the fragments were purified with the gel cleanup kit. The two fragments were used for step2 PCR (Table 16) to generate full-length NP and L with mutated XbaI site. The Step2 PCR products were directly used as template for step3 PCR (Table 17, standard condition) to amplify the mutated full-length NP and L, the products were analyzed via agarose gel electrophoresis and purified with the gel cleanup kit.

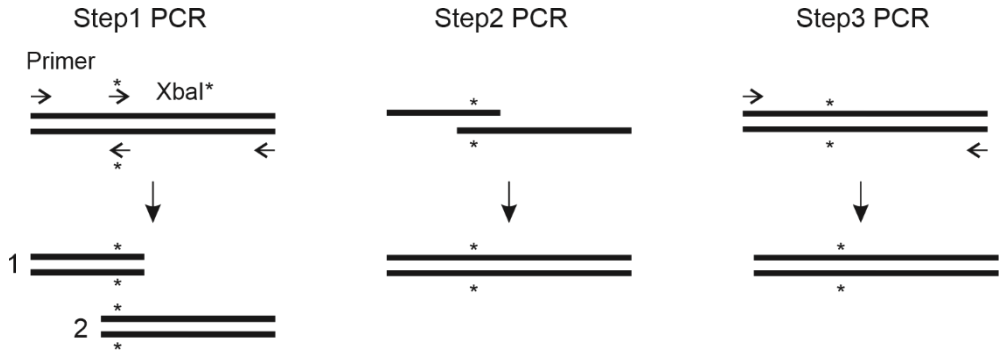

Fig. 6 Overlap extension PCR. Adapted from (302) and (303) and created with CorelDRAW.

Table 16 Step2 PCR

Reaction		Condition		
Component	Volume (µl)	Step	T (°C)	Time
5X Q5 Reaction Buffer	10	Initial denaturation	98	30 s
10 mM dNTPs	2	9 cycles	98	15 s
Q5 High-Fidelity DNA Polymerase	0.5		70	30 s/kb
5X Q5 High GC Enhancer	10	5 cycles	98	15 s
Fragment 1 (100 ng/kb)	x		65	15 s
Fragment 2 (100 ng/kb)	y		72	30 s/kb
Nuclease-Free Water	27.5-x-y	Final extension	72	2 min
Total	50	Hold	8	

Table 17 Step3 PCR reaction.

Component	Volume (µl)
5X Q5 Reaction Buffer	10
10 mM dNTPs	2
Q5 High-Fidelity DNA Polymerase	0.5
5X Q5 High GC Enhancer	10
Primer fw (2 µM)	1
Primer rv (2 µM)	1
Step2 PCR reaction	4
Nuclease-Free Water	21.5
Total	50

Restriction enzyme digestion

Plasmid vectors (around 2 µg) and purified PCR products were digested with FastDigest restriction enzymes to generate complementary overhangs for ligation. The enzyme digestion reaction was set up as the manufacture's protocol and was incubated at 37 °C for 30 min to 1h. FastAP phosphatase was occasionally added in plasmid digestion reaction. The digested products were analyzed via agarose gel electrophoresis and purified with the gel cleanup kit. To generate pPol II-4cis-vRNA-dGP-GFP, pPol II-4cis-vRNA-EBOV GP-GFP and pT7.1-4cis-vRNA-dGP-nluc were digested with EcoRI and EcoR81I, and the backbone of pPol II-4cis-vRNA-EBOV GP-GFP and insert of pT7.1-4cis-vRNA-dGP-nluc were cut from the gel and purified. The concentration of the purified DNA was measured by Nanodrop.

Ligation

Restriction enzyme digested plasmid vector (30 -100 ng) and insert DNA were ligated with T4 DNA ligase. The molar ratio between vector and insert was 1:3 to 1:6. 1 µl T4 DNA ligase and 2 µl 10× T4 DNA ligase buffer were used for the ligation reaction with total volume of 20 µl. The ligation reaction mixture was incubated at RT for 15 to 30 min before transformation.

Transformation

The E. coli competent cells NEB 10-beta (New England Biolabs) were thawed on ice. 20 to 50 µl of competent cells were added to 10 or 20 µl ligation reaction mixtures. After gentle mixing by tapping, the E. coli were incubated on ice for 30 min, followed by a heat shock at 42 °C for 45 s. The E. coli were put back on ice for 3-5 min and added with 200 µl LB medium. The E. coli were then incubated at 37 °C for 1 h with shaking and plated on LB agar plate with 100 µg/ml Ampicillin. The plate was incubated at 37 °C o/n.

Plasmid preparation

Single colonies were picked and inoculated into 3 ml LB medium with 100 µg/ml ampicillin. After incubation at 37 °C with shaking o/n, the E. coli were pelleted via centrifugation at 3300 g for 10 min. The plasmid DNA was prepared using either GeneJET Plasmid Miniprep System or lab established miniprep method. The latter procedure is following. The E. coli were suspended with 250 µl P1 buffer and lysed with 250 µl P2 buffer. 350 µl P3 buffer was added for neutralization, followed by centrifugation at 14000 rpm for 10 min. 700 µl supernatant were transferred to a new tube and added with 700 µl isopropanol for precipitation of the plasmid DNA. After incubation on ice for 15 min, the plasmid DNA was pelleted by centrifugation at 14000 rpm for 30 min at 4 °C. The supernatant was removed and the pellet was washed twice with 500 µl 70% Ethanol. After airdry, the plasmid DNA was dissolved in 30 µl HPLC grade H_2O. After confirmation by restriction enzyme digestion, the plasmids were prepared for sequencing by Eurofins. To prepare medium amount of plasmid, E. coli were inoculated in 50 ml LB medium with ampicillin or kanamycin. After incubation at 37 °C o/n, plasmids were prepared with PureYield Plasmid Midiprep System.

2.2.3 Transfection

Calcium Phosphate

293T cells were seeded one day before transfection. In a 6-well plate format, 5 µg plasmids and 13 µl 2 M $CaCl_2$ were mixed with H_2O in a total volume of 100

µl. The DNA mixture was dropwise added to 100 µl cold 2× HBS while vortexing. After vortexing for extra 10 s, the transfection mixture was incubated on ice for 15 min and dropwise added to the cells. 6 hours later, the medium was changed to fresh medium.

PEI

PEI was used for 293T cells transfection. In a 12-well plate format, 1 µg plasmids were mixed with 50 µl Opti-MEM, and 3 µl of 1 µg/µl PEI was mixed with 50 µl Opti-MEM. The PEI mixture was added to the plasmid mixture and mixed by pipetting. After incubation at RT for 15 min, the transfection mixture was dropwise added to the cells. 16h (o/n) later, the medium was changed to fresh medium. Transfection of other formats, the amount of plasmid was changed accordingly and the ratio between plasmid and PEI was 1:3.

jetPRIME

jetPRIME was used for 293T, Huh7.5 and Hela cells transfection. The cells were seeded 1 day before the transfection. The transfections were performed according to manufacturer's protocol.

DharmaFECT 4 Transfection Reagent

DharmaFECT 4 was used for human primary macrophages transfection with siRNA. Macrophages were seeded 1 day before transfection. 25 nM (final concentration) siRNA were transfected as the manufacture's protocol.

2.2.4 Generation of KO cells

293T CD81 KO cells and Hela control, CD81 KO, CD63 KO and CD9 KO cells were generated by transduction of lentiviruses expressing Cas9 only (control) or co-expressing Cas9 and gRNA targeting CD81, CD63 and CD9. In a 6-well plate format, 293T cells were transfected with 0.45 µg pMD2G/pVSV-G, 1.125 µg psPAX2 and 1.5 µg lentiviral CRISPR/Cas9 expression plasmid (Table 4) using PEI to produce lentiviruses. In parallel, 293T cells were transfected with 2.5 µg pSIV-vpr-vpx+ and 0.25 µg pVSV-G to produce Vpx-VLPs, which were used to

knock down SAMHD1 in target cells to improve lentivirus transduction efficiency (304). 24 h later, the supernatants containing lentiviruses and Vpx-VLPs were collected and centrifuged at 3200 g for 10 min to remove dead cells and cell debris. The cleared supernatants were collected for transduction. 293T and Hela cells seeded in 6-well plates were treated with Vpx-VLPs for 2 h and infected with lentiviruses for 24 h, followed by medium change. 24 h later, the cells were cultured in medium with 1 µg/ml puromycin for selection of successfully transduced cells. After around 2 weeks of selection, the KO efficiency of the cells was analyzed by flow cytometry. 293T CD81 KO cells stained with PE anti-human CD81 Antibody were subjected for fluorescence-activated cell sorting (FACS) at the FACS Core Facility (Tübingen university hospital). PE Mouse IgG1, κ Isotype Ctrl Antibody stained 293T CD81 KO cells were used for gating. Collected 293T CD81 KO cells from FACS are termed as 293T CD81 KO cells (sorted).

2.2.5 Flow cytometry

Surface staining

Surface staining was performed with 293T, Hela, Huh7.5 cells and human primary macrophages. Firstly, the cells were detached from the culture vessels. 293T cells were directly detached and suspended in PBS or medium by pipetting. Hela and Huh7.5 cells were detached by trypsin and suspended with medium. Human primary macrophages seeded in non-treated 96-well plate were detached by accutase (37 °C, 45-60 min) and suspended with medium. After detachment, the cells were transferred for centrifugation at 600g for 5 min and the supernatants were removed, followed by a wash with FACS buffer before staining. The cells were stained with PE conjugated antibodies (Table 9) diluted in FACS buffer for 30 min at 4 °C in dark. FACS buffer was filled to the cells for washing. The cells were centrifuged at 600 g for 5 min, and the wash step with FACS buffer was repeated once. Subsequently, the cells were either suspended with FACS buffer for direct measurement or suspended with 2% PFA and stored at 4 °C before measurement. Alternatively, the cells were fixed with 2% PFA at RT for 15 min and suspended with FACS buffer for measurement. For staining of

EBOV infected 293T cells, the cells were fixed as described in EBOV infection before staining.

Intracellular staining

PFA fixed (15 min at RT) surface stained cells were washed with PBS and permeabilized with ice-cold 90% methanol (in H_2O, stored at -20 °C) at 4 °C for 20 min. PE of surface stained antibodies were damaged by methanol (305). After the permeabilization, the cells were washed with FACS buffer and blocked with 10% FCS (in PBS) for 30 min at RT. The cells were then stained with PE conjugated antibodies and washed as surface staining. Cells were suspended with FACS buffer for measurements.

Total staining

Fixed (15 min at RT) surface stained cells were washed with PBS and permeablised with 0.2% saponin for 10 min at RT. The cells were then blocked with 10% FCS in 0.2% saponin for 30 min at RT. After a wash with FACS buffer, the cells were stained with PE conjugated antibodies and washed as surface staining. The cells were suspended in FACS buffer for measurement. For total staining of fixed EBOV infected 293T cells, the cells were permeabilized, blocked, stained and washed as intracellular staining.

All flow cytometry measurements were done with MACSquant VYB.

2.2.6 Western blot

12% or 15 % gel listed in Table 11 were prepared for SDS-PAGE. For detection of CD81, 15% gel was used. Gel running was done at 80-130 V for 90-120 min in 1× SDS-PAGE running buffer. PVDF membrane was activated by methanol for 15 s and assembled with the SDS-PAGE gel and filter paper as a sandwich. The transfer was done in 1x Transfer buffer at 80 V for 2 h, following by blocking with 5% milk in TBS for at least 1 h. The membranes were incubated with primary antibodies diluted in 5% milk o/n at 4 °C or 2-3 h at RT. The membranes were washed with 1x TBS-T 3× 10 min. Secondary antibodies were incubated with the

membranes in dark for 1 h at RT, followed by 3× 10 min with TBS-T. Detection was done with Odyssey Fc Imaging System.

2.2.7 Luciferase assay

The cells were lysed with 200 µl luciferase lysis buffer at RT for 15 min. For Fluc assay, Fluc assay buffer and substrate buffer was prepared as Table 11. 40 µl Fluc assay buffer was added to opaque white 96-well plates and mixed with 40 µl cell lysates and 40 µl Fluc substrate buffer (duplicates). For Nluc assay, Nluc substrate buffer was prepared by diluting Nluc substrate in Nluc assay buffer at ratio of 1/50 as the manufacture's protocol (Nano-Glo Luciferase Assay System). 40 µl cell lysates were added to opaque white 96-well plates and mixed with 40 µl Nluc substrate buffer. The measurements were done with Cytation3 Cell Imaging Multi-Mode Reader.

2.2.8 qRT-PCR

RNAs were extracted from the cells with RNeasy Mini Kit with on-column DNase digestion, and the concentration was measured with NanoDrop. 1 µg RNA were used for reverse transcription with QuantiTect Reverse Transcription kit. Specific primers in Table 8 were used for transcription of EBOV minigenome vRNA and cRNA, oligo(dT) was used for reverse transcription of mRNA. After reverse transcription, the reaction mixture (20 µl) was diluted with 40 µl RNase free water, and 5 µl diluted reverse transcription mixture was used for qPCR. qPCR reaction was prepared with Luna Universal qPCR Master Mix and 0.3 µM (final concentration) primers. Measurements were done with LightCycler 480 System. qPCR result was analyzed with the ΔΔCp method (306). Fluc (luc2) or GAPDH was used as reference gene.

2.2.9 BiFC assay

Kusabira-green (KG) based bimolecular fluorescence complementation (BiFC) assay from MBL life science (CoralHue® Fluo-chase Kit, a gift from AG Sauter) was used to analyze protein-protein interaction. 293T cells in 96-well plates were transfected with 75 ng KGN expression plasmids and 75 ng KGC expression

plasmids. In the assay to analyze whether CD81 interacts with NP in the presence of VP35, 50 ng KGN expression plasmids and 50 ng KGC expression plasmids together with 50 ng pCAGGS-VP35_v1.1 were transfected. 2 days post transfection, the cells were harvested and surface stained with PE conjugated CD81 antibody for flow cytometry.

2.2.10 Lentivirus pseudotypes production and infection

To produce EBOV GP or VSV G pseudotyped GFP expressing lentiviruses, 293T cells in 6-well plates were transfected with 1.125 µg psPAX2, 1.5 µg pWPXLd and 0.125 µg pVSV-G or pCAGGS ZEBOV GP wt using PEI. After incubation o/n, the medium was changed and medium containing lentivirus pseudotypes was harvested 3 days later. The lentiviruses containing medium was cleared by centrifugation at 3200g for 10 min. 0.9 ml cleared medium was used for infection with 293T cells in 12-well plates and the medium was changed 1-day post infection. 3 days post infection, the cells were harvested and fixed with 2% PFA at RT for 15 min. The cells were suspended with FACS buffer for flow cytometry.

2.2.11 EBOV trVLP assay

The trVLP production and infection assay was performed according to (111), this assay allows to model EBOV life cycle under BSL-1 condition. Briefly, a T7 RNA polymerase or RNA polymerase II driven plasmid encoding EBOV tetracistronic minigenome (4cis-vRNA) consisted of 3’ leader-nluc/GFP-VP40-GP-VP24-5’ trailer and plasmids encoding EBOV ribonucleoprotein (RNP: NP, VP35, VP30, VP24) responsible for minigenome replication and transcription were used for trVLP production. The produced trVLPs containing all EBOV proteins and a minigenome can be used for infection of target cells pretransfected with EBOV RNP, by which the minigenome can be replicated and transcribed. Tim1 (EBOV attachment factor) was also pretransfected to improve infection efficiency.

trVLP production

The transfection schemes shown in Table 18 were used to produce trVLP-nluc and trVLP-dGP-nluc. Cells were seeded in 12-well plates one day before

transfection. Transfection scheme 1 was used for transfection of 293T cells with PEI, medium was changed to fresh medium after o/n incubation. Transfection scheme 2 was used for transfection of Huh7.5 and Hela cells with jetPRIME, medium was changed to fresh medium 4 h post transfection. 3 d post transfection, the cells and medium were harvested for WB. The medium was transferred to 1.5 ml tubes and the cells were added with 1 ml PBS. The medium was centrifuged at 3200g for 10 min and the supernatants containing VLPs were taken and top layered on 200 µl 20% sucrose in a new tube. The VLPs were pelleted by centrifugation at 20000 × g at 4 °C for 90 min. The supernatants were removed and the pellets were suspended with 20-30 µl 1× Laemmli buffer (5× Laemmli buffer diluted with RIPA buffer). The cells were suspended with PBS and transferred to 1.5 ml tubes. After centrifugation at 300 g for 5 min, the cells were lysed with 50 to 80 µl RIPA buffer (containing protease inhibitor freshly added) > 20 min at 4 °C. The cell lysates were centrifuged at 12000 rpm for 10 min at 4 °C, and supernatants were taken and mixed with 5× Laemmli buffer. After mixing with Laemmli buffer, the VLPs and cell lysates were incubated at 95 °C for 10 min. The samples were stored at -20 °C before WB. In the CD81 restoration experiment, 293T CD81 KO cells in 12-well plates were pretransfected with pWPI-hCD81-HAHA-BLR (0, 0.0625, 0.125, 0.25, 0.5 and 1 µg) together with pWPI (1, 0.9375, 0.875, 0.75, 0.5 and 0 µg) in total 1 µg plasmids 1 day before the transfection to produce VLP, for which Table 18 scheme 2 was used to produce VLP-nluc and additionally 0.05 µg pCAGGS-luc2 were cotransfected as transfection control. 3 days post transfection, half of the cells were harvested for WB, half of the cells were prepared for luciferase assay. For RT-qPCR, 293T cells in 12-well plates were transfected as scheme 1 (Table 18 and Table 19) and additionally 0.1 µg pCAGGS-luc2 were cotransfected. 3 days post transfection, the cells were harvested for RT-qPCR.

Table 18 Transfection schemes to produce trVLP-nluc and trVLP-dGP-nluc

Plasmid	Mass (µg)-scheme 1	Mass (µg)-scheme 2
pCAGGS-NP-v1.1	0.125	0.0625
pCAGGS-VP35-v1.1	0.125	0.0625
pCAGGS-VP30-v1.1	0.075	0.0375

pCAGGS-L-v1.1	1	0.5
pCAGGS-T7opt	0.25	0.125
pT7.1-4cis-vRNA-EBOV GP-nLuc or pT7.1-4cis-vRNA-dGP-nluc	0.25	0.125

The transfection schemes to produce trVLP-GFP and trVLP-dGP-GFP were shown in Table 19. Scheme 2 was used to produce VLP-GFP in CD81 restoration experiment, the cells were harvested for WB 3 d post transfection. In live cell imaging experiment, cells in 96-well plates (triplicates) were transfected with 1/10 of scheme 2 (Table 19) together with 0.05 µg (10×) mCherry-C1 (transfection control). Live cell imaging started 6 h post transfection after medium change. To produce trVLP-GFP for infection, 293T cells in 6-well plates were transfected as scheme 1 (pPol II-4cis-vRNA-EBOV GP-GFP). After incubation o/n, medium was changed and trVLP-GFP containing medium was harvested 3 days later. The trVLP containing medium was clarified by centrifugation at 800 g for 5 min and supernatants were used for infection. The produced trVLPs were passaged twice and used for infection of target cells in the experiments. To produce trVLP-dGP-GFP pseudotyped with EBOV GP or VSV G (trVLP-dGP-GFP_EBOV GP or VSV G) for infection, 293T cells in 6-well plates were transfected with 2× scheme 1 (pPol II-4cis-vRNA-dGP-GFP) and 0.125 µg (2×) pCAGGS ZEBOV GP wt or pVSV-G. After incubation for 4 h or o/n, the medium was changed and VLP containing medium was harvested 3 days later. The VLP containing medium was centrifuged at 3200 g for 10 min and supernatants were taken for infection.

Table 19 Transfection scheme to produce trVLP-GFP and trVLP-dGP-GFP

Plasmid	**Mass (µg)-scheme 1**	**Mass (µg)-scheme 2**
pCAGGS-NP-v1.1	0.125	0.0625
pCAGGS-VP35-v1.1	0.125	0.0625
pCAGGS-VP30-v1.1	0.075	0.0375
pCAGGS-L-v1.1	1	0.5
pPol II-4cis-vRNA-EBOV GP-GFP or pPol II-4cis-vRNA-dGP-GFP	0.25	0.125

trVLP infection

For trVLP-GFP infection, 293T cells in 12- well plates were pretransfected with EBOV RNP and Tim1 as scheme 1 (Table 20) 1 day before infection. 1 ml cleared trVLP-GFP containing medium were added to the cells and medium was changed 1 day later. 3 days post infection, the cells and medium were harvested. 1/5 cells were collected for flow cytometry, remaining cells and medium were prepared for WB as trVLP production experiment. For flow cytometry, the cells were suspended with 2% PFA (0.5% FCS in PBS, ideally PBS) and stored at 4 °C before measurements. For infection of trVLP-dGP-GFP_ EBOV GP or VSV G (Fig. 15B), 293T cells in 12-well plates were pretransfected with EBOV RNP and Tim1 as scheme 1 (Table 20) and 0.1 µg pCAGGS-luc2 (transfection ctrl, optionally) was co-transfected 1 day before infection. The cells were infected with 0.9 ml cleared trVLP-dGP-GFP_EBOV GP or VSV G for 1 day and the medium was changed. 3 days post infection, the cells were harvested for flow cytometry. The cells were fixed with 2% PFA at RT for 15 min and suspended with FACS buffer for flow cytometry. For infection of trVLP-dGP-GFP_EBOV GP with 293T wt cells (Fig. 15D), the cells in 96-well plates (triplicates) were pretransfected with 1/10 scheme 2 (Table 20) + 0.05 µg (10×) pmtagBFP-C1 (transfection control) + 0.5 µg (10×) pWPI-hCD81-HAHA-BLR or pWPI_BLR. In case of Tim1-, pCAGGS-MCS instead of pCAGGS-Tim1-v1.2 was transfected. 1 day later, the cells were infected with 100 µl clarified trVLP-dGP-GFP_EBOV GP for 1 day, followed by medium change. 2 days post infection, the cells were harvested and surface stained with PE conjugated CD81 antibody for flow cytometry. In the CD81 antibody treatment experiment, 293T cells seeded in 96-well plates (triplicates) were pretransfected 1/10 of scheme 2 (Table 20) and 0.05 µg (10×) mCherry-C1. 1 day later, the medium was removed from the cells and 60 µl medium containing no antibody, 10 or 2 µg/ml Anti-human CD81 Antibody (5A6) or Mouse IgG1, κ Isotype Ctrl Antibody was added. 1 h later, the cells were added with 60 µl cleared trVLP-dGP-GFP, trVLP-dGP-GFP_EBOV GP or VSV G. 2 days post infection, the cells were harvested and suspended in FACS buffer for flow cytometry.

Table 20 Pretransfection scheme for trVLP infection

Plasmid	Mass (µg)-scheme 1	Mass (µg)-scheme 2
pCAGGS-NP-v1.1	0.125	0.0625
pCAGGS-VP35-v1.1	0.125	0.0625
pCAGGS-VP30-v1.1	0.075	0.0375
pCAGGS-L-v1.1	1	0.5
pCAGGS-Tim1-v1.2	0.25	0.125

2.2.12 EBOV infection

rgEBOV-iluc2 and rgEBOV-eGFP infection were performed by Dr. Thomas Hoenen and Dr. Lisa Wendt in Friedrich-Loeffler-Institut. For rgEBOV-iluc2 infection, 293T cells in 12-wel plates were infected with rgEBOV-iluc2 at MOI 0.5. 24 h and 48 h post infection, the cells were lysed with 300 µl 1x Glo Lysis buffer (Promega) at RT for 10 min. The cell lysates were centrifuged at 10000g for 3 min and the supernatants were taken for luciferase assay. In 96-well white bottom plate, 50 µl cleared cell lysates were mixed with 50 µl Bright Glo or Cell Titer-Glo reagent (Promega), and the luminescence was measured. For rgEBOV-eGFP infection, 293T cells in 6-well plates were infected with rgEBOV-eGFP at MOI 1. 24 h and 48 h post infection, the cells were harvested and fixed with 4% PFA at 4 °C for at least 24 h. Subsequently, the cells were suspended with PBS and shipped to Tübingen for flow cytometry analysis.

3. Results

3.1 Downregulation of CD81, CD63 and CD9 by EBOV GP

3.1.1 Modulation of surface receptors by EBOV GP

A variety of surface receptors modulated by EBOV GP in Hela cells were previously identified via a flow-cytometry based screen (by Julia Nehls). 20 downregulated receptors more than 2-fold and one upregulated receptor (CD55) were selected for validation. Hela and 293T cells were transfected to co-express EBOV GP and GFP through the internal ribosomal entry sequence of a bicistronic mRNA and stained with PE conjugated antibodies against the receptors for surface expression analysis by flow cytometry. In the flow cytometry analysis, the cells were gated into three populations according to GP expression level, GP- (no expression), GP+ (intermediate expression) and GP++ (high expression) (Fig. 7C and 7F). Receptors expression levels were normalized to the unstained control (Fig.7A and 7D). Receptors with expression levels (GP- population) two-fold higher than the unstained control were considered detectable. In Hela cells, 16 receptors, CD79b, HLA, CD59, CD9, CD276, CD24, CD81, CD277, CD137L, CD201, CD146, CD63, CD317, CD184, CD49c and CD55, had detectable expression (Fig. 7A). To analyze the modulation of the receptors in the presence of EBOV GP, receptor expression level of GP+ and GP++ cells were normalized to GP- cells (Fig.7B and 7E). In Hela cells, 6 receptors, CD79b, HLA, CD59, CD9, CD63 and CD184, were significantly downregulated by EBOV GP (Fig. 7B-7C). In 293T cells, 14 receptors, CD79b, HLA, CD59, CD9, CD276, CD81, CD277, CD137L, CD201, CD146, CD63, CD184, CD49c and CD55, had detectable expression (Fig. 7D). 10 receptors, HLA, CD59, CD9, CD276, CD81, CD201, CD146, CD63, CD184 and CD55, were significantly downregulated by GP in 293T cells (Fig. 7E-7F). Fold of modulation was calculated by dividing the receptor expression level (PE MFI) of GP- cells to GP++ cells, value greater than 1 indicates downregulation and value smaller than 1 indicates upregulation. 7 receptors, CD63, HLA, CD9, CD81, CD59, CD201(Endothelial protein C receptor) and CD184 (C-X-C chemokine receptor type 4), were downregulated more than 1,5-fold in both Hela and 293T cells (Fig. 7G). Among them, CD81, CD63 and CD9, are members of the tetraspanin superfamily. The downregulation

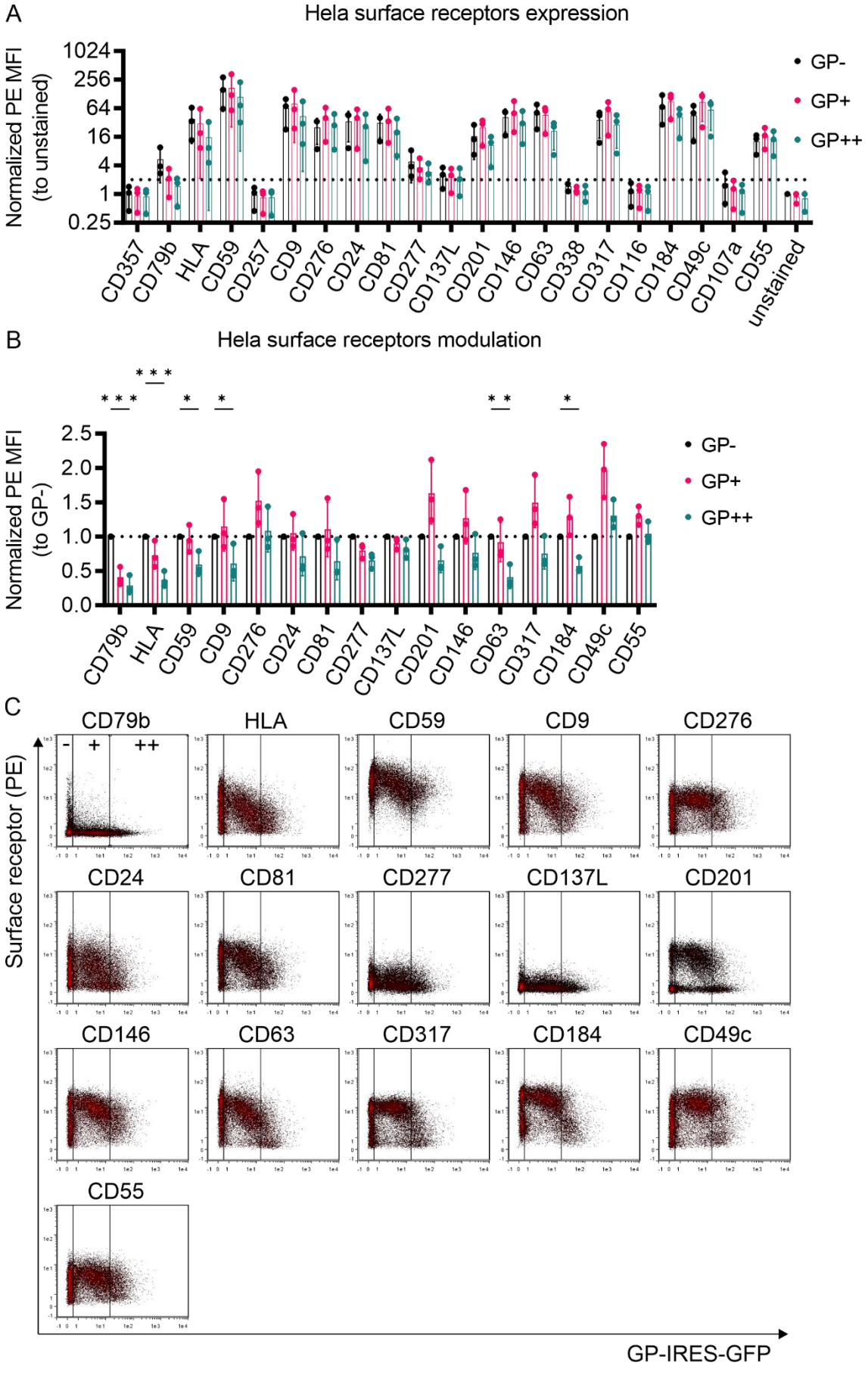
A
Hela surface receptors expression
Normalized PE MFI (to unstained)
1024
256
64
16
4
1
0.25
GP-
GP+
GP++
CD357
CD79b
HLA
CD59
CD257
CD9
CD276
CD24
CD81
CD277
CD137L
CD201
CD146
CD63
CD338
CD317
CD116
CD184
CD49c
CD107a
CD55
unstained
B
Hela surface receptors modulation
Normalized PE MFI (to GP-)
2.5
2.0
1.5
1.0
0.5
0.0
GP-
GP+
GP++
CD79b
HLA
CD59
CD9
CD276
CD24
CD81
CD277
CD137L
CD201
CD146
CD63
CD317
CD184
CD49c
CD55
C
CD79b
HLA
CD59
CD9
CD276
CD24
CD81
CD277
CD137L
CD201
CD146
CD63
CD317
CD184
CD49c
CD55
Surface receptor (PE)
GP-IRES-GFP

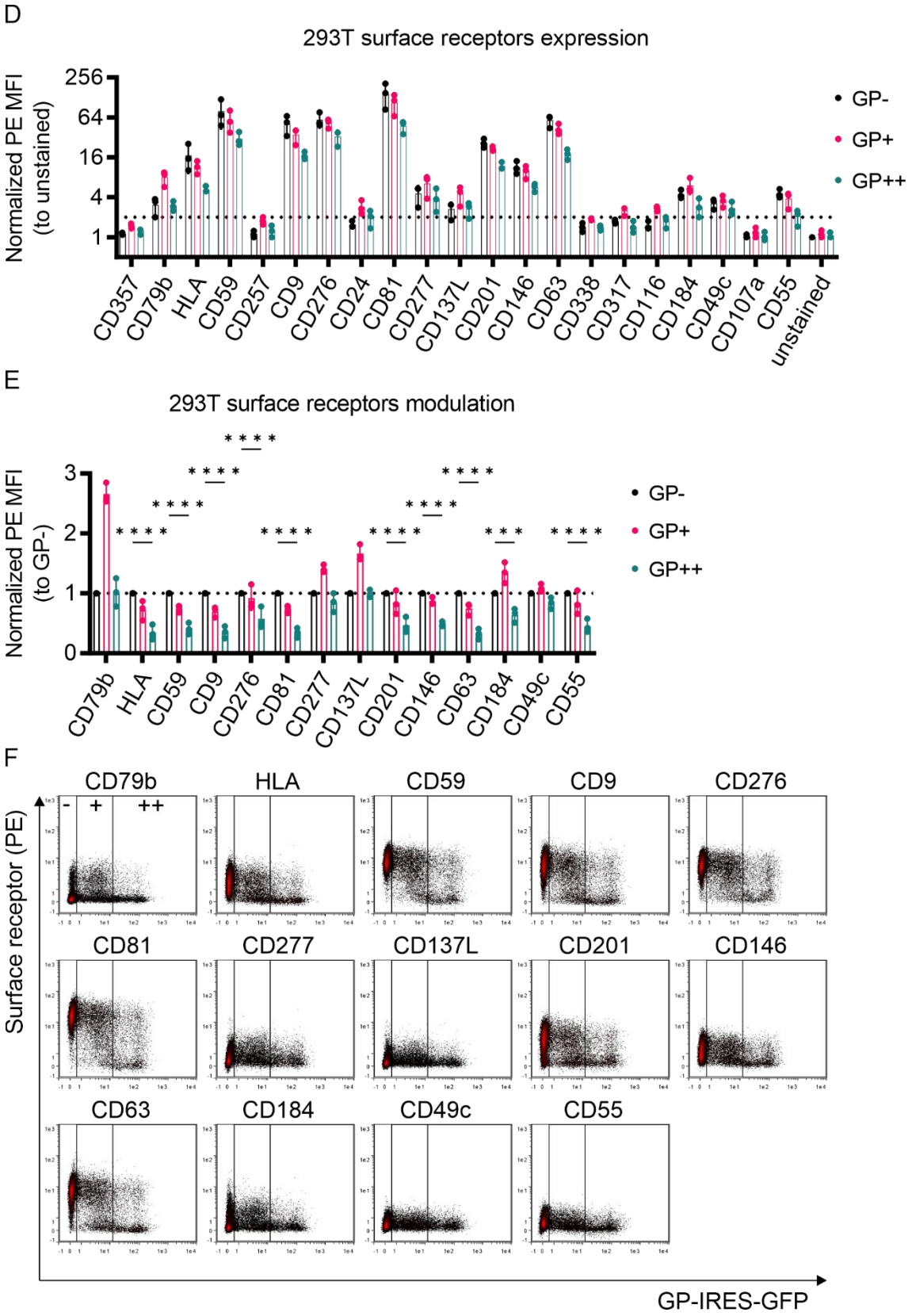
D
293T surface receptors expression
Normalized PE MFI (to unstained)
256
64
16
4
1
GP-
GP+
GP++
CD357
CD79b
HLA
CD59
CD257
CD9
CD276
CD24
CD81
CD277
CD137L
CD201
CD146
CD63
CD338
CD317
CD116
CD184
CD49c
CD107a
CD55
unstained
E
293T surface receptors modulation
Normalized PE MFI (to GP-)
3
2
1
0
GP-
GP+
GP++
CD79b
HLA
CD59
CD9
CD276
CD81
CD277
CD137L
CD201
CD146
CD63
CD184
CD49c
CD55
F
CD79b
HLA
CD59
CD9
CD276
CD81
CD277
CD137L
CD201
CD146
CD63
CD184
CD49c
CD55
-
+
++
Surface receptor (PE)
GP-IRES-GFP

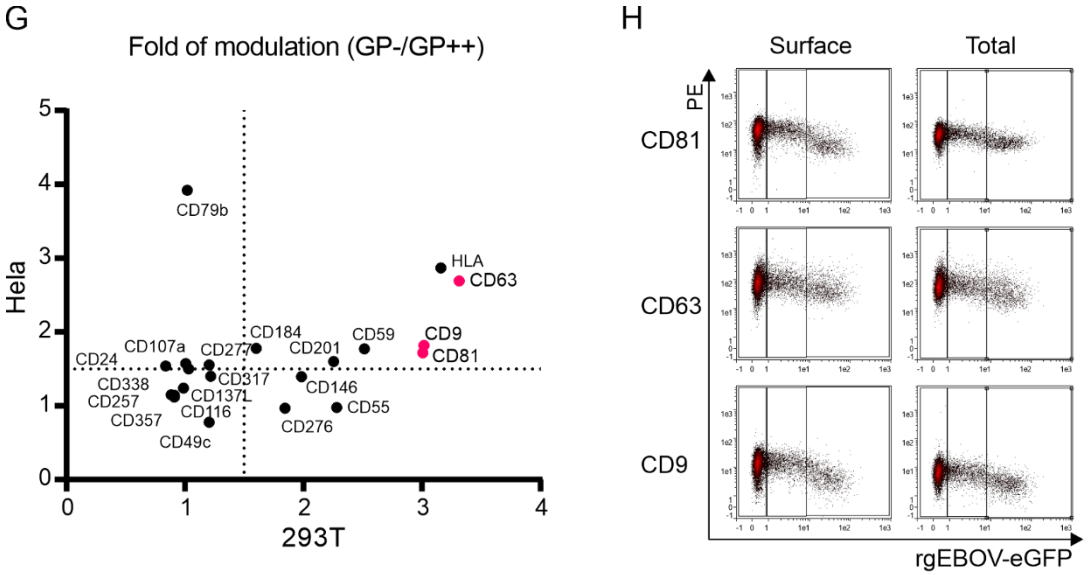

Figure 7 Modulation of surface receptors by EBOV GP. Hela (A-C) and 293T (D-F) cells were transfected with plasmids co-expressing EBOV GP and GFP. 2 d.p.t., the cells were harvested and stained with PE conjugated antibodies against the surface receptors for flow cytometry analysis (n=3). (A) and (D) shows surface receptors expression (PE MFI) normalized to unstained controls in Hela and 293T cells, respectively. Shown are mean values +/- SD. (B) and (E) are receptor surface expression (PE MFI) of GP+ and GP++ cells normalized to GP- cells in Hela and 293T cells. Indicated are mean values +/- SD, two-way ANOVA with Dunnett correction was used for statistics analysis (GP): 0,1234 (ns), 0,0332 (*), 0,0021 (**), 0,0002 (***), <0,0001 (****). Representative density plots of Hela (C) and 293T (F) cells shows GFP/GP and receptor surface expression. (G) Fold of modulation of the receptors in Hela and 293T cells is plotted, shown are mean values. (H) 293T control cells were infected with rgEBOV-eGFP (MOI=1). 1 d.p.i., the cells were harvested, fixed and stained with PE conjugated antibodies against CD81, CD63 and CD9 to analyze surface and total expression of the receptors via flow cytometry (n=1). Shown are density plots.

of CD81, CD63 and CD9 was also observed in authentic EBOV infection of 293T cells (by Thomas Hoenen and Lisa Wendt from Friedrich-Loeffler-Institut, Fig. 7H). Since several members of this superfamily appears to be downregulated in presence of GP, tetraspanins were selected for further investigations.

3.1.2 Modulation of CD81, CD63 and CD9 by viral GPs

To determine whether other viral glycoproteins, especially within the filoviridae family, modulate the previously identified tetraspanins, 293T cells were transfected to express GFP only or co-express viral GP and GFP. Then surface CD81, CD63 as well as CD9 expression levels were analyzed by flow cytometry. Four filoviral glycoproteins SUDV GP, RESTV GP, TAFV GP and MARV GP downregulated CD81, CD63 and CD9 (Fig. 8A-8B). Unlike the filoviral GPs, LASV

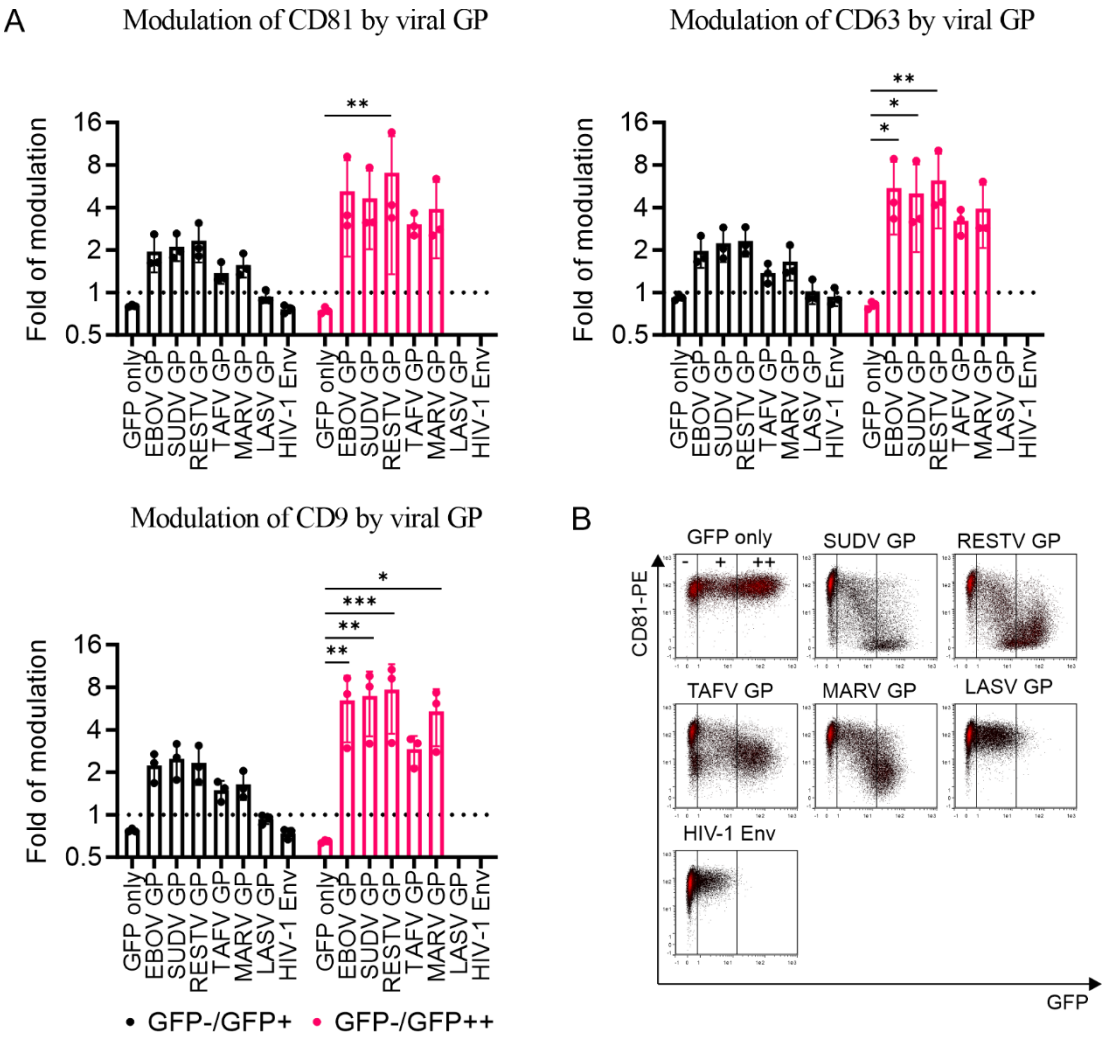

Figure 8 Modulation of CD81, CD63 and CD9 by viral GPs. (A-B) 293T cells were transfected with GFP only expression plasmid or viral GP and GFP co-expression plasmid. 2 d.p.t., the cells were harvested and stained with PE conjugated antibodies against CD81, CD63 and CD9 for flow cytometry analysis. (A) Fold of modulation was calculated by dividing the PE MFI of GFP- cells to GFP+ or GFP++ cells. n=3, shown are mean values +/- SD. Two-way ANOVA with Dunnett correction was used for statistics analysis (GP): 0,1234 (ns), 0,0332 (*), 0,0021 (**), 0,0002 (***), <0,0001 (****). LASV GP and HIV-1 Env were not included in the statistics analysis due to their relative low expression levels. (B) Representative density plots of cells stained with PE conjugated antibodies against CD81.

GP and HIV-1 (NL 4-3) Env were expressed mainly at intermediate level (GFP+) and did not modulate CD81, CD63 and CD9 expression (Fig. 8A-8B).

3.1.3 Modulation of CD81, CD63 and CD9 by EBOV GP subunits and mutants

To characterize the domains and residues of GP involved in the downregulation of CD81, CD63 and CD9, the capacity of a set of different GP subunits and

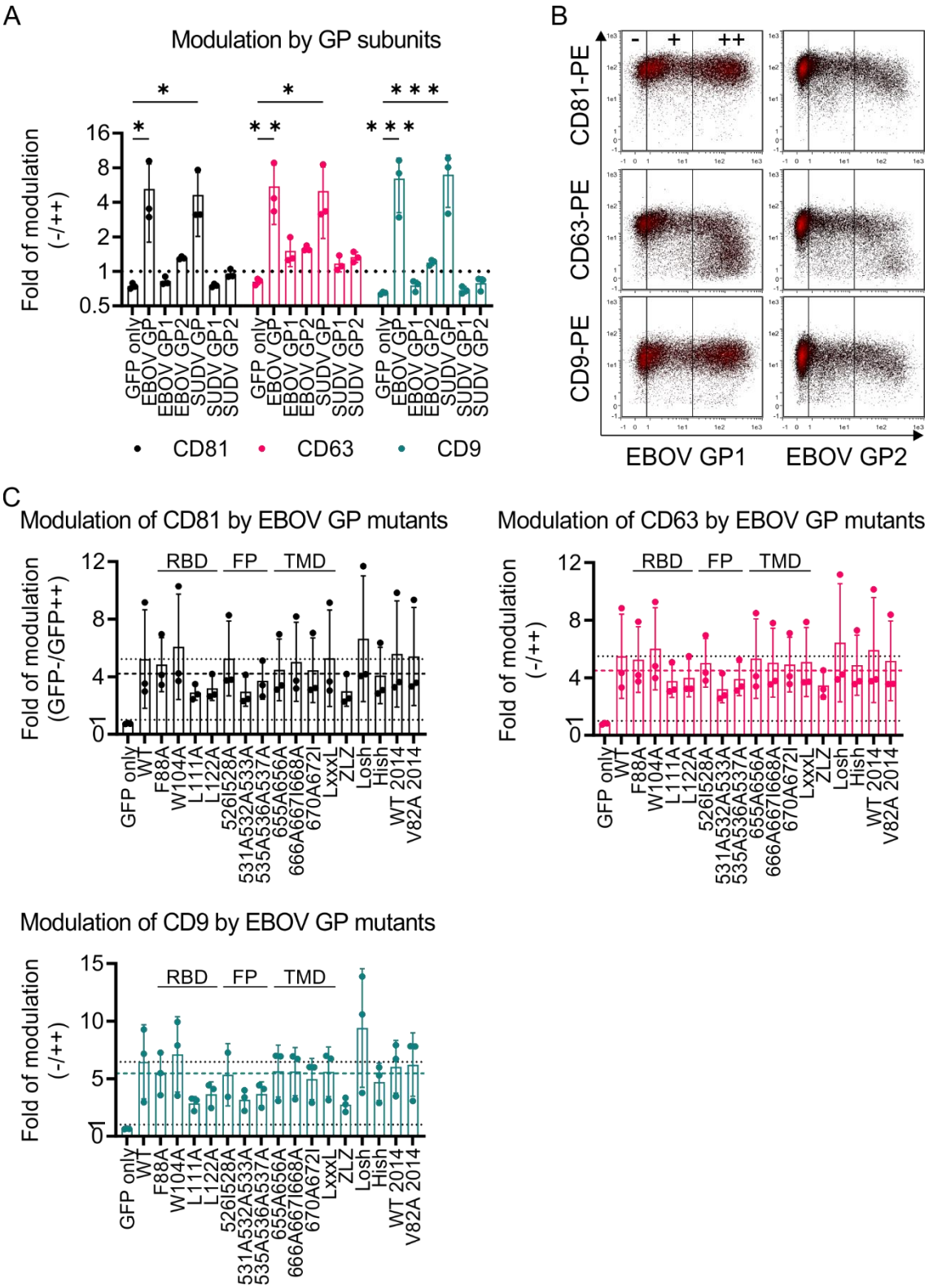

Figure 9 Modulation of CD81, CD63 and CD9 by EBOV GP subunits and mutants. 293T cells were transfected with plasmids expressing GFP only or Co-expressing GFP and GP (WT), GP subunits or mutants as indicated. 2 d.p.t., the cells were harvested and stained with PE conjugated antibodies against CD81, CD63 and CD9 for flow cytometry analysis (A-C). n=2-3, fold of modulation was calculated by dividing PE MFI of GFP- cells to GFP++ cells, shown are

mean values +/- SD. (A) Two-way ANOVA with Dunnett correction was used for statistics analysis (GP): 0,1234 (ns), 0,0332 (*), 0,0021 (**), 0,0002 (***), <0,0001 (****). This experiment was done with figure 8 together and the data of GFP only, EBOV GP (WT) and SUDV GP was plotted in both figure 8 and figure 9 as control for comparison.

mutants to modulate the surface expression of these three tetraspanin was investigated with flow cytometry. EBOV GP2 but not GP1 slightly downregulated CD81 and CD9, while CD63 was downregulated by both GP1 and GP2 (Fig.9A-9B). However, neither GP1 nor GP2 of EBOV and SUDV alone was able to downregulate surface CD81, CD63 and CD9 as efficient as full-length GP, suggesting both GP1 and GP2 are involved in the downregulation (Fig. 9A).

The GP mutants tested in this study mainly are mutants with characterized functions, that are described in the introduction. F88A, W104A, L111A and L122A locate within the RBD of GP, and 526I528A, 531A532A533A as well as 535A536A537A locate within the FP of GP. 655A656A, 666A667I668A, 670A672I and LxxxL are mutations within the TMD of GP. ZLZ is a chimera, in which the TMD is replaced by the TMD of LASV GP. Losh and Hish are mutants with low shedding and high shedding capacity to release the GP ectodomain (180). WT 2014 and V82A 2014 are GP of EBOV circulated during 2014 outbreak (307). All the GP tested were able to downregulate surface CD81, CD63 and CD9 (Fig. 9C). Mutants with the following features in terms of fold of modulation (mean value), WT-mutant>1 and mutant+SD<WT, were defined as mutants with impaired capacity in downregulation. L111A and L112A within RBD, 531A532A533A and 535A536A537A within FP and ZLZ with replaced TMD showed impaired capacity to downregulate surface CD81, CD63 and CD9 (Fig. 9C). Additionally, Hish showed impaired capacity to downregulate surface CD9 (Fig. 9C). The RBD is located in GP1 subunit while FP and TMD are located in GP2 subunit, again suggesting that the downregulation of surface CD81, CD63 and CD9 engages both GP1 and GP2 subunits.

3.2 CD81 suppresses EBOV minigenome replication and transcription

3.2.1 The role of CD81, CD63 and CD9 in EBOV trVLP production

To determine the role of TSP modulation by GP in EBOV replication, the EBOV trVLP assay was employed to model the EBOV life cycle (111). 293T control, CD81 KO, CD63 KO and CD9 KO cells were transfected with a tetracistronic minigenome plasmid encoding Nano-luciferase (nluc), VP40, GP and VP24 of EBOV (3'-5'), a T7 RNA polymerase expression plasmid (for initial transcription of tetracistronic minigenome plasmid to viral RNA minigenome) and four plasmids expressing EBOV NP, VP30, VP35 and L (RNP, for viral minigenome replication and transcription) to produce EBOV VLPs. As GP was shown to downregulate CD81, CD63 and CD9, the cells were transfected with a GP deficient minigenome to produce trVLP-dGP-nluc to see whether there is difference in replication between trVLP-nluc and trVLP-dGP-nluc. On the other hand, trVLP-dGP-nluc use allows analyzing the roles of the TSPs in EBOV replication and release beyond viral entry. The KO efficiency of CD81, CD63 and CD9 in 293T cells were analyzed by flow cytometry (Fig. 10A). Control cells were transduced with Cas9 lentivirus expressing no gRNA. In trVLP producer cells, the matrix protein VP40 expression in the cells (cell lysates, CL) as well as released trVLP (medium) were checked by WB (Fig. 10B). The quantification of the WB results demonstrated that CD81 KO, but not CD63 KO and CD9 KO, resulted in higher VP40 expression in both trVLP-nluc and trVLP-dGP-nluc producer cells (Fig. 10B). VP40 expression was generally lower in trVLP-nluc than trVLP-dGP-nluc producer cells, while CD81 KO resulted in higher fold of increase in VP40 expression when cells were producing trVLP-dGP-nluc (4,19~) as compared to trVLP-nluc (2,87~) (Fig. 10B). This result indicates that CD81 restricts trVLP expression. Furthermore, GP seems to counteract the negative effect of CD81 on EBOV VP40 expression. Similar to what has been observed in cell lysates, in the medium of 293T trVLP producer cells, more VP40 was released from CD81 KO cells than control cells, and similar amounts of VP40 were released from control, CD63 KO and CD9 KO cells (Fig. 10B). To analyze whether CD81, CD63 and CD9 have an effect on EBOV VLP release, released VP40 in medium was

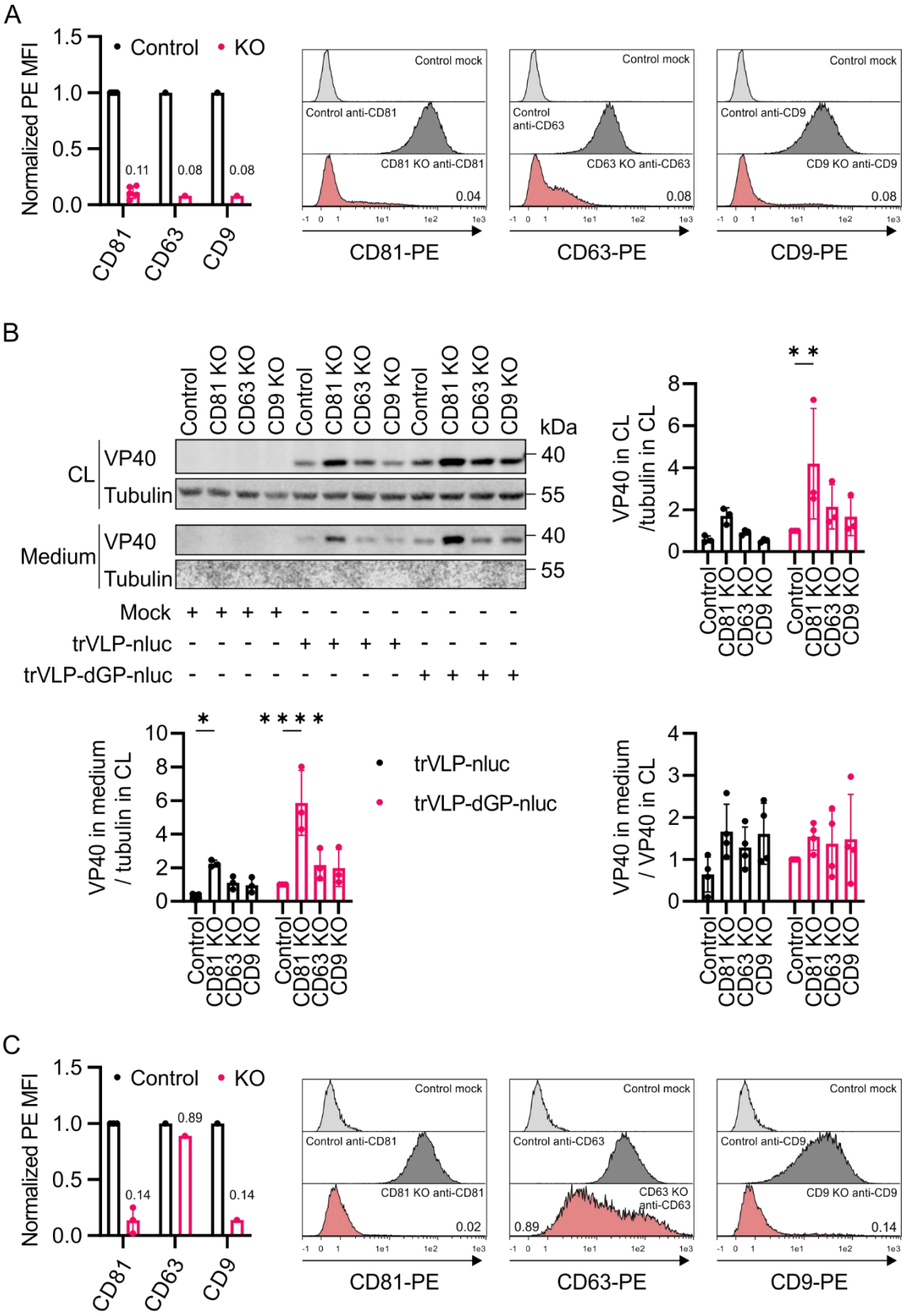
A
Normalized PE MFI
Control
KO
0.11
0.08
0.08
CD81
CD63
CD9
Control mock
Control anti-CD81
CD81 KO anti-CD81
0.04
CD81-PE
Control anti-CD63
CD63 KO anti-CD63
0.08
CD63-PE
Control anti-CD9
CD9 KO anti-CD9
0.08
CD9-PE
B
Control
CD81 KO
CD63 KO
CD9 KO
kDa
CL
VP40
Tubulin
Medium
40
55
Mock
trVLP-nluc
trVLP-dGP-nluc
VP40 in CL /tubulin in CL
VP40 in medium / tubulin in CL
VP40 in medium / VP40 in CL
trVLP-nluc
trVLP-dGP-nluc
C
Normalized PE MFI
Control
KO
0.14
0.89
0.14
CD81
CD63
CD9
Control mock
Control anti-CD81
CD81 KO anti-CD81
0.02
CD81-PE
Control anti-CD63
CD63 KO anti-CD63
0.89
CD63-PE
Control anti-CD9
CD9 KO anti-CD9
0.14
CD9-PE

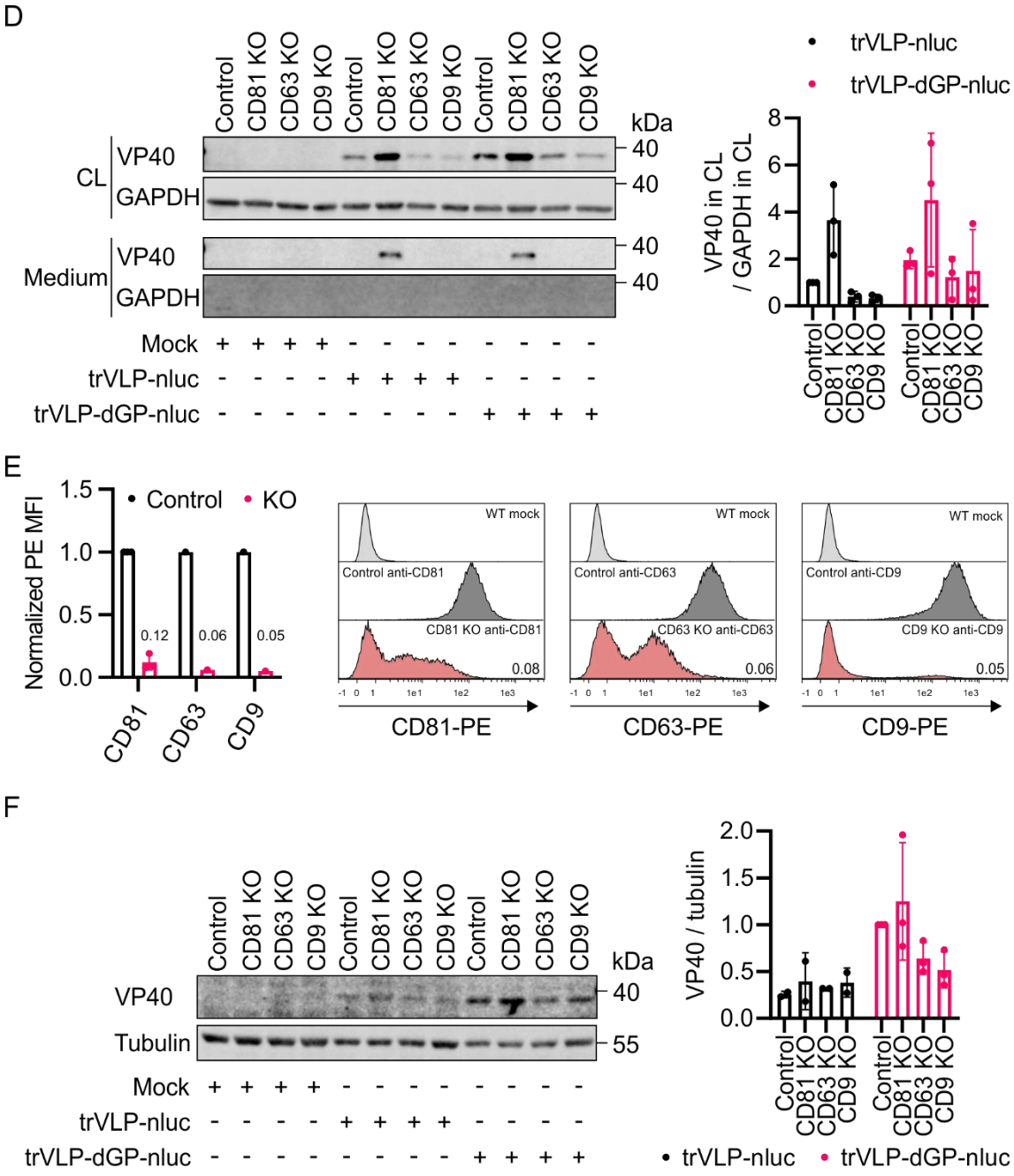

Figure 10 The role of CD81, CD63 and CD9 in EBOV trVLP production. (A) 293T (n=1-5), (C) Huh7.5 (n=1-3), (E) Hela (n=1-3) control, CD81 KO, CD63 KO and CD9 KO cells were mock stained or stained (surface) with PE conjugated antibodies against CD81, CD63 and CD9 for flow cytometry analysis. Shown are mean values of normalized PE MFI (to control cells) +/- SD (left) and histograms (right). (B) 293T, (D) Huh7.5, (F) Hela control, CD81 KO, CD63 KO and CD9 KO cells were mock transfected or transfected to produce EBOV trVLP-nluc or trVLP-dGP-nluc. 3 d.p.t., the cells and medium were harvested for WB to check EBOV VP40 and tubulin or GAPDH expression (n=3-4). (B, D and F) Bar graphs are quantification of WB result from 293T cells (B, normalized to control trVLP-dGP-nluc producer cells, n=3-4), Huh7.5 cells (D, normalized to control trVLP-nluc producer cells, n=3) and Hela cells (F, normalized to control trVLP-dGP-nluc producer cells, n=2-3). Indicated are mean values +/- SD. (B) Two-way ANOVA with Dunnett correction was used for statistics analyses (GP): 0,1234 (ns), 0,0332 (*), 0,0021 (**), 0,0002 (***), <0,0001 (****).

normalized to VP40 expressed in cells (CL). No significant difference was observed among the control and KO cells (Fig. 10B). These results suggest that CD81, but not CD63 and CD9, plays a negative role in EBOV trVLP production, while VLP release remains unaffected by CD81, CD63 and CD9 in 293T cells. EBOV trVLP production was also analyzed in Huh7.5 control, CD81 KO, CD63 KO and CD9 KO cells (Fig. 10C). Similarly, VP40 expression was higher in CD81 KO cell as compared to CD63 KO, CD9 KO and control cells in both trVLP-nluc and trVLP-dGP-nluc producer cells (Fig. 10D). In the medium of Huh7.5 trVLP producer cells, VP40 could only be detected from CD81 KO cells (Fig. 10D). The result suggests that CD81 also plays a negative role in EBOV trVLP production in Huh7.5 cells. The role of the tetraspanins in EBOV trVLP production in Hela cells, analyzed with control, CD81 KO, CD63 KO and CD9 KO cells (Fig. 10E), was less clear, which was associated with cytotoxicity (reduced tubulin expression, Fig. 10F).

Altogether, CD81, but not CD63 and CD9, reduced EBOV minigenome encoded VP40 expression and trVLP production in 293T and Huh7.5 cells.

3.2.2 CD81 suppresses EBOV minigenome encoded proteins expression

To further confirm the negative role of CD81 in EBOV minigenome encoded VP40 expression, 293T CD81 KO cells were transfected with gradient amounts of HA tagged CD81 (CD81-HA) to restore CD81 expression and the cells were transfected to produce trVLP-nluc and trVLP-dGP-nluc. VP40 expression in the trVLP producer cells was analyzed by WB, and the minigenome encoded nluc reporter expression was also determined via luciferase assay. In line with increased VP40 expression, KO of CD81 increased nluc expression (normalized to Fluc transfection ctrl) (Fig. 11A). Furthermore, restoring CD81 in CD81 KO cells reduced VP40 and nluc expression in a dose dependent manner (Fig. 11A). The suppression of both VP40 and nluc expression by CD81 suggests that CD81 plays a negative role in EBOV trVLP minigenome replication and/or transcription.

To clarify that the observed negative effect of CD81 on EBOV minigenome encoded proteins expression is not a result of its possible effect on T7 polymerase mediated initial transcription of the minigenome plasmid, an RNA

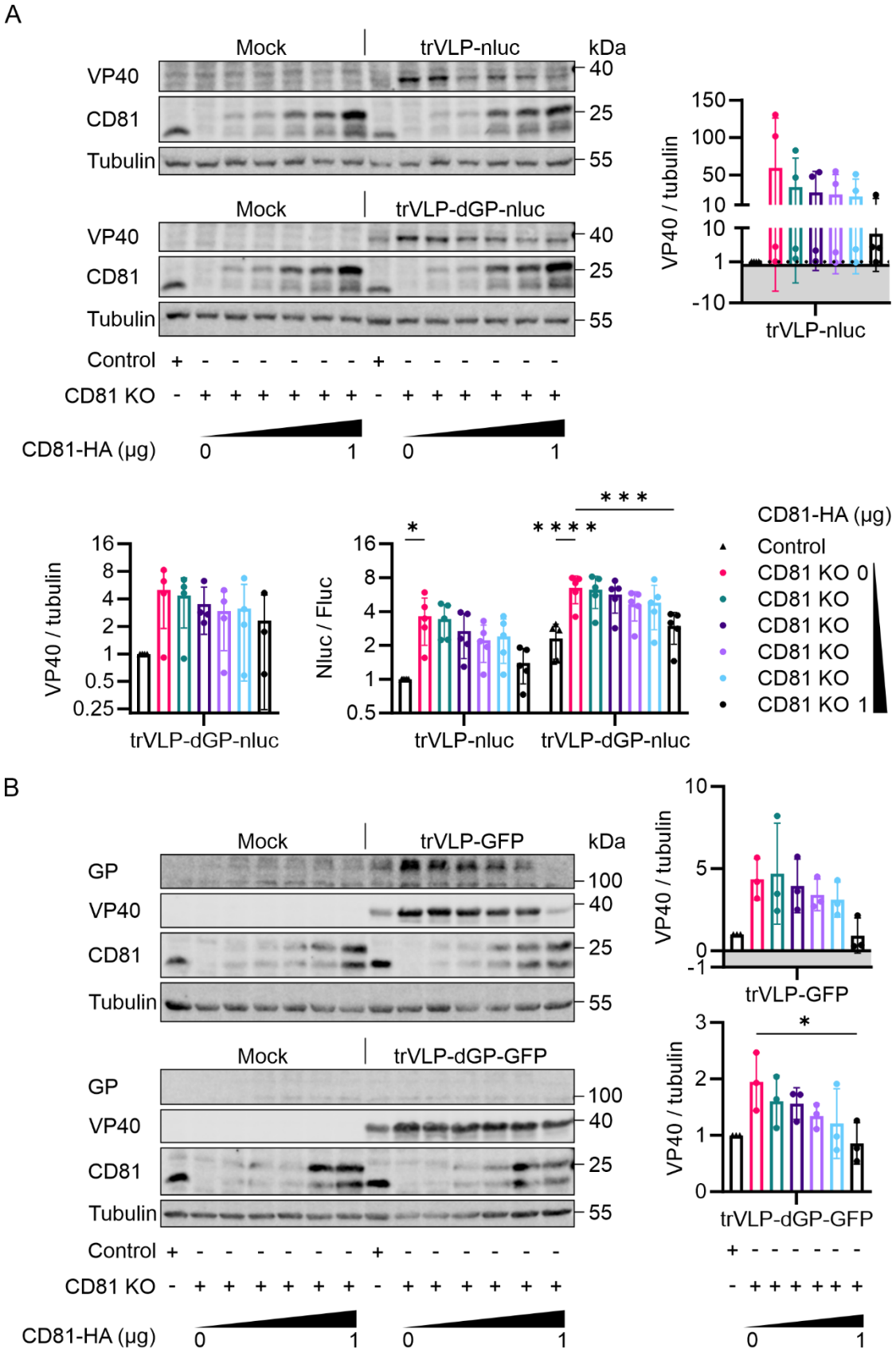
A
Mock
trVLP-nluc
kDa
VP40
CD81
Tubulin
40
25
55
Mock
trVLP-dGP-nluc
VP40
CD81
Tubulin
40
25
55
Control + - - - - - - + - - - - - -
CD81 KO - + + + + + + - + + + + + +
CD81-HA (µg) 0 1 0 1
VP40 / tubulin
150
100
50
10
10
1
-10
trVLP-nluc
VP40 / tubulin
16
8
4
2
1
0.5
0.25
trVLP-dGP-nluc
Nluc / Fluc
16
8
4
2
1
0.5
* * * *
* * *
trVLP-nluc
trVLP-dGP-nluc
CD81-HA (µg)
Control
CD81 KO 0
CD81 KO
CD81 KO
CD81 KO
CD81 KO
CD81 KO 1
B
Mock
trVLP-GFP
kDa
GP
VP40
CD81
Tubulin
100
40
25
55
Mock
trVLP-dGP-GFP
GP
VP40
CD81
Tubulin
100
40
25
55
Control + - - - - - - + - - - - - -
CD81 KO - + + + + + + - + + + + + +
CD81-HA (µg) 0 1 0 1
VP40 / tubulin
10
5
0
-1
trVLP-GFP
VP40 / tubulin
3
2
1
0
*
trVLP-dGP-GFP
+ - - - - - -
- + + + + + +
0 1

Figure 11 CD81 suppresses EBOV minigenome encoded proteins expression. (A) 293T control and CD81 KO cells were mock or pre- transfected with gradient amount of CD81-HA expression plasmids. Together with pWPI, the total transfected plasmids amount was the same. 1 day later, the cells were transfected to produce trVLP-nluc or trVLP-dGP-nluc and a Fluc expression plasmid was cotransfected as a transfection control. 3 days later, an aliquot of the cells was harvested for luciferase assay to analyze nluc and Fluc activities, and the remaining cells were harvested for WB to analyze VP40, CD81 and tubulin expression. n=4-5, shown are mean values of WB signals quantification (normalized to control cells) +/- SD and mean values of nluc activity (normalized to Fluc and further control cells producing trVLP-nluc) +/- SD. (B) 293T cells mock or pre- transfected with gradient amount of CD81-HA expression plasmids were transfected with EBOV RNP expression plasmids and a tetracistronic minigenome plasmid encoding GFP, EBOV VP40, GP and VP24 or a GP deficient minigenome plasmid to produce trVLP-GFP or trVLP-dGP-GFP. 3 d.p.t., the cells were harvested for WB to analyze GP, VP40 and tubulin expression. n=3, shown are mean values of WB signal quantification +/- SD. (A-B) Two/One-way ANOVA with Dunnett correction was used for statistics analysis (GP): 0,1234 (ns), 0,0332 (*), 0,0021 (**), 0,0002 (***), <0,0001 (****).

polymerase II (for initial transcription of the minigenome plasmid to RNA minigenome) driven minigenome plasmid with GFP instead of nluc as reporter was used in the trVLP assay. In agreement with previous results, GP and VP40 expression were higher in CD81 KO cells than control cells and restoring CD81 in CD81 KO cells reduced GP and VP40 expression (Fig. 11B).

In summary, CD81 suppresses EBOV minigenome encoded VP40, GP and nluc expression, indicating that EBOV minigenome replication and/or transcription are negatively regulated by CD81.

3.2.3 The effect of CD81 on EBOV minigenome encoded GFP expression assessed by live cell imaging

To analyze the effect of CD81 on the dynamics of EBOV minigenome encoded protein expression, 293T, Huh7.5 and Hela control and CD81 KO cells were transfected for trVLP-GFP and trVLP-dGP-GFP production and the GFP reporter expression in the cells was monitored by live cell imaging over time. Transfection without viral RNA polymerase L (L-) was included as negative control. An mCherry expression plasmid was cotransfected with the plasmids for trVLP assay. GFP expression was normalized to transfection ctrl mCherry expression (integrated green intensity / integrated mCherry intensity). Similar to increased VP40 expression, deletion of GP from the minigenome drastically increased GFP expression (Fig. 12). GFP expression (normalized to mCherry) of trVLP-dGP-GFP but not trVLP-GFP producer cells was slightly to moderately higher in CD81 KO cells than in control cells (Fig. 12), indicating limited negative effect of CD81

on EBOV minigenome encoded GFP expression and the antagonization of CD81 by GP.

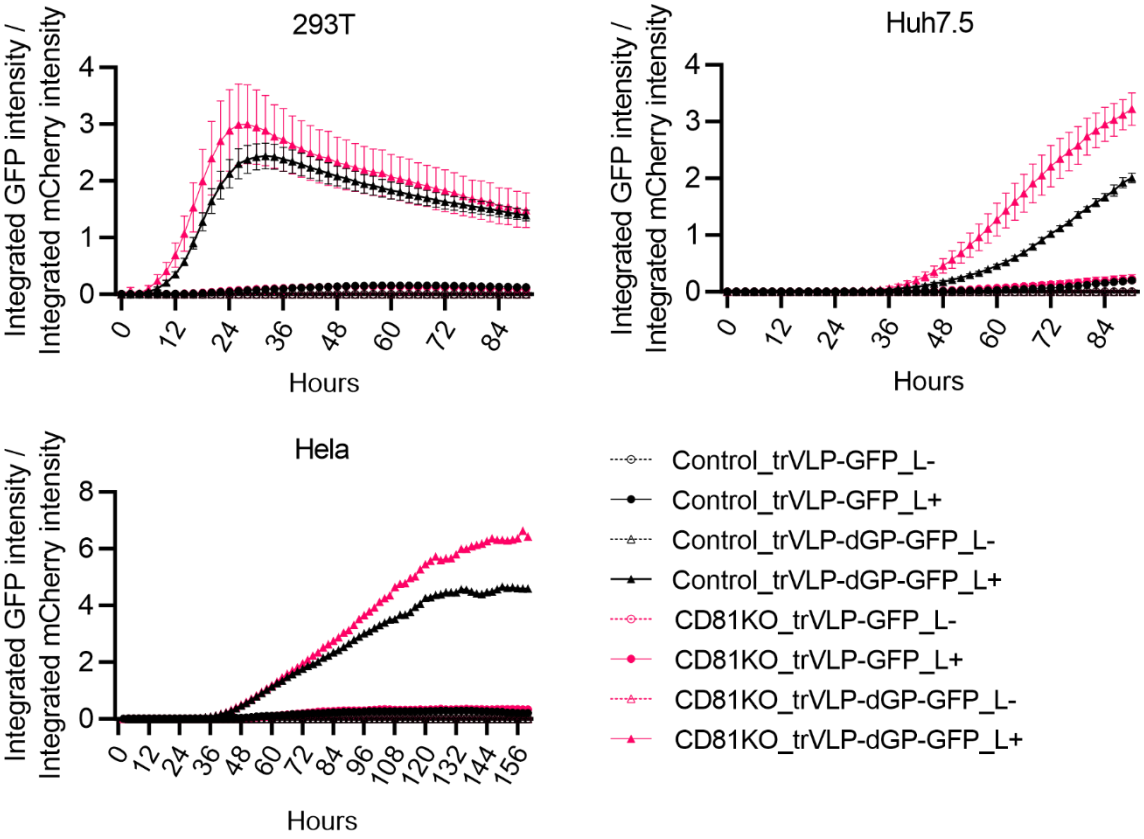

Figure 12 The effect of CD81 on EBOV minigenome replication and transcription-live cell imaging. 293T (n=4), Huh7.5 (n=3) and Hela (n=1) control and CD81KO cells were transfected for EBOV trVLP-GFP and trVLP-dGP-GFP production and mCherry expression plasmid was co-transfected as transfection ctrl. 6 h.p.t., the cells were imaged by Incucyte in green and red channel every two hours. Integrated green intensity (GFP expression) normalized to integrated red intensity (mCherry expression) was plotted, shown are mean values +/- SEM.

3.2.4 CD81 reduces EBOV minigenome RNA levels and negatively regulates NP oligomerization

To further elucidate the negative role of CD81 in EBOV minigenome encoded protein expression, the effect of CD81 on EBOV VP40 mRNA, vRNA (viral genomic RNA) and cRNA (complementary to vRNA) levels was determined by RT-qPCR in trVLP producer cells. VP40 mRNA and cRNA levels in trVLP-nluc and trVLP-dGP-nluc producer cells were higher in CD81 KO cells than control cells and vRNA level was higher in CD81 KO cells in trend as well (Fig. 13A and Sup. Fig. 1A). In the trVLP producer cells, vRNA is the only template for mRNA and cRNA synthesis, while both minigenome plasmid and cRNA are templates

for vRNA synthesis. It suggests a negative role of CD81 in vRNA dependent minigenome replication and transcription. Besides, whether the negative role of CD81 in EBOV minigenome RNA synthesis is dependent on the transcription activator VP30 was analyzed. mRNA and cRNA levels were higher in CD81 KO cells than control cells irrespective of VP30 expression, albeit the difference in trVLP-dGP-GFP producer cells was less evident than in trVLP-dGP-nluc producer cells (n=1-2, Sup. Fig. 1A). The mRNA and cRNA levels were much higher (~10 fold) in trVLP-dGP-GFP producer cells than in trVLP-dGP-nluc producer cells, probably due to the higher vRNA level (n=1-2, Sup. Fig. 1A). Additionally, luc2 (transfection ctrl, Fluc) mRNA level in trVLP producer cells seemed higher in CD81 KO cells than control cells (n=1-3, Sup. Fig. 1A), although the transfection efficiency in control and CD81 KO cells was shown to be similar (Sup. Fig. 5A).

Both EBOV genome replication and transcription occur in EBOV IB, and the formation of IB is dependent on NP oligomerization (105, 106, 112). Additionally, VP35 functions as a chaperone of NP in oligomerization and facilitates IB formation (118–120). VP35 also oligomerize to tetramers associated with EBOV RNA polymerase L (122). Therefore, whether CD81 has an effect on NP oligomerization, VP35 oligomerization and NP-VP35 interaction was analyzed with the Kusabira-green (KG) based BiFC assay by flow cytometry. 293T control and CD81 KO (sorted) cells were transfected to express NP and/or VP35 as fusion proteins with either N- or C- part of KG, and reconstitution of KG indicates protein oligomerization or interaction. KO of CD81 enhanced NP as well as VP35 oligomerization and NP-VP35 interaction (KG+ MFI, Fig. 13B) while had no effect on the percentage of cells showing oligomerization and interaction (KG+%, Sup. Fig. 1B). CD81 KO efficiency in CD81 KO (sorted) cells was analyzed by flow cytometry (Fig. 13C). To study the mechanism how CD81 regulates NP oligomerization, CD81 interaction with NP was assessed, in the absence or presence of VP35. No specific interaction between CD81 and NP was observed, due to the high background of the controls (Sup. Fig. 1C).

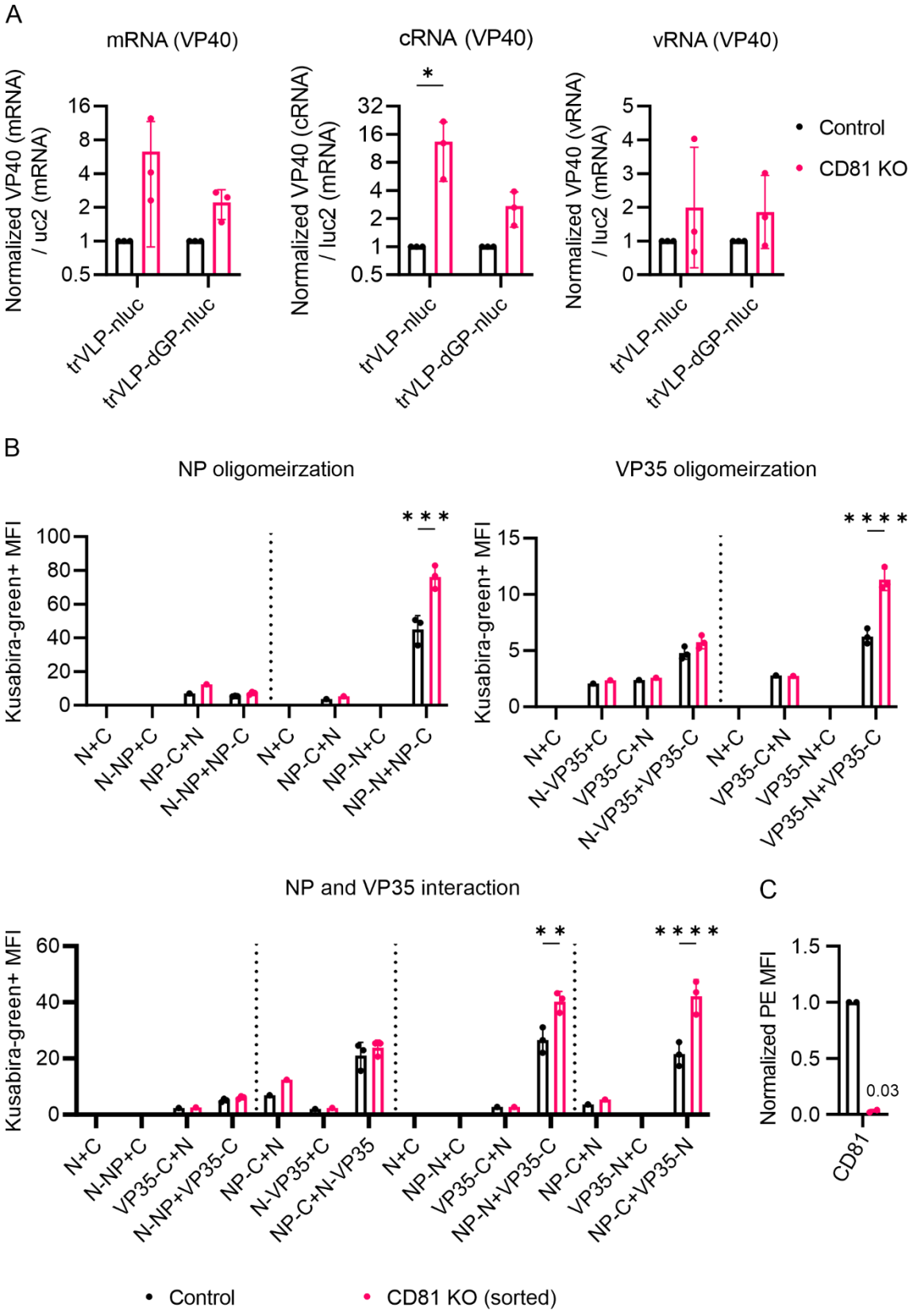

Figure 13 CD81 reduces EBOV minigenome RNA levels and negatively regulates NP oligomerization. (A) 293T control and CD81KO cells were transfected to produce trVLP. 3 d.p.t., the cells were harvested for RNA extraction, the plasmids DNA were removed by DNase.

Oligo(dT), for mRNA, and specific primers, for vRNA and cRNA, were used for reverse transcription. vRNA, cRNA as well as mRNA level of VP40 and luc2 (Fluc) mRNA level were determined by qPCR. n=3, indicated are mean values (normalized to luc2 and further the control cells) +/- SD. (B) 293T control and CD81KO (sorted) cells were co-transfected with two plasmids expressing N- and C- part of KG only or fused with NP/VP35 as indicated for the BiFC assay. 2 d.p.t., cells were harvested for flow cytometry analysis. n=1-3, shown are mean values +/- SD. (A-B) n=3, Two-way ANOVA with Šidák correction was used for statistics analysis (GP): 0,1234 (ns), 0,0332 (*), 0,0021 (**), 0,0002 (***), <0,0001 (****). (C) 293T control and CD81 KO (sorted) cells were surface stained with PE conjugated CD81 antibody for flow cytometry analysis, indicated are mean values of normalized PE MFI (to control cells) +/- SD (n=2).

3.3 CD81 plays a negative role in early steps of EBOV trVLP infection

3.3.1 The role of CD81, CD63 and CD9 in EBOV trVLP infection

To determine whether CD81, CD63 and CD9 play a role in EBOV infection including entry, 293T control, CD81 KO, CD63 KO and CD9 KO cells pretransfected with EBOV RNP and Tim1 (EBOV attachment factor) were infected with trVLP-GFP. The infection rate (GFP+ %) and viral proteins expression in trVLP infected cells were analyzed by flow cytometry and WB, respectively. GP and VP40 expression were higher in CD81 KO cells as compared to CD63 KO, CD9 KO and control cells, and more GP and VP40 were released from CD81 KO cells (Fig. 14, left and below). In agreement with previous results (Fig. 10B), the release step of EBOV trVLP (released VP40/VP40 expressed in cells) was not affected by CD81, CD63 or CD9 (Fig. 14, below). The infection rate was also higher in CD81 KO cells than control cells (Fig. 14, right and representative density plots in Sup. Fig. 2). Taken together, these results indicate that CD81, but not CD63 and CD9, plays a negative role in EBOV trVLP infection in 293T cells. The infection of recombinant authentic EBOV carrying a luciferase or GFP reporter was also analyzed in 293T control and CD81 KO cells (by Lisa Wendt and Thomas Hoenen). The firefly luciferase and GFP reporter expression of the recombinant EBOV was determined via luciferase activity assay and flow cytometry, respectively (n=1-2). It seems that KO of CD81 has no effect on rgEBOV-iluc2 infection while reduced rgEBOV-eGFP infection (Sup. Fig. 3).

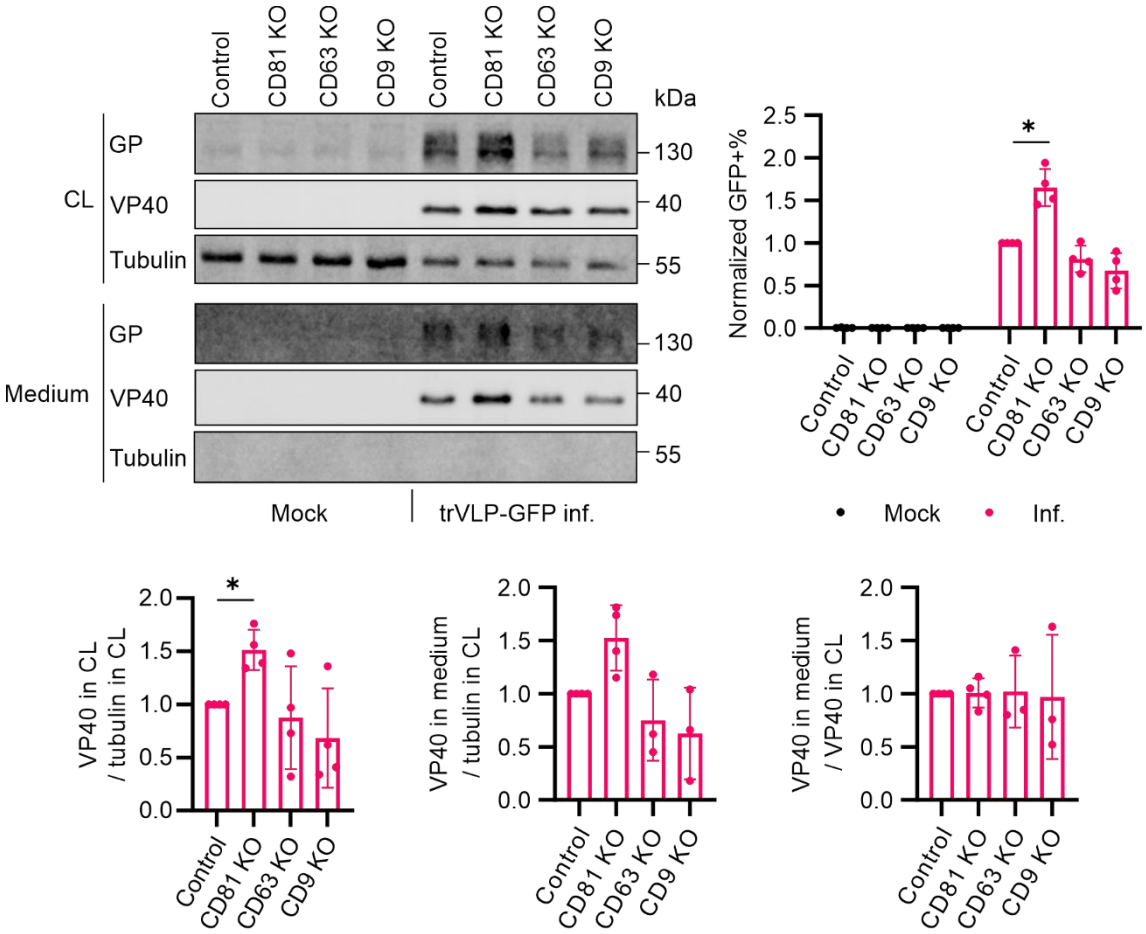

Figure 14 The role of CD81, CD63 and CD9 in EBOV trVLP infection. 293T cells were mock transfected or transfected with Tim1 and EBOV RNP (NP, L, VP35 and VP30). 1 day later, the cells were added with medium only (mock) or trVLP-GFP (inf.). 1 d.p.i., medium was changed to fresh medium. 3 d.p.i., the cells (CL) and medium were harvested for WB (left) and flow cytometry (right). The infection rates in control cells were normalized as 1. Below is quantification of VP40 in CL (left, normalized to tubulin), medium (middle, normalized to tubulin) as well as the release (right) from the infected cells in the WB result, the values were normalized to control cells. n=3-4, shown are mean values +/- SD. RM one-way ANOVA with Dunnett correction was used for statistics analyses (GP): 0,1234 (ns), 0,0332 (*), 0,0021 (**), 0,0002 (***), <0,0001 (****).

3.3.2 CD81 restricts early steps of EBOV trVLP infection

The changes in infection rate and viral proteins expression could result from altered minigenome replication and transcription as well as entry. Therefore, it was analyzed whether CD81, CD63 and CD9 play a role in EBOV GP mediated entry. 293T control, CD81 KO, CD63 KO and CD9 KO cells were infected with GFP expressing lentivirus (lenti-GFP) pseudotyped with EBOV GP or VSV G, and the infection rates were analyzed via flow cytometry. CD81 KO cells, but not CD63 KO and CD9 KO cells, had higher infection rates than control cells in lenti-GFP_EBOV GP, but not lenti-GFP_VSV G, infection (Fig. 15A), suggesting a

negative role of CD81 in EBOV GP mediated entry. As VSV G mediated entry was not affected by CD81, trVLP-dGP-GFP pseudotyped with VSV G infection was analyzed to verify the negative role of CD81 in EBOV minigenome replication and transcription. The minigenome replication and transcription in trVLP infected cells is only mediated by viral RNA polymerase and no T7 or RNA II polymerase is involved. The infection rate of both trVLP-dGP-GFP-_EBOV GP and trVLP-dGP-GFP_VSV G was higher in CD81 KO cells, but not CD63 KO and CD9 KO cells, than in control cells (Fig. 15B). The higher infection rate of trVLP-dGP-GFP_VSV G confirms the negative role of CD81 in EBOV minigenome replication and transcription. The role of CD81 in EBOV entry was further delineated. EBOV is known to be internalized mainly through macropinocytosis (76). Whether CD81 plays a role in macropinocytosis was analyzed by measuring Dextran-555 uptake by 293T control and CD81 KO (sorted) cells. High molecular weight Dextran is a commonly used marker for macropinocytosis (75, 76). Uptake of Dextran-555 was more efficient by 293T CD81 KO cells than control cells (Fig. 15C), implying a role of CD81 in macropinocytosis. Dextran-555 uptake was also analyzed in Huh7.5 cells and human primary macrophages. KO of CD81 in Huh7.5 cells and KD of CD81 in macrophages only slightly increased the uptake of Dextran-555 (Sup. Fig. 4A-4B). Additionally, whether overexpression of CD81 suppresses EBOV trVLP infection was determined. In parallel, whether Tim1, an EBOV attachment factor pretransfected in previous trVLP infection experiments (Fig. 14 and 15B), is required for the suppression of trVLP infection by CD81 was analyzed. 293T cells pretransfected with EBOV RNP, BFP (transfection ctrl), hCD81 or empty vector (Empty), Tim1 (Tim1+, n=3) or empty vector (Tim1-, n=1) were infected with trVLP-dGP-GFP pseudotyped with EBOV GP, and the infection rate was measured via flow cytometry. Overexpression of CD81 reduced the infection rate of trVLP regardless of Tim1 expression (Fig. 15D), which confirms the negative role of CD81 in EBOV trVLP infection. It seems that endogenous CD81 was downregulated by trVLP-dGP-GFP_EBOV GP infection expressing no GP in the absence of pretransfected Tim1 (Fig. 15D, bottom right).

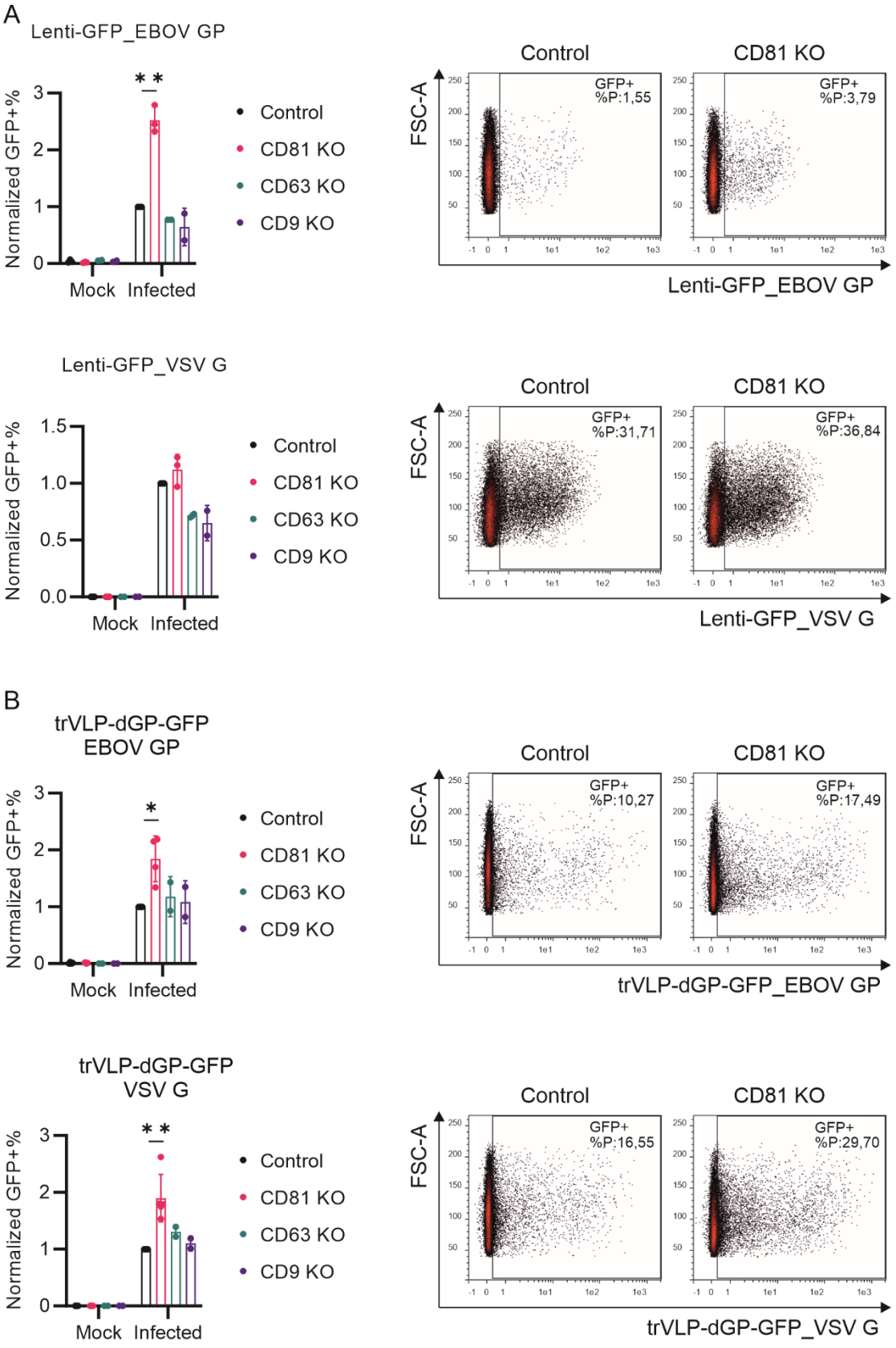
A
Lenti-GFP_EBOV GP
Normalized GFP+%
Mock
Infected
Control
CD81 KO
CD63 KO
CD9 KO
Control
CD81 KO
GFP+ %P:1,55
GFP+ %P:3,79
FSC-A
Lenti-GFP_EBOV GP
Lenti-GFP_VSV G
GFP+ %P:31,71
GFP+ %P:36,84
Lenti-GFP_VSV G
B
trVLP-dGP-GFP EBOV GP
GFP+ %P:10,27
GFP+ %P:17,49
trVLP-dGP-GFP_EBOV GP
trVLP-dGP-GFP VSV G
GFP+ %P:16,55
GFP+ %P:29,70
trVLP-dGP-GFP_VSV G

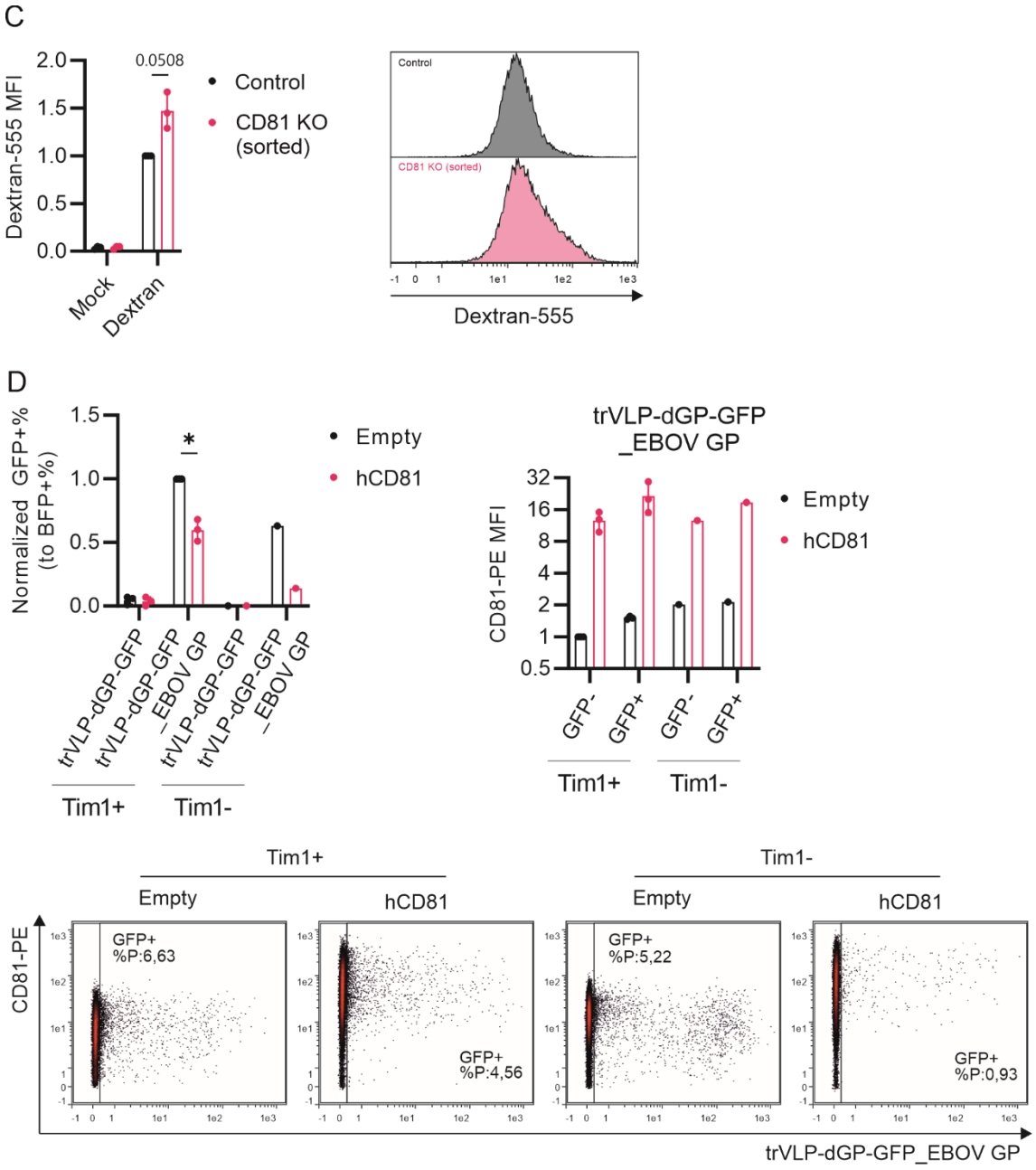

Figure 15 CD81 restricts early step of EBOV trVLP infection. (A) 293T cells were infected with GFP expressing lentiviruses pseudotyped with EBOV GP or VSV G. 3 d.p.i., the cells were harvested for flow cytometry (n=2-3), shown are mean values of normalized infection rate (to control cells) +/- SD and representative density plots with infection rates. (B) 293T cells were mock transfected or transfected with luc2 (transfection ctrl, n=3), Tim1 and EBOV RNP (NP, L, VP35 and VP30). 1 day later, the cells were mock infected or infected with trVLP-dGP-GFP pseudotyped with EBOV GP or VSV G. 3 d.p.i., the cells were harvested for flow cytometry (n=2-4), shown are mean values of normalized infection rate (to control cells) +/- SD and representative density plots with infection rates. (C) 293T cells were mock added or added with Dextran-555 (10K, 0,4 mg/ml). 15 min later, the cells were harvested for flow cytometry (n=3), shown are mean values of normalized MFI of Dextran-555 (to control cells) +/- SD and histogram. (D) 293T cells were transfected with Tim1, EBOV RNP (NP, L, VP35 and VP30), BFP (transfection ctrl) and hCD81 or empty vector (Empty). 1 day later, the cells were added with trVLP-dGP-GFP pseudotyped with no GP or EBOV GP. 2 d.p.i., the cells were harvested and stained with PE

conjugated CD81 antibody for flow cytometry (n=1-3), shown are mean values of normalized infection rate (to BFP+% and further Empty infected with trVLP-dGP-EBOV GP) and PE MFI (to GFP- of Empty) +/- SD and representative density plots with infection rates. n=3-4, Welch's t test was used for statistics analyses (GP): 0,1234 (ns), 0,0332 (*), 0,0021 (**), 0,0002 (***), <0,0001 (****).

3.4 Downregulation of CD81 by EBOV GP and VP40

3.4.1 Mechanism of EBOV GP and VP40 mediated downregulation of CD81

It is possible that EBOV evolves, in addition to GP, other proteins to downregulate CD81. To clarify this, 293T cells were transfected to express GFP only or co-express GFP and EBOV GP, L, NP, VP35, VP30, VP40 and VP24, and surface as well as intracellular CD81 expression were analyzed by flow cytometry. As L is not stable when it is solely expressed (105), L was co-transfected with NP, VP35 and VP30 (components of EBOV RNP). CD81 was downregulated by VP40 as well at both surface and intracellular level, although less efficient compared to GP (Fig. 16A). There was no modulation of CD81 either with L alone or upon co-expression of L, NP, VP35 and VP30.

Moreover, the mechanism of EBOV GP and VP40 mediated downregulation of CD81 was studied. To analyze whether the downregulation of CD81 is due to proteasomal or lysosomal protein degradation, 293T cells were transfected to express GFP only or co-express GFP and GP/VP40 and treated with DMSO, proteasome inhibitor MG132 or V-ATPase inhibitor bafilomycin A1 (BafiA1, lysosome inhibitor). Surface and total CD81 expression was determined via flow cytometry. MG132 and bafilomycin partially blocked GP mediated downregulation of surface and total CD81 (Fig. 16B). Notably, bafilomycin A1 treatment reduced CD81 surface expression in cells with no GP/VP40 expression (Fig. 16B). VP40 mediated downregulation of surface CD81 was partially blocked by MG132 and fully blocked by bafilomycin A1 (Fig. 16B). Both MG132 and bafilomycin partially blocked the downregulation of total CD81 by VP40 (Fig. 16B). Altogether, GP and VP40 mediated downregulation of CD81 is partially due to proteasomal and lysosomal protein degradation.

As both GP and CD81 are membrane proteins and VP40 is a membrane binding protein, whether CD81 interacts with GP and VP40 was analyzed with the Kusabira-green based BiFC assay. 293T cells were transfected to express CD81

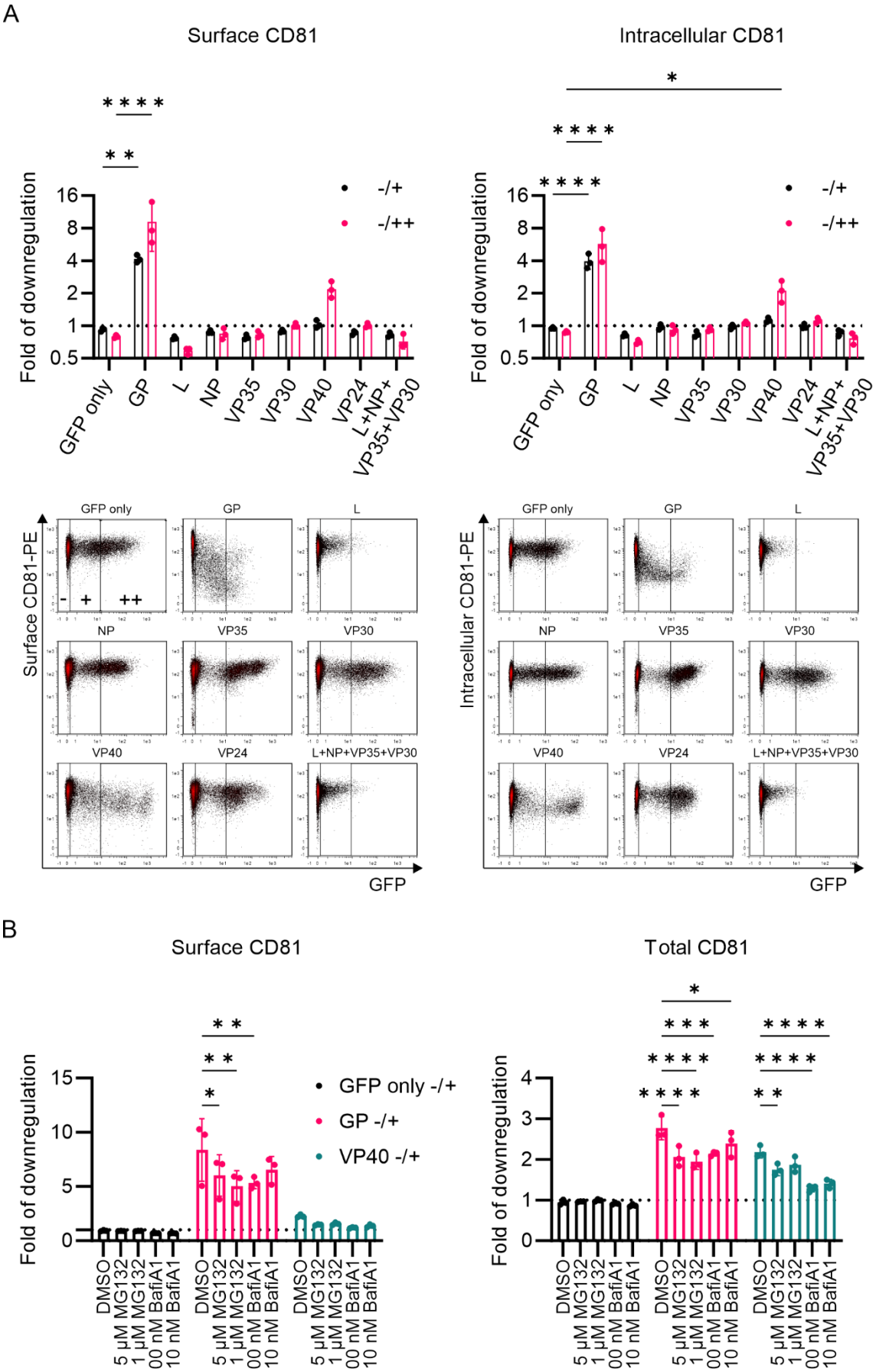
A
Surface CD81
Intracellular CD81
Fold of downregulation
-/+
-/++
GFP only
GP
L
NP
VP35
VP30
VP40
VP24
L+NP+ VP35+VP30
Surface CD81-PE
Intracellular CD81-PE
GFP
B
Surface CD81
Total CD81
GFP only -/+
GP -/+
VP40 -/+
DMSO
5 µM MG132
1 µM MG132
100 nM BafiA1
10 nM BafiA1

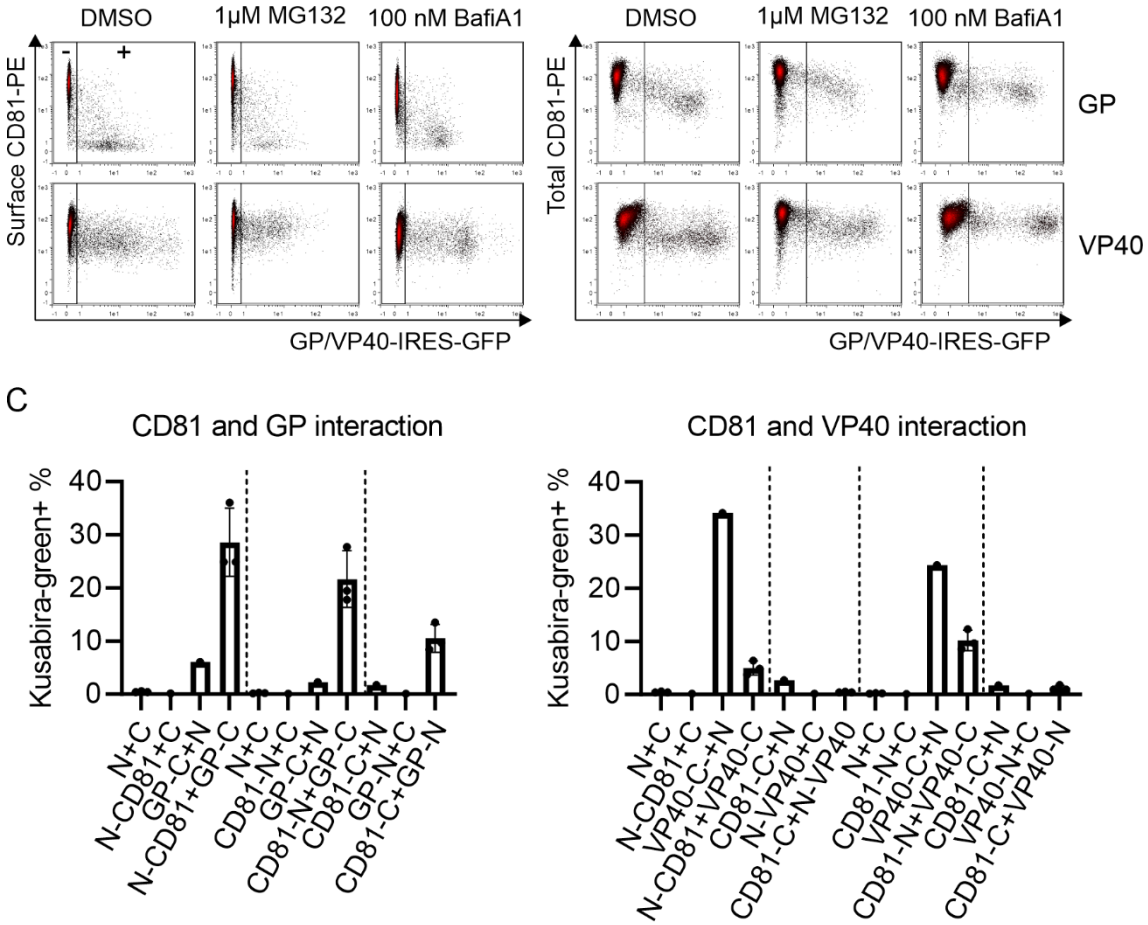

Figure 16 Mechanism of EBOV GP and VP40 mediated downregulation of CD81. (A) 293T cells were transfected to express GFP only or co-express GFP and EBOV proteins. 2 d.p.t., the cells were harvested and stained with PE conjugated CD81 antibodies for flow cytometry to measure the surface and intracellular CD81 expression. n=3, shown are mean values of fold of downregulation, calculated by dividing the PE MFI of GFP- (no GFP expression) cells with the PE MFI of GFP++ (high GFP expression) cells, +/- SD and representative density plots. (B). 293T cells were transfected to express GFP only or co-express GFP and GP/VP40. 6 h.p.t., the cells were treated with DMSO (mock), MG132 or bafilomycin A1. 24 h.p.t., the cells were harvested and stained with PE conjugated CD81 antibodies for flow cytometry to analyze surface and total CD81 expression. n=3, shown are fold of downregulation, calculated by dividing the PE MFI of GFP- (GFP negative) cells with PE MFI of GFP+ (GFP positive) cells, +/- SD and representative density plots. (A-B) Two-way ANOVA with Dunnett correction was used for statistics analysis (GP): 0,1234 (ns), 0,0332 (*), 0,0021 (**), 0,0002 (***), <0,0001 (****). (C) 293T cells were co-transfected with plasmids expressing N- and C- part of KG only or fused with CD81 (cytoplasmic tail)/GP (cytoplasmic tail)/VP40 as indicated for the BiFC assay. n=1-3, shown are KG+% (percentage of KG expressing cells) or mean values of KG+% +/- SD.

and GP/VP40 fused with N/C part of KG, and the percentage of cells with reconstructed KG expression (a result of protein-protein interaction) was measured via flow cytometry. Co-expression of CD81 and GP drastically increased the percentage of KG expressing cells (KG+) (Fig. 16C), suggesting

CD81 interacts with GP. It is less clear whether CD81 interacts with VP40, due to the high background of the controls (Fig. 16C).

3.4.2 Downregulation of CD81 is dispensable for the downregulation of CD63 and CD9

The KO cells-based experiments showed that only CD81, but not CD63 and CD9, had negative effect on trVLP production and infection. As tetraspanins heterooligomerize (223, 308), it was studied whether downregulation of CD63 and CD9 is a byproduct of CD81 downregulation. As CD81 was additionally downregulated by EBOV VP40, whether CD63 and CD9 are downregulated by EBOV VP40 was also analyzed. 293T control and CD81 KO (sorted) cells as well as Huh7.5 control and CD81KO cells were mock transfected or transfected to express GFP only or co-express GFP and EBOV GP/VP40, and surface CD81, CD63 and CD9 expression were analyzed by flow cytometry. CD81 was downregulated by both GP and VP40 in 293T control cells (Fig. 17A). CD63 and CD9 were downregulated by GP similarly in control and CD81 KO (sorted) cells, and CD9 was additionally downregulated by VP40 irrespective of CD81 expression in 293T cells (Fig. 17A). Apart from that, CD63 and CD9 expression was not affected by KO of CD81 in 293T cells (Fig. 17A). In Huh7.5 (control) cells, CD81 was downregulated only by GP but not VP40 (Fig. 17B). In line with 293T cells, CD63 and CD9 were downregulated by GP irrespective of CD81 expression in Huh7.5 cells (Fig. 17B). CD63 expression was not notably affected by KO of CD81 in Huh7.5 cells, while CD9 expression in Huh7.5 cells was higher in CD81 KO. Whether CD81 has an effect on transfection was also analyzed. Transfection efficiency was similar in control and CD81 KO cells in both 293T and Huh7.5 cells, while GFP expression (MFI) by the transfected plasmids was slightly higher in CD81 KO cells than control cells in Huh7.5 cells (Sup. Fig. 5A-5B).

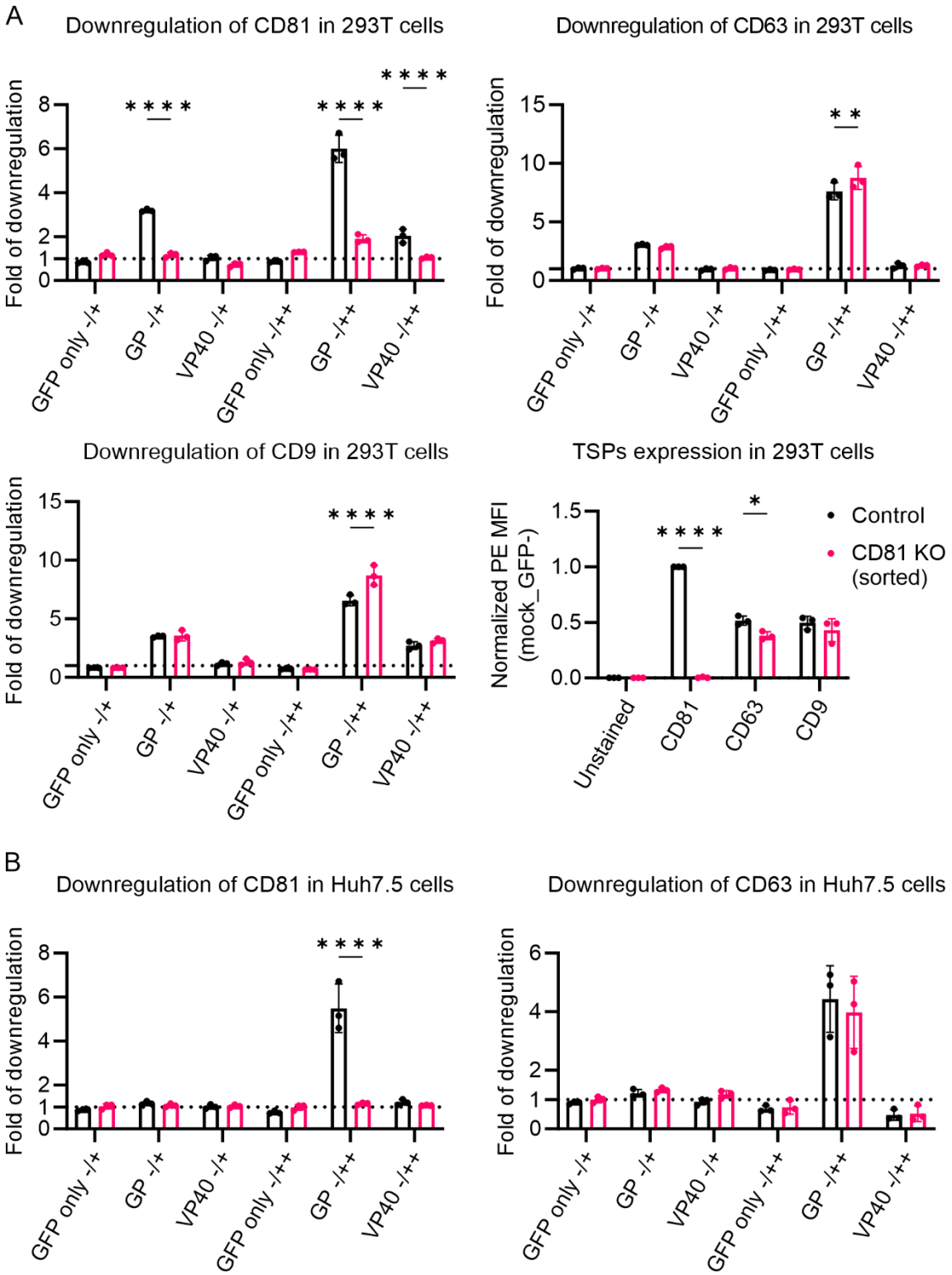
A
Downregulation of CD81 in 293T cells
Fold of downregulation
GFP only -/+
GP -/+
VP40 -/+
GFP only -/++
GP -/++
VP40 -/++
Downregulation of CD63 in 293T cells
Downregulation of CD9 in 293T cells
TSPs expression in 293T cells
Normalized PE MFI (mock_GFP-)
Control
CD81 KO (sorted)
Unstained
CD81
CD63
CD9
B
Downregulation of CD81 in Huh7.5 cells
Downregulation of CD63 in Huh7.5 cells

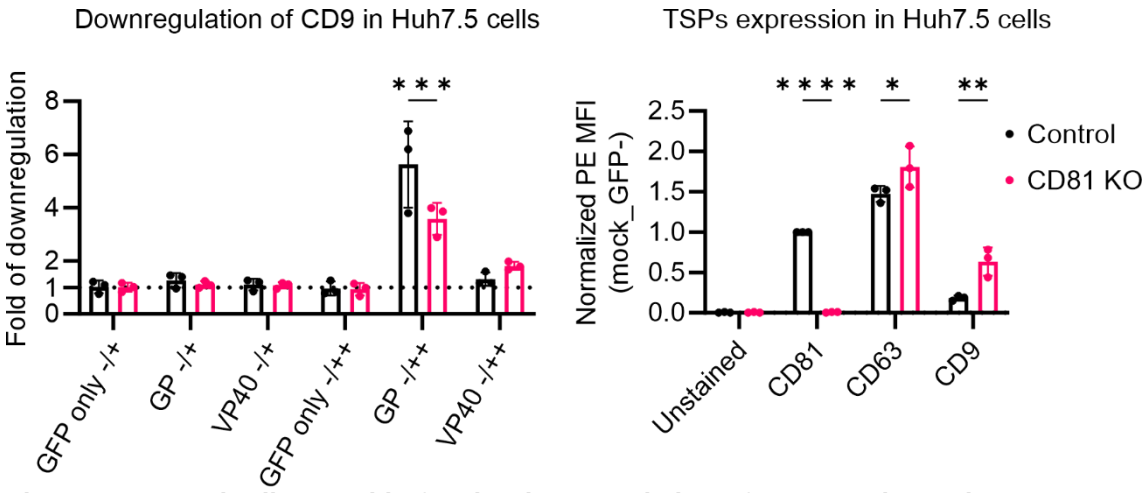

Figure 17 CD81 is dispensable for the downregulation of CD63 and CD9 by EBOV GP. (A)293T and (B) Huh7.5 cells were mock transfected or transfected to express GFP only or co-express GFP and GP/VP40. 2 d.p.t., the cells were harvested and stained with PE conjugated antibodies against CD81, CD63 and CD9 to analyze the surface expression of the receptors by flow cytometry (n=3). Shown are mean values +/- SD, fold of downregulation was calculated by dividing the PE MFI of GFP- (no GFP expression) cells to PE MFI of GFP+ (intermediate GFP expression) or GFP++ (high GFP expression) cells and PE MFI showing the TSPs expression was normalized to CD81-PE MFI of control cells. Two-way ANOVA with Šidák correction was used for statistics analysis (GP): 0,1234 (ns), 0,0332 (*), 0,0021 (**), 0,0002 (***), <0,0001 (****).

3.5 CD81 antibody suppresses EBOV trVLP infection

As CD81 was shown to suppress EBOV trVLP infection, it was hypothesized that ligation of CD81 with a CD81 antibody might inhibit EBOV trVLP infection. The CD81 antibody used in this experiment is 5A6, which initially identified CD81 and showed antiproliferative effect on lymphoma cell line (224). 5A6 binds to the large extracellular loop of CD81 and induces conformational changes as well as clustering of CD81 at the cell surface (255, 309). 293T control and CD81 KO cells treated with no antibody (Ab), CD81 antibody or isotype antibody were infected with trVLP-dGP-GFP pseudotyped with EBOV GP or VSV G, and the infection rate was determined by flow cytometry. CD81 antibody, but not the isotype antibody, significantly suppressed EBOV GP or VSV G pseudotyped EBOV trVLP infection of control cells but not CD81 KO cells (Fig. 18A-18B). Altogether, not only CD81 but also CD81 antibody suppresses EBOV trVLP infection.

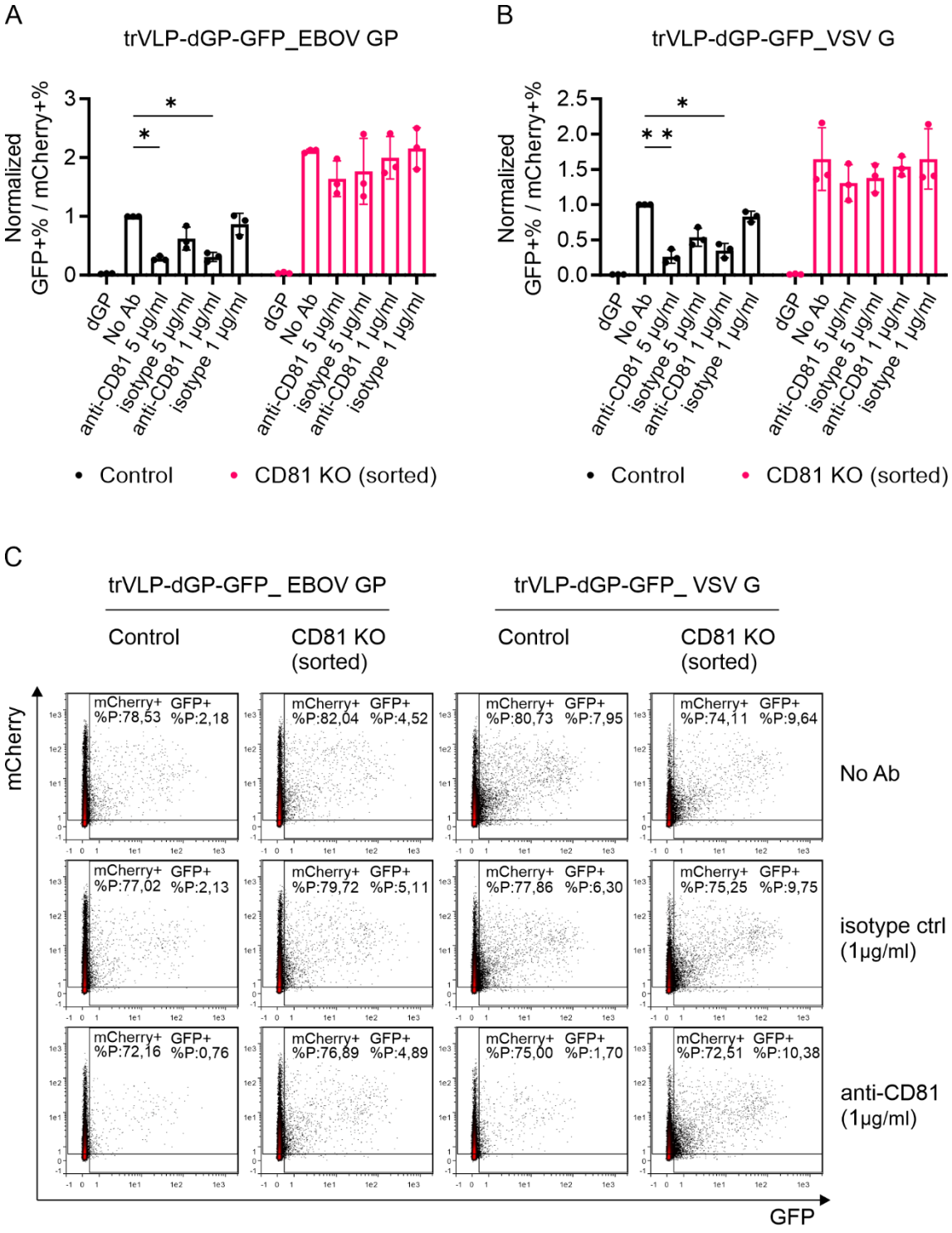

Figure 18 CD81 antibody suppresses EBOV trVLP infection. 293T cells were transfected with Tim1, mCherry (transfection ctrl) and EBOV RNP (NP, L, VP35 and VP30). 1 day later, the cells were treated with no antibody (Ab), CD81 antibody (5A6) or the isotype ctrl antibody.1 hour later, the cells were added with trVLP-dGP-GFP (dGP, no Ab) or trVLP-dGP-GFP pseudotyped with EBOV GP (A) or VSV-G (B). 2 d.p.i., the cells were harvested for flow cytometry (n=3), shown are mean values of normalized infection rate (to mCherry+% and further control cells with No Ab treatment) +/- SD and density plots with transfections rates and infection rates. Two-way ANOVA with Dunnett correction was used for statistics analyses (GP): 0,1234 (ns), 0,0332 (*), 0,0021 (**), 0,0002 (***), <0,0001 (****).

4. Discussion

4.1 EBOV GP mediated downregulation of surface receptors

Amongst the 20 receptors identified to be modulated by EBOV GP in Hela cells via a flow cytometry-based screen (by Julia Nehls), seven receptors, CD184, CD201, CD59, HLA, CD81, CD63 and CD9, were confirmed being downregulated more than 1.5-fold by EBOV GP in both Hela and 293T cells, although there was only a trend to downregulate CD201 and CD81 in Hela cells (Fig. 7A-7G). EBOV GP is known to sterically shield HLA on the cell surface and thereby to render it less accessible (187). However, the modulation of the other six receptors is reported for the first time. CD59, a complement lysis restriction factor, is incorporated into the membrane attack complex during complement activation (310). Moreover, CD59 was found to be incorporated into HIV-1, HCMV, HTLV-1, extracellular enveloped vaccinia virus, HCV and IBV particles and protect HIV-1, extracellular enveloped vaccinia virus, IBV and HCV from complement destruction (311–316). It's unknown whether CD59 is incorporated into EBOV particles yet. On the other hand, CD59 is known to be downregulated by HBV infection, which sensitizes hepatocytes to complement dependent cytotoxicity (317). The downregulation of CD59 by EBOV GP could be potentially related with EBOV pathogenicity. CD201, known as endothelial cell protein C receptor, augments protein C activation that negatively regulates blood coagulation (318). Decrease of activated protein C level was observed in EBOV infected primates, which is correlated with abnormal coagulation (319). It would be interesting to study whether EBOV GP mediated downregulation of CD201 decreases protein C activation. CD184 (CXCR4) is, the receptor for chemokine CXCL12, migration inhibitory factor, extracellular ubiquitin, human beta defensin-3 and HIV-1, engaged in cell migration and multiple other cellular processes (reviewed in (320), (321–325)). Multiple CXCR4 signaling pathways might be modulated by GP in EBOV infected cells. As outlined in the introduction, CD81, CD63 and CD9, the members of the tetraspanin superfamily, are known to be involved in various cellular processes, including cell fusion, adhesion, migration and proliferation, and also the life cycle of several viruses. The downregulation of three members of the tetraspanin superfamily features their potential role in the EBOV life cycle.

As mentioned, CD81, CD63 and CD9 were downregulated by authentic EBOV infection as well (Fig. 7H).

Not only EBOV (1976, Mayinga) but also other members of Ebolavirus genus tested, SUDV, RESTV and TAFV, and MARV GP downregulate surface CD81, CD63 and CD9 (Fig. 8), suggesting a conserved function among the filoviral GPs. The GP of HIV-1 (Env) and LASV, with relative low expression level, did not modulate the tetraspanins, while CD81 is known to be downregulated by HIV-1 Vpu (271). Both subunits of EBOV GP, GP1 and GP2, were required for the downregulation of the tetraspanins, and more specifically residues located with the RBD, FP and TMD (ZLZ) seemed involved in the downregulation (Fig. 9). The involvement of same residues of GP implies common mechanism is employed by GP to downregulate the tetraspanins. Neither GP1 (33-501 aa) nor GP2 (502-676 aa) alone were able to significantly downregulate the tetraspanins (Fig. 9A-9B). However, increased shedding efficacy (326) of EBOV GP did not significantly affect the downregulation of the tetraspanins (Fig. 9C), suggesting remaining uncleaved GP was sufficient to mediate the downregulation. Additionally, GP of EBOV that circulated during the 2014 outbreak in West Africa, differed in 20 amino acids from the GP of EBOV circulated in 1976 (307), preserved the capacity to downregulate the tetraspanins (Fig. 9C).

4.2 CD81 and the life cycle of EBOV trVLP

Whether TSP modulation by EBOV GP plays a role in the EBOV life cycle was studied with the EBOV trVLP assay. The trVLP assay allows to study the different steps of the EBOV life cycle under BSL 1/2 conditions, including entry, genome replication and transcription as well as release, with expression of all EBOV proteins (111).

4.2.1 CD81 and EBOV minigenome replication and transcription

Firstly, EBOV trVLP production was analyzed in control (no sgRNA), CD81 KO, CD63 KO and CD9 KO cells. KO of CD81 enhanced EBOV minigenome encoded VP40 expression and more VP40 were released from the CD81KO cells (Fig. 10B and 10D). VP40 is released into exosomes as well, which have smaller size than EBOV VLPs (216, 217). In the trVLP assay, 20,000 g was used to pellet the

trVLPs through 20% sucrose from the medium, which is lower than the centrifugation speed commonly used to pellet exosomes, 100,000 g (327). Moreover, it was shown that exosomes containing MHC II molecules were barely pelleted by centrifugation at 10,000 g (328). Thus, the VP40 detected in medium is supposed to originate mainly from trVLPs. Higher VP40 expression in trVLP-dGP-nluc producer cells was observed as compared to trVLP-nluc producer cells (Fig. 10B and 10D). This could be related with the inverse correlation between minigenome length and encoded protein expression (111). Regardless, altogether, the cumulated results show that CD81 plays a negative role in minigenome encoded VP40 expression and trVLP production.

The suppressive role of CD81 in the minigenome encoded VP40 expression was further confirmed by restoration of CD81 expression in CD81 KO cells. In addition to T7 RNA polymerase driven minigenome plasmid (with nluc reporter), an RNA polymerase II driven minigenome plasmid (with GFP reporter) was used to exclude possible effects of CD81 on initial transcription of the minigenome plasmids. Not only VP40 expression but also GP and nluc reporter expression, encoded by the minigenome, were suppressed by CD81 expression (Fig. 11). GP was detected in trVLP-GFP but not trVLP-nluc (data not shown) producer cells, which could be related to more efficient transcription in the RNA polymerase II system (329). On the other hand, KO of CD81 had no or only minor effect on GFP expression (Fig. 12) in trVLP-GFP and trVLP-dGP-GFP producer cells could be due to counteraction of CD81 by GP and higher expression of GFP than VP40, as the EBOV genome is gradiently transcribed from 3’ to 5’ (115).

Next, whether EBOV minigenome RNA level is affected by CD81 was determined, and a negative role of CD81 in vRNA dependent minigenome replication and transcription is suggested (Fig. 13A). The transcription activator VP30 was shown to be dispensable for the negative effect of CD81 on VP40 mRNA and cRNA level (Sup. Fig. 1A). However, a negative role of CD81 in minigenome transcription cannot be excluded, as both replication and transcription occur in the inclusion bodies and requires common viral proteins NP, L and VP35 (103, 105, 106). In the trVLP assay, higher transcription level

does not necessarily lead to higher minigenome replication, as EBOV RNP, responsible for minigenome replication and transcription, are expressed by co-transfected plasmids but not the minigenome. On the other hand, increased minigenome replication can result in higher mRNA level. Increased RNA level could also result from impaired RNA decay/degradation. However, it has been shown that EBOV RNP (NP, L and VP35) encapsidated minigenome RNA is nuclease resistant (103), which makes RNA decay unfavorable.

Furthermore, KO of CD81 enhanced NP homo-oligomerization, NP-VP35 interaction and VP35 homo-oligomerization (Fig. 13B). NP oligomerization was shown to play a key role in EBOV inclusion bodies formation, and VP35 is a chaperone for NP oligomerization and forms tetramer as cofactor of EBOV polymerase L (112, 118, 120, 122). Robust NP homo-oligomerization could be observed when C/N of KG is fused at the C, but not N, terminus of NP (Fig. 13B, left), which could indicate that the N terminus of NP is essential for oligomerization (118, 120). Regarding VP35 homo-oligomerization and NP-VP35 interaction, the enhancement effect could be observed when N/C part is fused to the C, but not N, terminus of VP35 (Fig. 13B, right and bottom). This could be explained by the fact that the NP-chaperoning domain (20-48 aa) and homo-oligomerization domain (82-145 aa) of VP35 (1-340) are located closely to the N terminus (120, 330).

CD81 is a four-transmembrane protein. Therefore, how CD81 may modulate the formation of EBOV inclusion bodies, known to be membraneless liquid organelle (112), sounds counterintuitive. Colocalization between membrane structure and membraneless organelle has been demonstrated. Lee at al showed that membraneless organelle P bodies can localize with ER tubes, which appears to regulate P bodies fission (331). Moreover, Dolnik et al. demonstrated that Lamp1 and LC3, respectively a membrane protein of late endosomes/lysosomes and a marker of autophagosomal membranes, are localized to MARV NP inclusion bodies (332). So far no membrane proteins has been identified in EBOV inclusion bodies, but EBOV inclusion bodies (viral factories) were observed to be in close proximity to several membrane organelles, including ER, vesicles, mitochondria

and nucleus (333). Therefore, CD81 may regulate EBOV inclusion bodies formation through direct interaction with the components/regulators of the inclusion bodies. On the other hand, CD81 involved signaling might be engaged in EBOV genome replication and transcription. As discussed in the introduction, CD81 is associated with several integrins. Integrin signaling pathways are associated with multiple cellular responses including cell survival, which favors virus replication at the early phase (334, 335).

4.2.2 CD81 and EBOV trVLP entry

CD81 also suppresses EBOV GP mediated entry (Fig. 15A). This could be related to that CD81 interacts with integrin αV and β1, and αVβ1 that were shown to be required for EBOV-GP, but not VSV G, mediated entry by regulating cathepsins (238, 336). Although CD63 and CD9 had no effect on EBOV trVLP infection, their possible role in trVLP infectivity cannot be ruled out. Especially CD9 is known to inhibit the shedding activity of ADAM17/TACE, which can remove the ectodomain of EBOV GP (180, 289). However, it would be hard to study their role, including CD81, in EBOV infectivity, as the tetraspanins are downregulated by EBOV GP (Fig. 7). CD63 is a receptor of the tissue inhibitor of metalloproteinase-1 (TIMP-1), which was shown to promote inflammation in influenza infection (277, 337). So far, involvement of TIMP-1 in EBOV infection has not been reported. Role of CD63 in EBOV in vivo infection cannot be excluded. CD9 and CD81 were shown to have essentially similar structures (220, 221). The two tetraspanins share around 60% sequence similarity, mainly in the transmembrane domain, and the extracellular loops as well as short C terminal cytoplasmic tails differ from each other (221). Therefore, it is likely and interesting to study in the future, if the differed extracellular loops and C terminal cytoplasmic tail of CD81 confers its negative role in EBOV trVLP infection.

Moreover, CD81 seems play a role in macropinocytosis, the major internalization pathway of EBOV (Fig. 15C). CD81, but not CD9, is known to interact with Rac1 via its C terminal cytoplasmic domain and regulate Rac1 activation, which plays an essential role in macropinocytosis (232, 338). It is not clear how EBOV induces macropinocytosis. Moller-Trank and Maury discussed and suggested that

macropinocytosis occurs through PtdSer/PtdSer receptor and/or glycan(GP)/lectin interaction (62). They have listed the following evidences. Firstly, PtdSer/PtdSer receptor interaction mediates internalization of EBOV VLP (VP40-GFP) without GP (339, 340). Secondly, VSV, known to be internalized via clathrin mediated endocytosis, pseudotyped with EBOV GP is internalized through macropinocytosis (74). Their assumption is supported by other studies. Stewart et al. demonstrated that bald EBOV VLPs comprised of NP and VP40 can activate Akt, an event occurs during macropinocytosis (87, 341). Saeed el al. showed that EBOV GP pseudotyped EBOV VLP is internalized through macropinocytosis, while VSV G pseudotyped EBOV VLP is internalized via clathrin mediated endocytosis (75). On the other hand, Bhattacharyya et al. showed that EBOV GP pseudotyped HIV uses clathrin mediated endocytosis as entry pathway while macropinocytosis was not studied (342). Aleksandrowicz et al. indicated that EBOV takes macropinocytosis as a major route and clathrin mediated endocytosis as an alternative route for entry (76). More recently, tyrosine kinase receptors were shown to be required for EBOV or EBOV VLP induced Akt activation (86, 87). Considering CD81 is associated with multiple membrane proteins, it would be interesting to study whether CD81 interacts with EBOV attachment factors and tyrosine kinase receptors. Furthermore, the negative role of CD81 in EBOV trVLP infection shown by the KO cells-based experiments (Fig. 14 and 15B) was confirmed in 293T cells overexpressing CD81 (Fig. 15D). Tim1, the pretransfected PtdSer receptor, was not required for CD81 mediated suppression of EBOV trVLP infection (Fig. 15D), indicating other EBOV attachment factors expressed by 293T cells might be involved.

On top of that, the role of CD81 in authentic EBOV infection remains unclear (Sup. Fig. 3). Notably, CD81 was downregulated by both GP and VP40 in 293T cells, which likely compromised the effect of CD81 in authentic EBOV infection.

4.3 EBOV GP and VP40 mediated downregulation of CD81

Both proteasome and lysosome protein degradation contribute to EBOV GP and VP40 mediated downregulation of CD81 (Fig. 16). It is known that the CD81 N terminus contains ubiquitination sites (K8 and K11) promoting CD81 proteasomal

degradation and internalization of surface CD81 for lysosome degradation (343, 344). The ubiquitination sites also exist in the N terminus of other tetraspanins, including CD63 and CD9 (343). Moreover, the BiFC assay showed that CD81 interacts with GP (Fig. 16C). CD81 was shown to be degraded by ubiquitin ligase MARCH8, which is an interaction partner of EBOV GP and impairs GP maturation (345, 346). It is reasonable to assume that GP targets CD81 for degradation through its interaction with MARCH8, whereas MARCH8 expression was not detected in 293T cells by WB (346). Nevertheless, MARCH8 is highly expressed in macrophages and dendritic cells, the primary target cells of EBOV (346, 347). Similar to EBOV GP, HIV-1 Vpu is known to interact with and downregulate CD81 through proteasomal and lysosomal degradation (271). Other mechanism may contribute to the downregulation of CD81. It was shown that GP forms microvesicles and results in more CD81 released from cells (182). Moreover, GP is known to sterically shield MHC I and β1 integrin via its glycan (187). Whether glycan shield contributes to the observed CD81 downregulation needs to be addressed. It's not clear whether VP40 interacts with CD81 (Fig. 16C). VP40 is known to be a membrane binding protein and interact with several ubiquitin ligase for budding (153, 165–168). It might be interesting to study whether membrane binding is required for VP40 to downregulate CD81. Considering the downregulation of CD81 by both GP and VP40, the effect of CD81 mutant, lacking the ubiquitination sites, on EBOV infection should be studied.

4.4 CD81 antibody and EBOV trVLP infection

EBOV GP or VSV G pseudotyped trVLP infection was suppressed by the CD81 antibody 5A6 (Fig. 18). The epitope of 5A6 is located within the large extracellular loop of CD81, and the binding of 5A6 leads to conformation change and clustering of CD81 (255, 309). The clustering of CD81 might resemble CD81 overexpression. 5A6 has been implicated in modulation of virus infection and restriction of cancer cells. HCV E2 is known to interact with CD81 large extracellular loop for entry, which was shown to be inhibited by 5A6 (262, 348). In contrast, 5A6 was shown to improve HIV-1 transmission from T cells to macrophages via cell to cell fusion (266). CD81 was demonstrated to negatively regulate the heterotypic cell fusion through the RhoA/actomyosin pathway (266).

5A6 was shown to kill B lymphoma cells via direct killing, antibody-dependent cell cytotoxicity, complement-dependent cytotoxicity and antibody-dependent cell phagocytosis while spare the normal lymphocytes (349). Additionally, 5A6 was indicated to inhibit human breast cancer cell invasion and migration, and this inhibition involves JAM-A (309). Further study indicates that the CD81 interaction partners transferrin receptor1, integrin α6, α5, and β5 are engaged in the antimetastatic effect of 5A6 (308). It is attempting to hypothesize that 5A6 may modulate CD81 and its interaction partners to restrict EBOV trVLP infection. Of note, EBOV GP and VSV G pseudotyped VLPs (EBOV) are internalized through different pathways, macropinocytosis and clathrin mediated endocytosis, respectively (75). Thus, 5A6 may target CD81 to suppress EBOV minigenome replication and transcription. Nonetheless, the possible suppression of macropinocytosis by 5A6 cannot be excluded. As Rac1, a key regulator of macropinocytosis, is known to interact with CD81 cytoplasmic tail and its activity is regulated by CD81 (232, 338). The antiviral effect of 5A6 should be further studied with authentic EBOV infection and its primary target cells, macrophages and dendritic cells. Additionally, CD81 was identified as host factor for influenza virus, HSV-1 and CHIKV (264, 272, 273). It might be interesting to determine the antiviral effect of 5A6 on infection of these viruses.

4.5 Conclusion

Among other receptors, tetraspanin CD81, CD63 and CD9 are downregulated by EBOV GP and authentic EBOV infection. The downregulation of the tetraspanins by GP is conserved within filovirus family and both subunits of GP are engaged. CD81, but not CD63 and CD9, suppresses EBOV minigenome replication and transcription as well as NP oligomerization, a determinant of EBOV replication complex inclusion body formation. Moreover, CD81 plays a negative role in early steps of EBOV entry including EBOV GP mediated entry and likely macropinocytosis. Remarkably, a CD81 antibody, 5A6, can suppress EBOV trVLP infection. The CD81 downregulation mechanism was also studied. CD81 is downregulated by not only GP but also VP40, which is partially due to proteasomal and lysosomal protein degradation. In addition, EBOV GP can interact with CD81, which might be the mechanism that CD81 is targeted by GP

for downregulation/degradation. Taken together, tetraspanin CD81, downregulated by EBOV, is a restriction factor of EBOV and might serve as a druggable target for EBOV infection treatment.

5. Summary

EBOV, a highly pathogenic filovirus, causes Ebola virus disease to humans with high case fatalities. A broad range of cell types are susceptible for EBOV infection. EBOV entry into host cells is mediated by the viral surface glycoprotein GP, which is also known to play roles in immune evasion by modulating cell surface receptors.

Following a flow cytometry-based screen to comprehensively identify EBOV GP modulated surface receptors, this thesis confirmed the downregulations of three tetraspanins, CD81, CD63 and CD9. The downregulations could also be observed in authentic EBOV infection. Moreover, GP of other filoviruses, SUDV, RESTV, TAFV and MARV, can downregulate these tetraspanins as well. The tetraspanins are known to interact with other host proteins and form the tetraspanin enriched microdomains involved in multiple signaling pathways and cellular processes. The functional relevance of the tetraspanins in the EBOV life cycle was characterized by using the EBOV trVLP assay and tetraspanin KO cells. KO of CD81, but not CD63 and CD9, enhanced EBOV minigenome replication and transcription as well as NP oligomerization, which plays an essential role in the formation of EBOV inclusion body, the EBOV replication complex. Conversely, restoration of CD81 expression in CD81 KO cells suppressed EBOV minigenome encoded proteins expression. Moreover, KO of CD81 increased EBOV GP mediated entry and seems to enhance macropinocytosis, the major internalization pathway of EBOV. CD81 was shown to be downregulated by both GP and VP40 of EBOV, which involves lysosomal and proteasomal protein degradation. Notably, a CD81 antibody, 5A6, showed inhibitory effects on EBOV trVLP infection.

In summary, EBOV downregulates tetraspanin CD81, as a novel immune evasion mechanism, to create a replication friendly environment. With further investigations of authentic EBOV infection of its primary target cells, CD81 antibody 5A6 might be used as an antiviral treatment.

6. Zusammenfassung

Das Ebolavirus (EBOV) ist ein hoch pathogenes Filovirus, das beim Menschen eine komplexe Symptomatik mit hämorrhagischen Fiebern verursacht und eine hohe Sterblichkeitsrate hat. Ein breites Spektrum von Zelltypen ist für eine EBOV-Infektion empfänglich. Das Eindringen von EBOV in Wirtszellen wird durch das virale Oberflächenglykoprotein GP vermittelt, von dem auch bekannt ist, dass es durch die Modulation von Zelloberflächenrezeptoren eine Rolle bei der viralen Immunevasion spielt.

Nach einem Screening zur umfassenden Identifizierung von EBOV-GP-modulierten Oberflächenrezeptoren bestätigte diese Arbeit die Herunterregulierung von drei Tetraspaninen, CD81, CD63 und CD9. Es konnte gezeigt werden, dass diese Rezeptoren auch in EBOV-infizierten Zellen herunter reguliert werden. Darüber hinaus können GPs anderer Filoviren, SUDV, RESTV, TAFV und MARV, die Tetraspanine ebenfalls modulieren. Tetraspanine interagieren mit anderen Wirtsproteinen und bilden sogenannte TEMs, Englisch für „tetraspanin-enriched microdomains“, die an zahlreichen Signalwegen und zellulären Prozessen beteiligt sind. Die funktionelle Bedeutung der Tetraspanine im EBOV-Lebenszyklus wurde mit Hilfe des EBOV trVLP-Systems, ein Surrogat-System für Infektionen mit EBOV, und genetischen „knock-out“ Zellen untersucht. Die Inaktivierung von CD81, nicht aber von CD63 und CD9, verstärkte die EBOV-Minigenom-Replikation und -Transkription sowie die Oligomerisierung des Nucleokapsidproteins (NP), was eine wesentliche Rolle bei der Bildung der EBOV-Replikationskomplexe spielt. Umgekehrt unterdrückte die CD81-Überexpression in CD81-KO-Zellen die Expression von EBOV-Minigenom-kodierten Proteinen. Darüber hinaus erhöhte der KO von CD81 den GP-vermittelten Eintritt von EBOV und verstärkt die Makropinozytose, den wichtigsten Internalisierungsweg von EBOV. Außer GP ist noch ein anderes EBOV Protein, VP40, dazu in der Lage, CD81 herunter zu regulieren. Mechanistisch schleusen GP und VP40 CD81 in den lysosomalen und proteasomalen Abbauweg ein. Interessanter Weise konnte durch den CD81 spezifischen Antikörper 5A6 die Infektion mit EBOV trVLPs gehemmt werden.

Zusammenfassend konnte in dieser Arbeit gezeigt werden, dass EBOV das Tetraspanin CD81 als neuartigen Mechanismus zur Umgehung des Immunsystems herunterreguliert, um eine replikationsfreundliche Umgebung zu schaffen. Bei weiterer Untersuchung der EBOV-Infektion in primären Zielzellen könnte der CD81-Antikörper 5A6 ein neuer therapeutischer Ansatz darstellen.

7. Supplement

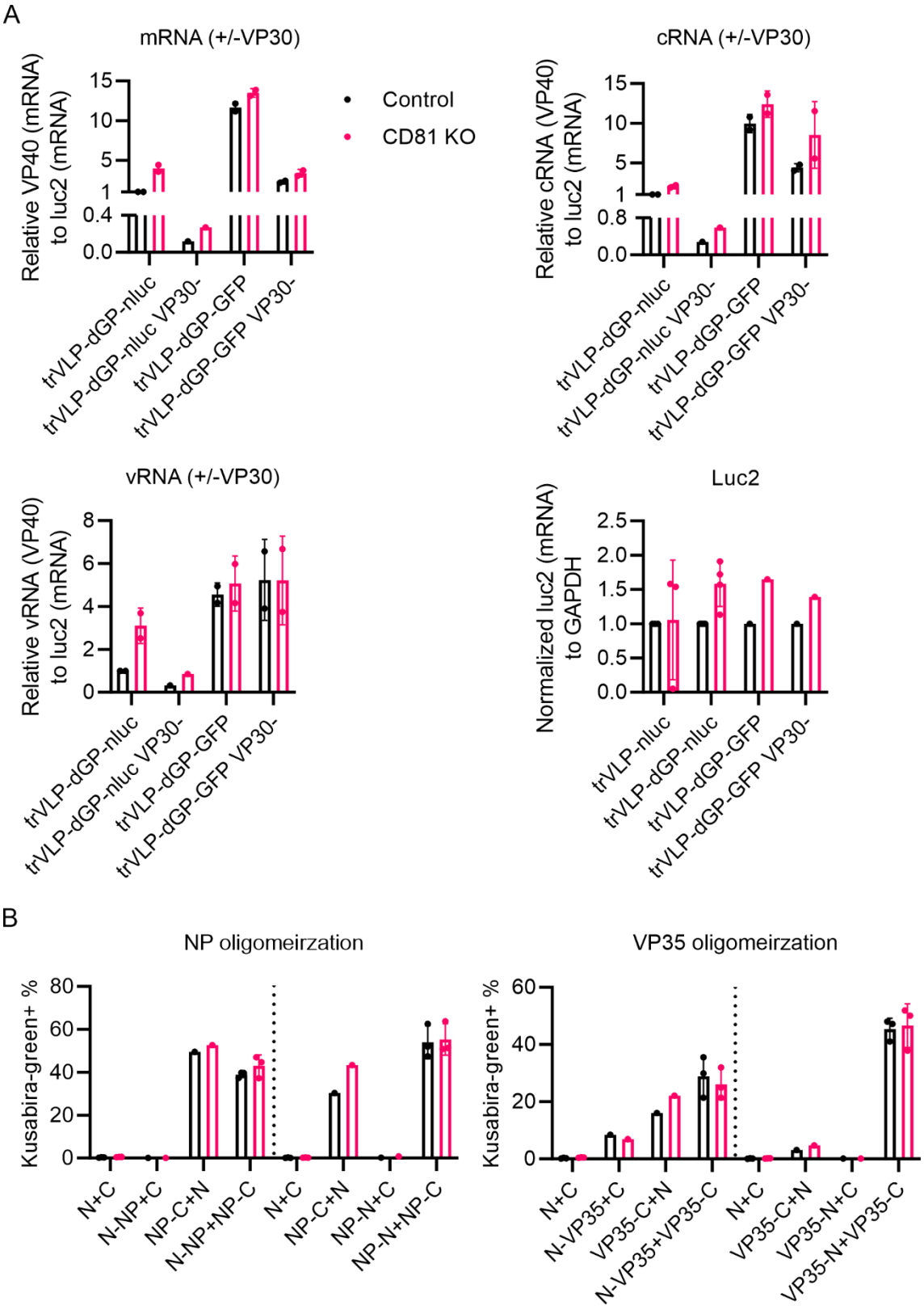

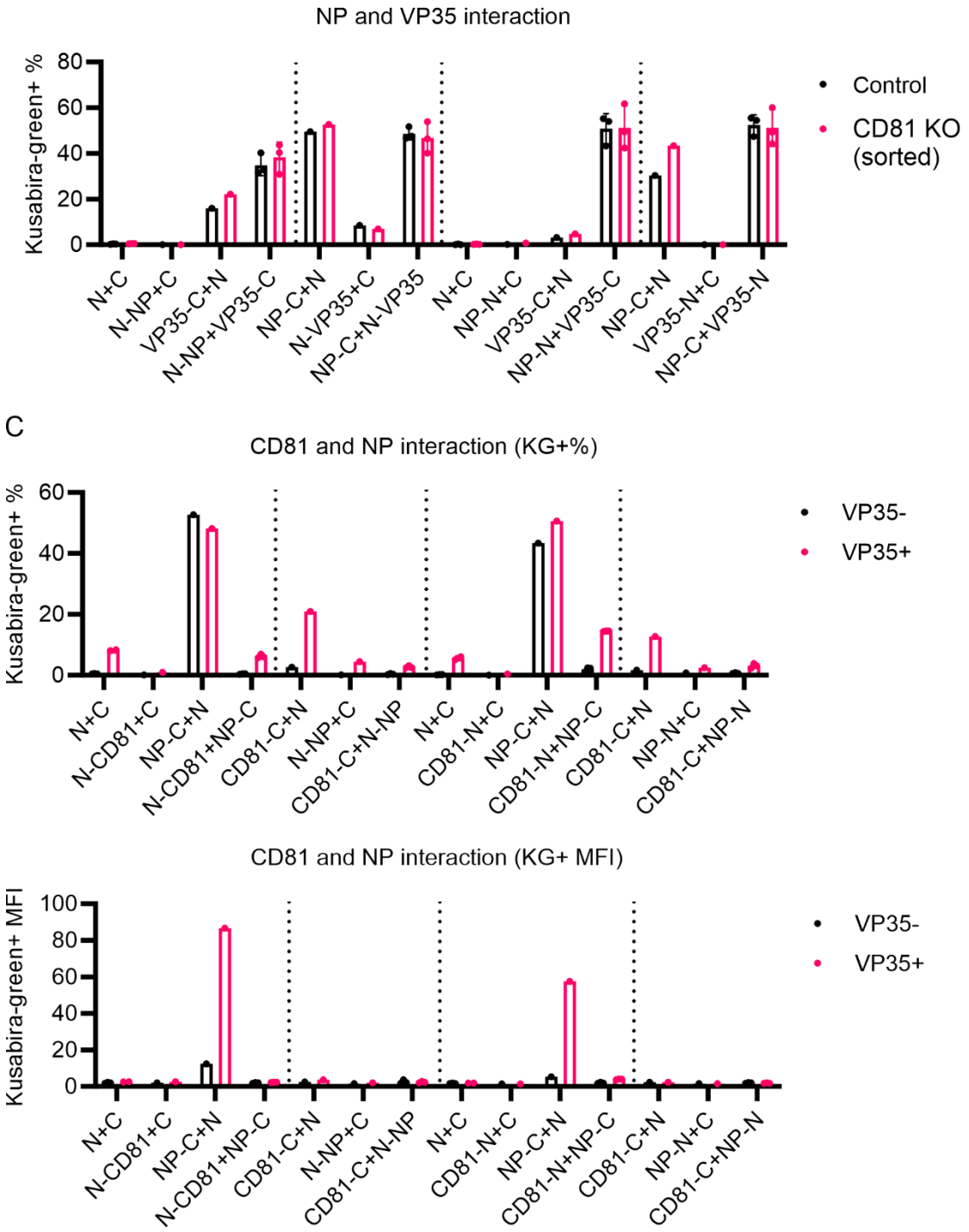

Sup. Figure 1 EBOV trVLP RNA levels and BiFC assay. (A) 293T control and CD81 KO cells were transfected to produce trVLP-dGP-nluc/-GFP with or without VP30 (+/-VP30), and luc2 expression plasmids were co-transfected as transfection control. 3 d.p.t., the cells were harvested and prepared for RT-qPCR. Shown are relative RNA levels or mean values of relative RNA levels +/- SD, EBOV mRNA, cRNA and vRNA levels were normalized to control cells producing trVLP-dGP-nluc and luc2 mRNA levels were normalized to the control cells (n=1-2). (B) The percentage of cells with reconstitution of KG, resulted from oligomerization of NP and VP35 as well as NP-VP35 interaction, in 293T control and CD81 KO (sorted) cells in the BiFC assay (Fig. 13B). (C) 293T CD81 KO (sorted) cells were co-transfected to express N- and C- part of KG only or fused with CD81/NP with or without VP35 as indicated for the BiFC assay. 2 d.p.t., the cells were

harvested for flow cytometry to analyze the percentage of KG+ cells and MFI of KG+ cells. n=1-3, shown are mean values +/- SD.

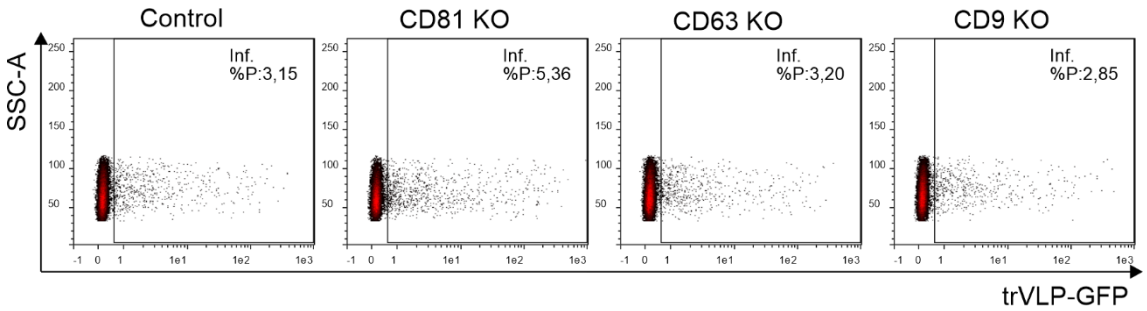

Sup. Figure 2 EBOV trVLP infection with 293T TSP KO cells. (A) 293T control, CD81 KO, CD63 KO and CD9 KO cells were transfected with Tim1 and EBOV RNP (NP, L, VP35 and VP30). 1 day later, the cells were infected with trVLP-GFP (inf.). 3 d.p.i., the cells were harvested for flow cytometry (n=4). Shown are representative density plots with infection rates.

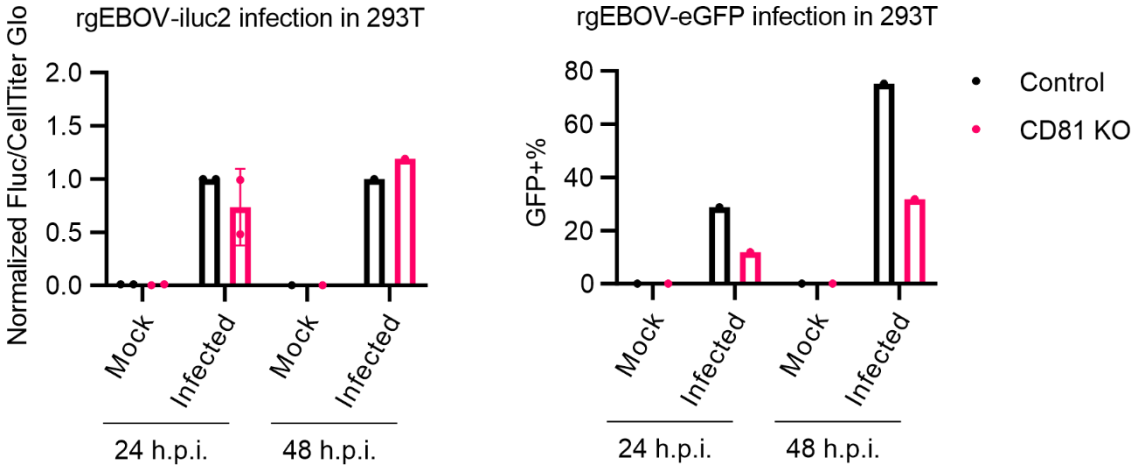

Sup. Figure 3 The role of CD81 in recombinant authentic EBOV infection. 293T control and CD81 KO cells were infected with rgEBOV-iluc2 at MOI of 0.5 (left). 24 and 48 h.p.i, the cells were harvested and lysed for luciferase assay, the luciferase activities were normalized to control cells. n=1-2, indicated are mean values +/- SD. 293T control and CD81 KO cells were infected with rgEBOV-eGFP at MOI of 1 (right). 24 and 48 h.p.i., the cells were harvested and fixed for flow cytometry analysis (n=1). The authentic EBOV infection experiments were performed by Thomas Hoenen and Lisa Wendt.

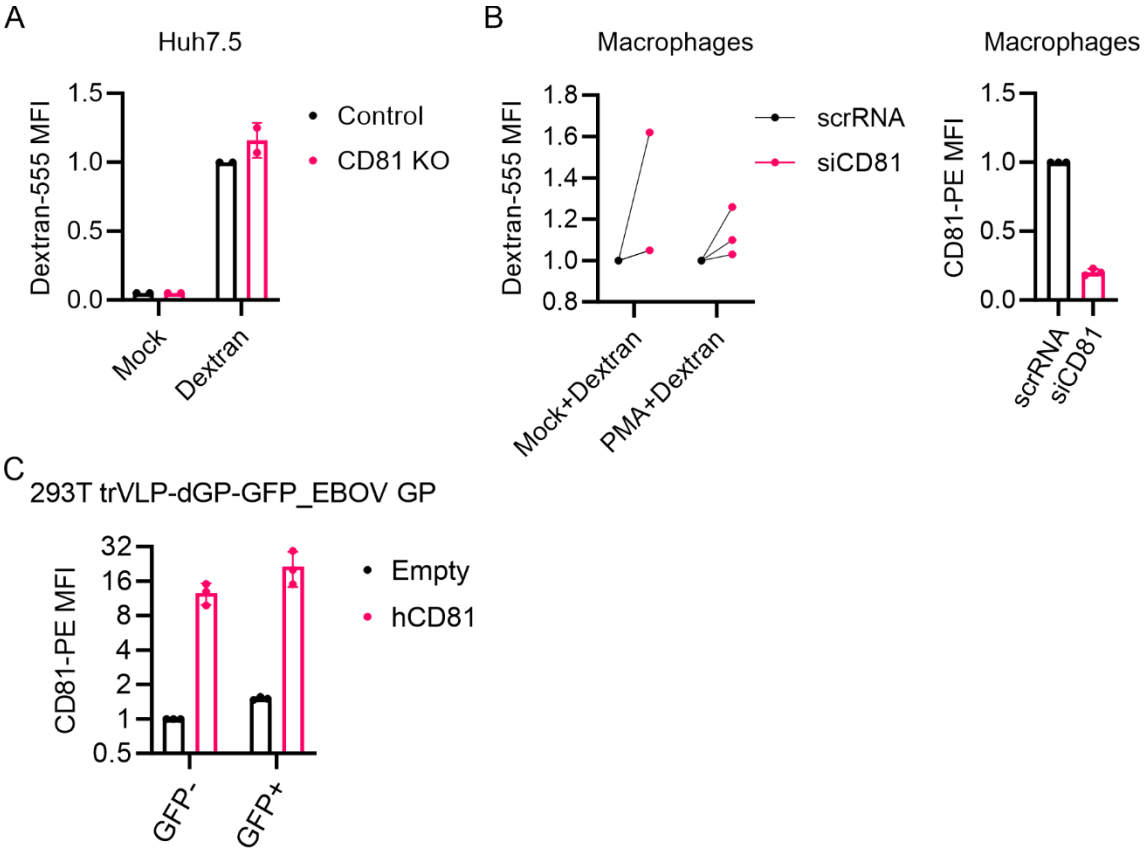

Sup. Figure 4 The role of CD81 in macropinocytosis. (A) Huh7.5 control and CD81 KO cells were added with medium only (mock) or Dextran-555 (10K, 0,4 mg/ml). 15 min later, the cells were harvested for flow cytometry (n=2), shown are mean values of normalized MFI of Dextran-555 (to control cells) +/- SD. (B) Human primary macrophages were transfected with non-targeting siRNA (scrRNA) or siRNA against CD81 (siCD81). 4 d.p.t., the cells were mock treated or treated with PMA (1 µM). 30 min later, the PMA was removed and Dextran-555 (10K, 0,4 mg/ml) was added. 15 min later, the cells were harvested for flow cytometry to analyze Dextran uptake, shown are normalized Dextran-555 MFI (to scrRNA transfected cells) of macrophages from three independent donors (left). Macrophages without PMA and Dextran-555 treatment were harvested and stained with PE conjugated antibody against CD81 to measure surface CD81 expression by flow cytometry, shown are CD81-PE MFI (normalized to scrNRA) of macrophages from the three donors.

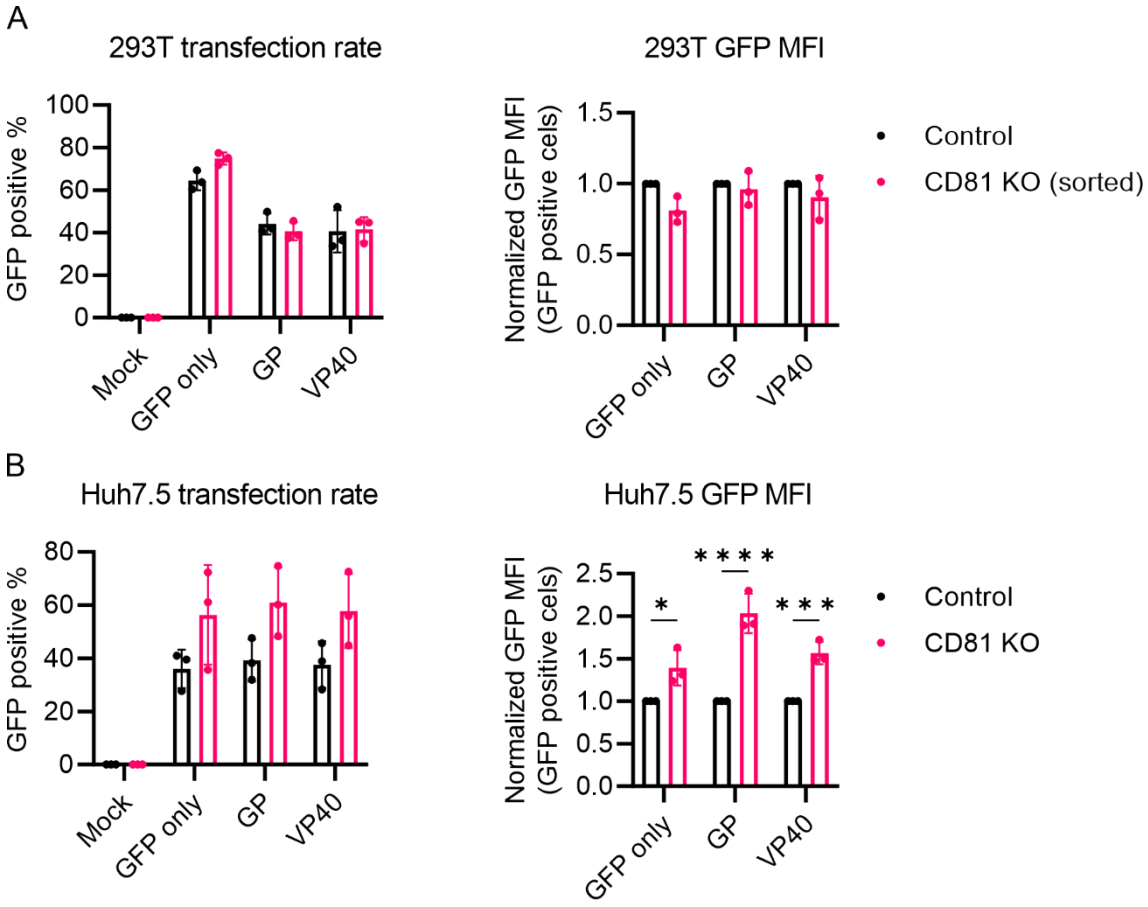

Sup. Figure 5 The effect of CD81 on transfection efficiency. 293T (A) and Huh7.5 (B) cells were transfected to express GFP only or co-express GFP and GP/VP40. 2 d.p.t., the cells were harvested for flow cytometry analysis (n=3). Shown are mean values of percentage of GFP positive cells and normalized GFP MFI (to control cells) +/- SD, two-way ANOVA with Šidák correction was used for statistics analysis (GP): 0,1234 (ns), 0,0332 (*), 0,0021 (**), 0,0002 (***), <0,0001 (****).

8. References

1. Kuhn JH, Amarasinghe GK, Basler CF, Bavari S, Bukreyev A, Chandran K, Crozier I, Dolnik O, Dye JM, Formenty PBH, Griffiths A, Hewson R, Kobinger GP, Leroy EM, Mühlberger E, Netesov (Нетёсов Сергей Викторович) SV, Palacios G, Pályi B, Pawęska JT, Smither SJ, Takada (高田礼人) A, Towner JS, Wahl V, ICTV Report Consortium. 2019. ICTV Virus Taxonomy Profile: Filoviridae. J Gen Virol 100:911–912.
2. Kuhn JH, Adachi T, Adhikari NKJ, Arribas JR, Bah IE, Bausch DG, Bhadelia N, Borchert M, Brantsæter AB, Brett-Major DM, Burgess TH, Chertow DS, Chute CG, Cieslak TJ, Colebunders R, Crozier I, Davey RT, de Clerck H, Delgado R, Evans L, Fallah M, Fischer WA, Fletcher TE, Fowler RA, Grünewald T, Hall A, Hewlett A, Hoepelman AIM, Houlihan CF, Ippolito G, Jacob ST, Jacobs M, Jakob R, Jacquerioz FA, Kaiser L, Kalil AC, Kamara RF, Kapetshi J, Klenk H-D, Kobinger G, Kortepeter MG, Kraft CS, Kratz T, Bosa HSK, Lado M, Lamontagne F, Lane HC, Lobel L, Lutwama J, Lyon GM, Massaquoi MBF, Massaquoi TA, Mehta AK, Makuma VM, Murthy S, Musoke TS, Muyembe-Tamfum J-J, Nakyeyune P, Nanclares C, Nanyunja M, Nsio-Mbeta J, O'Dempsey T, Pawęska JT, Peters CJ, Piot P, Rapp C, Renaud B, Ribner B, Sabeti PC, Schieffelin JS, Slenczka W, Soka MJ, Sprecher A, Strong J, Swanepoel R, Uyeki TM, van Herp M, Vetter P, Wohl DA, Wolf T, Wolz A, Wurie AH, Yoti Z. 2019. New filovirus disease classification and nomenclature. Nat Rev Microbiol 17:261–263.
3. 2023. History of Ebola Disease Outbreaks | History | Ebola (Ebola Virus Disease) | CDC. https://www.cdc.gov/vhf/ebola/history/chronology.html. Retrieved 22 August 2023.
4. Genus: Ebolavirus | ICTV. https://ictv.global/report/chapter/filoviridae/filoviridae/ebolavirus. Retrieved 13 May 2023.
5. Ebola virus disease. https://www.who.int/news-room/fact-sheets/detail/ebola-virus-disease. Retrieved 6 January 2023.
6. Formenty P, Hatz C, Le Guenno B, Stoll A, Rogenmoser P, Widmer A. 1999. Human Infection Due to Ebola Virus, Subtype Côte d'Ivoire: Clinical and Biologic Presentation. J Infect Dis 179:S48–S53.
7. Miranda MEG, Miranda NLJ. 2011. Reston ebolavirus in Humans and Animals in the Philippines: A Review. J Infect Dis 204:S757–S760.
8. Miranda MaryEG, White MarkE, Dayrit ManuelM, Hayes CurtisG, Ksiazek ThomasG, Burans JamesP. 1991. Seroepidemiological study of filovirus related to Ebola in the Philippines. The Lancet 337:425–426.
9. Goldstein T, Anthony SJ, Gbakima A, Bird BH, Bangura J, Tremeau-Bravard A, Belaganahalli MN, Wells HL, Dhanota JK, Liang E, Grodus M, Jangra RK, DeJesus VA, Lasso G, Smith BR, Jambai A, Kamara BO, Kamara S, Bangura W, Monagin C, Shapira S, Johnson CK, Saylors K, Rubin EM, Chandran K, Lipkin WI, Mazet JAK. 2018. The discovery of Bombali virus adds further support for bats as hosts of ebolaviruses. Nat Microbiol 3:1084–1089.
10. Marburg virus disease. https://www.who.int/news-room/fact-sheets/detail/marburg-virus-disease. Retrieved 6 January 2023.
11. Jacob ST, Crozier I, Fischer WA, Hewlett A, Kraft CS, Vega M-A de L, Soka MJ, Wahl V, Griffiths A, Bollinger L, Kuhn JH. 2020. Ebola virus disease. Nat Rev Dis Primer 6:13.
12. Dowell SF, Mukunu R, Ksiazek TG, Khan AS, Rollin PE, Peters CJ, the Commission de Lutte contre les Epidémies à Kikwit. 1999. Transmission of Ebola Hemorrhagic Fever: A Study of Risk Factors in Family Members, Kikwit, Democratic Republic of the Congo, 1995. J Infect Dis 179:S87–S91.
13. Bausch DG, Towner JS, Dowell SF, Kaducu F, Lukwiya M, Sanchez A, Nichol ST, Ksiazek TG, Rollin PE. 2007. Assessment of the Risk of Ebola Virus Transmission from Bodily Fluids and Fomites. J Infect Dis 196:S142–S147.
14. Okoror L, Kamara A, Kargbo B, Bangura J, Lebby M. 2018. Transplacental Transmission: A Rare Case of Ebola Virus Transmission. Infect Dis Rep 10:7725.
15. Feldmann H, Sprecher A, Geisbert TW. 2020. Ebola. N Engl J Med 382:1832–1842.
16. Xu Z, Jin B, Teng G, Rong Y, Sun L, Zhang J, Du N, Liu L, Su H, Yuan Y, Chen H. 2016. Epidemiologic characteristics, clinical manifestations, and risk factors of 139 patients with Ebola virus disease in western Sierra Leone. Am J Infect Control 44:1285–1290.

17. Qin E, Bi J, Zhao M, Wang Y, Guo T, Yan T, Li Z, Sun J, Zhang J, Chen S, Wu Y, Li J, Zhong Y. 2015. Clinical Features of Patients With Ebola Virus Disease in Sierra Leone. Clin Infect Dis 61:491–495.
18. Barry M, Toure A, Traore FA, Sako F-B, Sylla D, Kpamy DO, Bah EI, Bangoura M, Poncin M, Keita S, Tounkara TM, Cisse M, Vanhems P. 2015. Clinical Predictors of Mortality in Patients With Ebola Virus Disease. Clin Infect Dis 60:1821–1824.
19. Schieffelin JS, Shaffer JG, Goba A, Gbakie M, Gire SK, Colubri A, Sealfon RSG, Kanneh L, Moigboi A, Momoh M, Fullah M, Moses LM, Brown BL, Andersen KG, Winnicki S, Schaffner SF, Park DJ, Yozwiak NL, Jiang P-P, Kargbo D, Jalloh S, Fonnie M, Sinnah V, French I, Kovoma A, Kamara FK, Tucker V, Konuwa E, Sellu J, Mustapha I, Foday M, Yillah M, Kanneh F, Saffa S, Massally JLB, Boisen ML, Branco LM, Vandi MA, Grant DS, Happi C, Gevao SM, Fletcher TE, Fowler RA, Bausch DG, Sabeti PC, Khan SH, Garry RF. 2014. Clinical Illness and Outcomes in Patients with Ebola in Sierra Leone. N Engl J Med 371:2092–2100.
20. Feldmann H, Geisbert TW. 2011. Ebola haemorrhagic fever. The Lancet 377:849–862.
21. Geisbert TW, Hensley LE, Larsen T, Young HA, Reed DS, Geisbert JB, Scott DP, Kagan E, Jahrling PB, Davis KJ. 2003. Pathogenesis of Ebola Hemorrhagic Fever in Cynomolgus Macaques. Am J Pathol 163:2347–2370.
22. Connolly BM, Steele KE, Davis KJ, Geisbert TW, Kell WM, Jaax NK, Jahrling PB. 1999. Pathogenesis of Experimental Ebola Virus Infection in Guinea Pigs. J Infect Dis 179:S203–S217.
23. Geisbert TW, Young HA, Jahrling PB, Davis KJ, Larsen T, Kagan E, Hensley LE. 2003. Pathogenesis of Ebola Hemorrhagic Fever in Primate Models. Am J Pathol 163:2371–2382.
24. Gibb TR, Bray M, Geisbert TW, Steele KE, Kell WM, Davis KJ, Jaax NK. 2001. Pathogenesis of Experimental Ebola Zaire Virus Infection in BALB/c Mice. J Comp Pathol 125:233–242.
25. Geisbert TW, Hensley LE, Gibb TR, Steele KE, Jaax NK, Jahrling PB. 2000. Apoptosis Induced In Vitro and In Vivo During Infection by Ebola and Marburg Viruses. Lab Invest 80:171–186.
26. Wauquier N, Becquart P, Padilla C, Baize S, Leroy EM. 2010. Human Fatal Zaire Ebola Virus Infection Is Associated with an Aberrant Innate Immunity and with Massive Lymphocyte Apoptosis. PLoS Negl Trop Dis 4:e837.
27. Iampietro M, Younan P, Nishida A, Dutta M, Lubaki NM, Santos RI, Koup RA, Katze MG, Bukreyev A. 2017. Ebola virus glycoprotein directly triggers T lymphocyte death despite of the lack of infection. PLOS Pathog 13:e1006397.
28. Younan P, Santos RI, Ramanathan P, Iampietro M, Nishida A, Dutta M, Ammosova T, Meyer M, Katze MG, Popov VL, Nekhai S, Bukreyev A. 2019. Ebola virus-mediated T-lymphocyte depletion is the result of an abortive infection. PLOS Pathog 15:e1008068.
29. Woolsey C, Geisbert TW. 2021. Current state of Ebola virus vaccines: A snapshot. PLOS Pathog 17:e1010078.
30. Commissioner O of the. 2020. First FDA-approved vaccine for the prevention of Ebola virus disease, marking a critical milestone in public health preparedness and response. FDA. FDA. https://www.fda.gov/news-events/press-announcements/first-fda-approved-vaccine-prevention-ebola-virus-disease-marking-critical-milestone-public-health. Retrieved 22 August 2023.
31. EMA. 2019. Ervebo. Eur Med Agency. Text. https://www.ema.europa.eu/en/medicines/human/EPAR/ervebo. Retrieved 22 August 2023.
32. EMA. 2020. Zabdeno. Eur Med Agency. Text. https://www.ema.europa.eu/en/medicines/human/EPAR/zabdeno. Retrieved 22 August 2023.
33. EMA. 2020. Mvabea. Eur Med Agency. Text. https://www.ema.europa.eu/en/medicines/human/EPAR/mvabea. Retrieved 22 August 2023.
34. NMPA Database. https://www.nmpa.gov.cn/datasearch/en/search-info-en.html?nmpa=aWQ95Zu96I2v5YeG5a2XUzIwMTcwMDA4Jml0ZW1JZD0yYzliYTM4MTc5ZDA4ZjRmMDE3OWQxM2NhNGY0MDA0ZQ==. Retrieved 22 August 2023.
35. Ebola. https://gamaleya.org/en/research/ebola/. Retrieved 22 August 2023.
36. Henao-Restrepo AM, Camacho A, Longini IM, Watson CH, Edmunds WJ, Egger M, Carroll MW, Dean NE, Diatta I, Doumbia M, Draguez B, Duraffour S, Enwere G, Grais R, Gunther S, Gsell P-S, Hossmann S, Watle SV, Kondé MK, Kéïta S, Kone S, Kuisma E, Levine MM,

Mandal S, Mauget T, Norheim G, Riveros X, Soumah A, Trelle S, Vicari AS, Røttingen J-A, Kieny M-P. 2017. Efficacy and effectiveness of an rVSV-vectored vaccine in preventing Ebola virus disease: final results from the Guinea ring vaccination, open-label, cluster-randomised trial (Ebola Ça Suffit!). The Lancet 389:505–518.
37. Markham A. 2021. REGN-EB3: First Approval. Drugs 81:175–178.
38. Lee A. 2021. Ansuvimab: First Approval. Drugs 81:595–598.
39. Mulangu S, Dodd LE, Davey RT, Tshiani Mbaya O, Proschan M, Mukadi D, Lusakibanza Manzo M, Nzolo D, Tshomba Oloma A, Ibanda A, Ali R, Coulibaly S, Levine AC, Grais R, Diaz J, Lane HC, Muyembe-Tamfum J-J, the PALM Writing Group. 2019. A Randomized, Controlled Trial of Ebola Virus Disease Therapeutics. N Engl J Med 381:2293–2303.
40. Brauburger K, Boehmann Y, Tsuda Y, Hoenen T, Olejnik J, Schümann M, Ebihara H, Mühlberger E. 2014. Analysis of the Highly Diverse Gene Borders in Ebola Virus Reveals a Distinct Mechanism of Transcriptional Regulation. J Virol 88:12558–12571.
41. Sanchez A, Kiley MP, Holloway BP, Auperin DD. 1993. Sequence analysis of the Ebola virus genome: organization, genetic elements, and comparison with the genome of Marburg virus. Virus Res 29:215–240.
42. Volchkov VE, Volchkova VA, Chepurnov AA, Blinov VM, Dolnik O, Netesov SV, Feldmann H. 1999. Characterization of the L gene and 5' trailer region of Ebola virus. J Gen Virol 80:355–362.
43. Weik M, Enterlein S, Schlenz K, Mühlberger E. 2005. The Ebola Virus Genomic Replication Promoter Is Bipartite and Follows the Rule of Six. J Virol 79:10660–10671.
44. Calain P, Monroe MC, Nichol ST. 1999. Ebola Virus Defective Interfering Particles and Persistent Infection. Virology 262:114–128.
45. Hoenen T, Jung S, Herwig A, Groseth A, Becker S. 2010. Both matrix proteins of Ebola virus contribute to the regulation of viral genome replication and transcription. Virology 403:56–66.
46. Mühlberger E. 2007. Filovirus replication and transcription. Future Virol 2:205–215.
47. Hume AJ, Mühlberger E. 2019. Distinct genome replication and transcription strategies within the growing filovirus family. J Mol Biol 431:4290–4320.
48. Sanchez A, Rollin PE. 2005. Complete genome sequence of an Ebola virus (Sudan species) responsible for a 2000 outbreak of human disease in Uganda. Virus Res 113:16–25.
49. Volchkov VE, Becker S, Volchkova VA, Ternovoj VA, Kotov AN, Netesov SV, Klenk H-D. 1995. GP mRNA of Ebola Virus Is Edited by the Ebola Virus Polymerase and by T7 and Vaccinia Virus Polymerases1. Virology 214:421–430.
50. Sanchez A, Trappier SG, Mahy BW, Peters CJ, Nichol ST. 1996. The virion glycoproteins of Ebola viruses are encoded in two reading frames and are expressed through transcriptional editing. Proc Natl Acad Sci 93:3602–3607.
51. Mehedi M, Falzarano D, Seebach J, Hu X, Carpenter MS, Schnittler H-J, Feldmann H. 2011. A New Ebola Virus Nonstructural Glycoprotein Expressed through RNA Editing. J Virol 85:5406–5414.
52. Bharat TAM, Noda T, Riches JD, Kraehling V, Kolesnikova L, Becker S, Kawaoka Y, Briggs JAG. 2012. Structural dissection of Ebola virus and its assembly determinants using cryo-electron tomography. Proc Natl Acad Sci 109:4275–4280.
53. Beniac DR, Melito PL, deVarennes SL, Hiebert SL, Rabb MJ, Lamboo LL, Jones SM, Booth TF. 2012. The Organisation of Ebola Virus Reveals a Capacity for Extensive, Modular Polyploidy. PLOS ONE 7:e29608.
54. Ruigrok RWH, Schoehn G, Dessen A, Forest E, Volchkov V, Dolnik O, Klenk H-D, Weissenhorn W. 2000. Structural characterization and membrane binding properties of the matrix protein VP40 of ebola virus. J Mol Biol 300:103–112.
55. Han Z, Boshra H, Sunyer JO, Zwiers SH, Paragas J, Harty RN. 2003. Biochemical and Functional Characterization of the Ebola Virus VP24 Protein: Implications for a Role in Virus Assembly and Budding. J Virol 77:1793–1800.
56. Licata JM, Johnson RF, Han Z, Harty RN. 2004. Contribution of Ebola Virus Glycoprotein, Nucleoprotein, and VP24 to Budding of VP40 Virus-Like Particles. J Virol 78:7344–7351.
57. Su Y, Stahelin RV. 2020. The Minor Matrix Protein VP24 from Ebola Virus Lacks Direct Lipid-Binding Properties. Viruses 12:869.
58. Elliott LH, Kiley MP, McCormick JB. 1985. Descriptive analysis of Ebola virus proteins. Virology 147:169–176.

59. Huang Y, Xu L, Sun Y, Nabel GJ. 2002. The Assembly of Ebola Virus Nucleocapsid Requires Virion-Associated Proteins 35 and 24 and Posttranslational Modification of Nucleoprotein. Mol Cell 10:307–316.
60. Takamatsu Y, Yoshikawa T, Kurosu T, Fukushi S, Nagata N, Shimojima M, Ebihara H, Saijo M, Noda T. 2022. Role of VP30 Phosphorylation in Ebola Virus Nucleocapsid Assembly and Transport. J Virol 96:e01083-22.
61. Wan W, Kolesnikova L, Clarke M, Koehler A, Noda T, Becker S, Briggs JAG. 2017. Structure and assembly of the Ebola virus nucleocapsid. 7680. Nature 551:394–397.
62. Moller-Tank S, Maury W. 2015. Ebola Virus Entry: A Curious and Complex Series of Events. PLOS Pathog 11:e1004731.
63. Alvarez CP, Lasala F, Carrillo J, Muñiz O, Corbí AL, Delgado R. 2002. C-Type Lectins DC-SIGN and L-SIGN Mediate Cellular Entry by Ebola Virus in *cis* and in *trans*. J Virol 76:6841–6844.
64. Simmons G, Reeves JD, Grogan CC, Vandenberghe LH, Baribaud F, Whitbeck JC, Burke E, Buchmeier MJ, Soilleux EJ, Riley JL, Doms RW, Bates P, Pöhlmann S. 2003. DC-SIGN and DC-SIGNR Bind Ebola Glycoproteins and Enhance Infection of Macrophages and Endothelial Cells. Virology 305:115–123.
65. Takada A, Fujioka K, Tsuiji M, Morikawa A, Higashi N, Ebihara H, Kobasa D, Feldmann H, Irimura T, Kawaoka Y. 2004. Human Macrophage C-Type Lectin Specific for Galactose and *N* -Acetylgalactosamine Promotes Filovirus Entry. J Virol 78:2943–2947.
66. Powlesland AS, Fisch T, Taylor ME, Smith DF, Tissot B, Dell A, Pöhlmann S, Drickamer K. 2008. A Novel Mechanism for LSECtin Binding to Ebola Virus Surface Glycoprotein through Truncated Glycans. J Biol Chem 283:593–602.
67. Brudner M, Karpel M, Lear C, Chen L, Yantosca LM, Scully C, Sarraju A, Sokolovska A, Zariffard MR, Eisen DP, Mungall BA, Kotton DN, Omari A, Huang I-C, Farzan M, Takahashi K, Stuart L, Stahl GL, Ezekowitz AB, Spear GT, Olinger GG, Schmidt EV, Michelow IC. 2013. Lectin-Dependent Enhancement of Ebola Virus Infection via Soluble and Transmembrane C-type Lectin Receptors. PLoS ONE 8:e60838.
68. Moller-Tank S, Albritton LM, Rennert PD, Maury W. 2014. Characterizing Functional Domains for TIM-Mediated Enveloped Virus Entry. J Virol 88:6702–6713.
69. Yuan S, Cao L, Ling H, Dang M, Sun Y, Zhang X, Chen Y, Zhang L, Su D, Wang X, Rao Z. 2015. TIM-1 acts a dual-attachment receptor for Ebolavirus by interacting directly with viral GP and the PS on the viral envelope. Protein Cell 6:814–824.
70. Shimojima M, Takada A, Ebihara H, Neumann G, Fujioka K, Irimura T, Jones S, Feldmann H, Kawaoka Y. 2006. Tyro3 Family-Mediated Cell Entry of Ebola and Marburg Viruses. J Virol 80:10109–10116.
71. Morizono K, Xie Y, Olafsen T, Lee B, Dasgupta A, Wu AM, Chen ISY. 2011. The Soluble Serum Protein Gas6 Bridges Virion Envelope Phosphatidylserine to the TAM Receptor Tyrosine Kinase Axl to Mediate Viral Entry. Cell Host Microbe 9:286–298.
72. O'Hearn A, Wang M, Cheng H, Lear-Rooney CM, Koning K, Rumschlag-Booms E, Varhegyi E, Olinger G, Rong L. 2015. Role of EXT1 and Glycosaminoglycans in the Early Stage of Filovirus Entry. J Virol 89:5441–5449.
73. Favier A-L, Gout E, Reynard O, Ferraris O, Kleman J-P, Volchkov V, Peyrefitte C, Thielens NM. 2016. Enhancement of Ebola Virus Infection via Ficolin-1 Interaction with the Mucin Domain of GP Glycoprotein. J Virol 90:5256–5269.
74. Nanbo A, Imai M, Watanabe S, Noda T, Takahashi K, Neumann G, Halfmann P, Kawaoka Y. 2010. Ebolavirus Is Internalized into Host Cells via Macropinocytosis in a Viral Glycoprotein-Dependent Manner. PLoS Pathog 6:e1001121.
75. Saeed MF, Kolokoltsov AA, Albrecht T, Davey RA. 2010. Cellular Entry of Ebola Virus Involves Uptake by a Macropinocytosis-Like Mechanism and Subsequent Trafficking through Early and Late Endosomes. PLoS Pathog 6:e1001110.
76. Aleksandrowicz P, Marzi A, Biedenkopf N, Beimforde N, Becker S, Hoenen T, Feldmann H, Schnittler H-J. 2011. Ebola Virus Enters Host Cells by Macropinocytosis and Clathrin-Mediated Endocytosis. J Infect Dis 204:S957–S967.
77. Lin XP, Mintern JD, Gleeson PA. 2020. Macropinocytosis in Different Cell Types: Similarities and Differences. Membranes 10:177.

78. Canton J, Schlam D, Breuer C, Gütschow M, Glogauer M, Grinstein S. 2016. Calcium-sensing receptors signal constitutive macropinocytosis and facilitate the uptake of NOD2 ligands in macrophages. Nat Commun 7:11284.
79. Bohdanowicz M, Schlam D, Hermansson M, Rizzuti D, Fairn GD, Ueyama T, Somerharju P, Du G, Grinstein S. 2013. Phosphatidic acid is required for the constitutive ruffling and macropinocytosis of phagocytes. Mol Biol Cell 24:1700–1712.
80. Commisso C, Davidson SM, Soydaner-Azeloglu RG, Parker SJ, Kamphorst JJ, Hackett S, Grabocka E, Nofal M, Drebin JA, Thompson CB, Rabinowitz JD, Metallo CM, Vander Heiden MG, Bar-Sagi D. 2013. Macropinocytosis of protein is an amino acid supply route in Ras-transformed cells. Nature 497:633–637.
81. Salloum G, Jakubik CT, Erami Z, Heitz SD, Bresnick AR, Backer JM. 2019. PI3Kβ is selectively required for growth factor-stimulated macropinocytosis. J Cell Sci jcs.231639.
82. Lee E, Knecht DA. 2002. Visualization of Actin Dynamics During Macropinocytosis and Exocytosis. Traffic 3:186–192.
83. Araki N, Johnson MT, Swanson JA. 1996. A role for phosphoinositide 3-kinase in the completion of macropinocytosis and phagocytosis by macrophages. J Cell Biol 135:1249–1260.
84. Quinn SE, Huang L, Kerkvliet JG, Swanson JA, Smith S, Hoppe AD, Anderson RB, Thiex NW, Scott BL. 2021. The structural dynamics of macropinosome formation and PI3-kinase-mediated sealing revealed by lattice light sheet microscopy. Nat Commun 12:4838.
85. Saeed MF, Kolokoltsov AA, Freiberg AN, Holbrook MR, Davey RA. 2008. Phosphoinositide-3 Kinase-Akt Pathway Controls Cellular Entry of Ebola Virus. PLoS Pathog 4:e1000141.
86. Kuroda M, Halfmann P, Kawaoka Y. 2020. HER2-mediated enhancement of Ebola virus entry. PLOS Pathog 16:e1008900.
87. Stewart CM, Phan A, Bo Y, LeBlond ND, Smith TKT, Laroche G, Giguère PM, Fullerton MD, Pelchat M, Kobasa D, Côté M. 2021. Ebola virus triggers receptor tyrosine kinase-dependent signaling to promote the delivery of viral particles to entry-conducive intracellular compartments. PLOS Pathog 17:e1009275.
88. Mingo RM, Simmons JA, Shoemaker CJ, Nelson EA, Schornberg KL, D'Souza RS, Casanova JE, White JM. 2015. Ebola Virus and Severe Acute Respiratory Syndrome Coronavirus Display Late Cell Entry Kinetics: Evidence that Transport to NPC1 $^{+}$ Endolysosomes Is a Rate-Defining Step. J Virol 89:2931–2943.
89. Simmons JA, D'Souza RS, Ruas M, Galione A, Casanova JE, White JM. 2016. Ebolavirus Glycoprotein Directs Fusion through NPC1 $^{+}$ Endolysosomes. J Virol 90:605–610.
90. Spence JS, Krause TB, Mittler E, Jangra RK, Chandran K. 2016. Direct Visualization of Ebola Virus Fusion Triggering in the Endocytic Pathway. mBio 7:e01857-15.
91. Qiu S, Leung A, Bo Y, Kozak RA, Anand SP, Warkentin C, Salambanga FDR, Cui J, Kobinger G, Kobasa D, Côté M. 2018. Ebola virus requires phosphatidylinositol (3,5) bisphosphate production for efficient viral entry. Virology 513:17–28.
92. Bo Y, Qiu S, Mulloy RP, Côté M. 2020. Filoviruses Use the HOPS Complex and UVRAG To Traffic to Niemann-Pick C1 Compartments during Viral Entry. J Virol 94:e01002-20.
93. Sakurai Y, Kolokoltsov AA, Chen C-C, Tidwell MW, Bauta WE, Klugbauer N, Grimm C, Wahl-Schott C, Biel M, Davey RA. 2015. Two-pore channels control Ebola virus host cell entry and are drug targets for disease treatment. Science 347:995–998.
94. Chandran K, Sullivan NJ, Felbor U, Whelan SP, Cunningham JM. 2005. Endosomal Proteolysis of the Ebola Virus Glycoprotein Is Necessary for Infection. Science 308:1643–1645.
95. Schornberg K, Matsuyama S, Kabsch K, Delos S, Bouton A, White J. 2006. Role of Endosomal Cathepsins in Entry Mediated by the Ebola Virus Glycoprotein. J Virol 80:4174–4178.
96. Hood CL, Abraham J, Boyington JC, Leung K, Kwong PD, Nabel GJ. 2010. Biochemical and Structural Characterization of Cathepsin L-Processed Ebola Virus Glycoprotein: Implications for Viral Entry and Immunogenicity. J Virol 84:2972–2982.
97. Côté M, Misasi J, Ren T, Bruchez A, Lee K, Filone CM, Hensley L, Li Q, Ory D, Chandran K, Cunningham J. 2011. Small molecule inhibitors reveal Niemann–Pick C1 is essential for Ebola virus infection. Nature 477:344–348.
98. Carette JE, Raaben M, Wong AC, Herbert AS, Obernosterer G, Mulherkar N, Kuehne AI, Kranzusch PJ, Griffin AM, Ruthel G, Cin PD, Dye JM, Whelan SP, Chandran K,

Brummelkamp TR. 2011. Ebola virus entry requires the cholesterol transporter Niemann–Pick C1. Nature 477:340–343.
99. Miller EH, Obernosterer G, Raaben M, Herbert AS, Deffieu MS, Krishnan A, Ndungo E, Sandesara RG, Carette JE, Kuehne AI, Ruthel G, Pfeffer SR, Dye JM, Whelan SP, Brummelkamp TR, Chandran K. 2012. Ebola virus entry requires the host-programmed recognition of an intracellular receptor: Niemann-Pick C1 is a critical filovirus receptor. EMBO J 31:1947–1960.
100. Lee J, Kreutzberger AJB, Odongo L, Nelson EA, Nyenhuis DA, Kiessling V, Liang B, Cafiso DS, White JM, Tamm LK. 2021. Ebola virus glycoprotein interacts with cholesterol to enhance membrane fusion and cell entry. Nat Struct Mol Biol 28:181–189.
101. Dolnik O, Becker S. 2022. Assembly and transport of filovirus nucleocapsids. PLOS Pathog 18:e1010616.
102. Hoenen T, Groseth A, Kolesnikova L, Theriault S, Ebihara H, Hartlieb B, Bamberg S, Feldmann H, Ströher U, Becker S. 2006. Infection of Naïve Target Cells with Virus-Like Particles: Implications for the Function of Ebola Virus VP24. J Virol 80:7260–7264.
103. Mühlberger E, Weik M, Volchkov VE, Klenk H-D, Becker S. 1999. Comparison of the Transcription and Replication Strategies of Marburg Virus and Ebola Virus by Using Artificial Replication Systems. J Virol 73:2333–2342.
104. Biedenkopf N, Lier C, Becker S. 2016. Dynamic Phosphorylation of VP30 Is Essential for Ebola Virus Life Cycle. J Virol 90:4914–4925.
105. Hoenen T, Shabman RS, Groseth A, Herwig A, Weber M, Schudt G, Dolnik O, Basler CF, Becker S, Feldmann H. 2012. Inclusion Bodies Are a Site of Ebolavirus Replication. J Virol 86:11779–11788.
106. Lier C, Becker S, Biedenkopf N. 2017. Dynamic phosphorylation of Ebola virus VP30 in NP-induced inclusion bodies. Virology 512:39–47.
107. Weik M, Modrof J, Klenk H-D, Becker S, Mühlberger E. 2002. Ebola Virus VP30-Mediated Transcription Is Regulated by RNA Secondary Structure Formation. J Virol 76:8532–8539.
108. Martínez MJ, Biedenkopf N, Volchkova V, Hartlieb B, Alazard-Dany N, Reynard O, Becker S, Volchkov V. 2008. Role of Ebola Virus VP30 in Transcription Reinitiation. J Virol 82:12569–12573.
109. Nanbo A, Watanabe S, Halfmann P, Kawaoka Y. 2013. The spatio-temporal distribution dynamics of Ebola virus proteins and RNA in infected cells. Sci Rep 3:1206.
110. Wu L, Jin D, Wang D, Jing X, Gong P, Qin Y, Chen M. 2022. The two-stage interaction of Ebola virus VP40 with nucleoprotein results in a switch from viral RNA synthesis to virion assembly/budding. Protein Cell 13:120–140.
111. Watt A, Moukambi F, Banadyga L, Groseth A, Callison J, Herwig A, Ebihara H, Feldmann H, Hoenen T. 2014. A Novel Life Cycle Modeling System for Ebola Virus Shows a Genome Length-Dependent Role of VP24 in Virus Infectivity. J Virol 88:10511–10524.
112. Bodmer BS, Vallbracht M, Ushakov DS, Wendt L, Chlanda P, Hoenen T. 2023. Ebola virus inclusion bodies are liquid organelles whose formation is facilitated by nucleoprotein oligomerization. Emerg Microbes Infect 12:2223727.
113. Groseth A, Charton JE, Sauerborn M, Feldmann F, Jones SM, Hoenen T, Feldmann H. 2009. The Ebola virus ribonucleoprotein complex: A novel VP30–L interaction identified. Virus Res 140:8–14.
114. Sanchez A, Kiley MP. 1987. Identification and analysis of ebola virus messenger RNA. Virology 157:414–420.
115. Shabman RS, Jabado OJ, Mire CE, Stockwell TB, Edwards M, Mahajan M, Geisbert TW, Basler CF. 2014. Deep Sequencing Identifies Noncanonical Editing of Ebola and Marburg Virus RNAs in Infected Cells. mBio 5:e02011-14.
116. Trunschke M, Conrad D, Enterlein S, Olejnik J, Brauburger K, Mühlberger E. 2013. The L–VP35 and L–L interaction domains reside in the amino terminus of the Ebola virus L protein and are potential targets for antivirals. Virology 441:135–145.
117. Hartlieb B, Muziol T, Weissenhorn W, Becker S. 2007. Crystal structure of the C-terminal domain of Ebola virus VP30 reveals a role in transcription and nucleocapsid association. Proc Natl Acad Sci 104:624–629.
118. Kirchdoerfer RN, Abelson DM, Li S, Wood MR, Saphire EO. 2015. Assembly of the Ebola Virus Nucleoprotein from a Chaperoned VP35 Complex. Cell Rep 12:140–149.

119. Miyake T, Farley CM, Neubauer BE, Beddow TP, Hoenen T, Engel DA. 2020. Ebola Virus Inclusion Body Formation and RNA Synthesis Are Controlled by a Novel Domain of Nucleoprotein Interacting with VP35. J Virol 94:e02100-19.
120. Leung DW, Borek D, Luthra P, Binning JM, Anantpadma M, Liu G, Harvey IB, Su Z, Endlich-Frazier A, Pan J, Shabman RS, Chiu W, Davey RA, Otwinowski Z, Basler CF, Amarasinghe GK. 2015. An Intrinsically Disordered Peptide from Ebola Virus VP35 Controls Viral RNA Synthesis by Modulating Nucleoprotein-RNA Interactions. Cell Rep 11:376–389.
121. Lin AE, Diehl WE, Cai Y, Finch CL, Akusobi C, Kirchdoerfer RN, Bollinger L, Schaffner SF, Brown EA, Saphire EO, Andersen KG, Kuhn JH, Luban J, Sabeti PC. 2020. Reporter Assays for Ebola Virus Nucleoprotein Oligomerization, Virion-Like Particle Budding, and Minigenome Activity Reveal the Importance of Nucleoprotein Amino Acid Position 111. Viruses 12:105.
122. Yuan B, Peng Q, Cheng J, Wang M, Zhong J, Qi J, Gao GF, Shi Y. 2022. Structure of the Ebola virus polymerase complex. Nature 610:394–401.
123. Reid StP, Cárdenas WB, Basler CF. 2005. Homo-oligomerization facilitates the interferon-antagonist activity of the ebolavirus VP35 protein. Virology 341:179–189.
124. Hartlieb B, Modrof J, Mühlberger E, Klenk H-D, Becker S. 2003. Oligomerization of Ebola Virus VP30 Is Essential for Viral Transcription and Can Be Inhibited by a Synthetic Peptide. J Biol Chem 278:41830–41836.
125. Modrof J, Mu¨hlberger E, Klenk H-D, Becker S. 2002. Phosphorylation of VP30 Impairs Ebola Virus Transcription*. J Biol Chem 277:33099–33104.
126. Biedenkopf N, Hartlieb B, Hoenen T, Becker S. 2013. Phosphorylation of Ebola Virus VP30 Influences the Composition of the Viral Nucleocapsid Complex. J Biol Chem 288:11165–11174.
127. Biedenkopf N, Schlereth J, Grünweller A, Becker S, Hartmann RK. 2016. RNA Binding of Ebola Virus VP30 Is Essential for Activating Viral Transcription. J Virol 90:7481–7496.
128. Takamatsu Y, Krähling V, Kolesnikova L, Halwe S, Lier C, Baumeister S, Noda T, Biedenkopf N, Becker S. 2020. Serine-Arginine Protein Kinase 1 Regulates Ebola Virus Transcription. mBio 11:e02565-19.
129. Kruse T, Biedenkopf N, Hertz EPT, Dietzel E, Stalmann G, López-Méndez B, Davey NE, Nilsson J, Becker S. 2018. The Ebola Virus Nucleoprotein Recruits the Host PP2A-B56 Phosphatase to Activate Transcriptional Support Activity of VP30. Mol Cell 69:136-145.e6.
130. Dolnik O, Gerresheim GK, Biedenkopf N. 2021. New Perspectives on the Biogenesis of Viral Inclusion Bodies in Negative-Sense RNA Virus Infections. Cells 10:1460.
131. Takahashi K, Halfmann P, Oyama M, Kozuka-Hata H, Noda T, Kawaoka Y. 2013. DNA Topoisomerase 1 Facilitates the Transcription and Replication of the Ebola Virus Genome. J Virol 87:8862–8869.
132. Fang J, Pietzsch C, Ramanathan P, Santos RI, Ilinykh PA, Garcia-Blanco MA, Bukreyev A, Bradrick SS. 2018. Staufen1 Interacts with Multiple Components of the Ebola Virus Ribonucleoprotein and Enhances Viral RNA Synthesis. mBio 9:e01771-18.
133. Chen J, He Z, Yuan Y, Huang F, Luo B, Zhang J, Pan T, Zhang H, Zhang J. 2019. Host factor SMYD3 is recruited by Ebola virus nucleoprotein to facilitate viral mRNA transcription. Emerg Microbes Infect 8:1347–1360.
134. Brandt J, Wendt L, Bodmer BS, Mettenleiter TC, Hoenen T. 2020. The Cellular Protein CAD is Recruited into Ebola Virus Inclusion Bodies by the Nucleoprotein NP to Facilitate Genome Replication and Transcription. Cells 9:1126.
135. Zhu L, Gao T, Huang Y, Jin J, Wang D, Zhang L, Jin Y, Li P, Hu Y, Wu Y, Liu H, Dong Q, Wang G, Zheng T, Song C, Bai Y, Zhang X, Liu Y, Yang W, Xu K, Zou G, Zhao L, Cao R, Zhong W, Xia X, Xiao G, Liu X, Cao C. 2022. Ebola virus VP35 hijacks the PKA-CREB1 pathway for replication and pathogenesis by AKIP1 association. Nat Commun 13:2256.
136. Batra J, Hultquist JF, Liu D, Shtanko O, Von Dollen J, Satkamp L, Jang GM, Luthra P, Schwarz TM, Small GI, Arnett E, Anantpadma M, Reyes A, Leung DW, Kaake R, Haas P, Schmidt CB, Schlesinger LS, LaCount DJ, Davey RA, Amarasinghe GK, Basler CF, Krogan NJ. 2018. Protein Interaction Mapping Identifies RBBP6 as a Negative Regulator of Ebola Virus Replication. Cell 175:1917-1930.e13.
137. Wendt L, Brandt J, Bodmer BS, Reiche S, Schmidt ML, Traeger S, Hoenen T. 2020. The Ebola Virus Nucleoprotein Recruits the Nuclear RNA Export Factor NXF1 into Inclusion Bodies to Facilitate Viral Protein Expression. Cells 9:187.

138. Wendt L, Brandt J, Ushakov DS, Bodmer BS, Pickin MJ, Groseth A, Hoenen T. 2022. Evidence for Viral mRNA Export from Ebola Virus Inclusion Bodies by the Nuclear RNA Export Factor NXF1. J Virol 96:e00900-22.
139. Zhang Q, Sharma NR, Zheng Z-M, Chen M. 2019. Viral Regulation of RNA Granules in Infected Cells. Virol Sin 34:175–191.
140. Nelson EV, Schmidt KM, Deflubé LR, Doğanay S, Banadyga L, Olejnik J, Hume AJ, Ryabchikova E, Ebihara H, Kedersha N, Ha T, Mühlberger E. 2016. Ebola Virus Does Not Induce Stress Granule Formation during Infection and Sequesters Stress Granule Proteins within Viral Inclusions. J Virol 90:7268–7284.
141. Messaoudi I, Amarasinghe GK, Basler CF. 2015. Filovirus pathogenesis and immune evasion: insights from Ebola virus and Marburg virus. Nat Rev Microbiol 13:663–676.
142. Cárdenas WB, Loo Y-M, Gale M, Hartman AL, Kimberlin CR, Martínez-Sobrido L, Saphire EO, Basler CF. 2006. Ebola Virus VP35 Protein Binds Double-Stranded RNA and Inhibits Alpha/Beta Interferon Production Induced by RIG-I Signaling. J Virol 80:5168–5178.
143. Luthra P, Ramanan P, Mire CE, Weisend C, Tsuda Y, Yen B, Liu G, Leung DW, Geisbert TW, Ebihara H, Amarasinghe GK, Basler CF. 2013. Mutual Antagonism between the Ebola Virus VP35 Protein and the RIG-I Activator PACT Determines Infection Outcome. Cell Host Microbe 14:74–84.
144. Schümann M, Gantke T, Mühlberger E. 2009. Ebola Virus VP35 Antagonizes PKR Activity through Its C-Terminal Interferon Inhibitory Domain. J Virol 83:8993–8997.
145. Prins KC, Cárdenas WB, Basler CF. 2009. Ebola Virus Protein VP35 Impairs the Function of Interferon Regulatory Factor-Activating Kinases IKKε and TBK-1. J Virol 83:3069–3077.
146. Chang T-H, Kubota T, Matsuoka M, Jones S, Bradfute SB, Bray M, Ozato K. 2009. Ebola Zaire Virus Blocks Type I Interferon Production by Exploiting the Host SUMO Modification Machinery. PLOS Pathog 5:e1000493.
147. Reid StP, Leung LW, Hartman AL, Martinez O, Shaw ML, Carbonnelle C, Volchkov VE, Nichol ST, Basler CF. 2006. Ebola Virus VP24 Binds Karyopherin α1 and Blocks STAT1 Nuclear Accumulation. J Virol 80:5156–5167.
148. Schudt G, Dolnik O, Kolesnikova L, Biedenkopf N, Herwig A, Becker S. 2015. Transport of Ebolavirus Nucleocapsids Is Dependent on Actin Polymerization: Live-Cell Imaging Analysis of Ebolavirus-Infected Cells. J Infect Dis 212:S160–S166.
149. Takamatsu Y, Kolesnikova L, Becker S. 2018. Ebola virus proteins NP, VP35, and VP24 are essential and sufficient to mediate nucleocapsid transport. Proc Natl Acad Sci 115:1075–1080.
150. Frick CT, Stahelin RV. 2015. The Ebola Virus Matrix Protein VP40 Interacts With Several Host Protein Networks to Facilitate Viral Replication. Curr Clin Microbiol Rep 2:137–141.
151. Stahelin RV. 2014. Membrane binding and bending in Ebola VP40 assembly and egress. Front Microbiol 5.
152. Yamayoshi S, Noda T, Ebihara H, Goto H, Morikawa Y, Lukashevich IS, Neumann G, Feldmann H, Kawaoka Y. 2008. Ebola Virus Matrix Protein VP40 Uses the COPII Transport System for Its Intracellular Transport. Cell Host Microbe 3:168–177.
153. Scianimanico S. 2000. Membrane association induces a conformational change in the Ebola virus matrix protein. EMBO J 19:6732–6741.
154. Adu-Gyamfi E, Johnson KA, Fraser ME, Scott JL, Soni SP, Jones KR, Digman MA, Gratton E, Tessier CR, Stahelin RV. 2015. Host Cell Plasma Membrane Phosphatidylserine Regulates the Assembly and Budding of Ebola Virus. J Virol 89:9440–9453.
155. Johnson KA, Taghon GJF, Scott JL, Stahelin RV. 2016. The Ebola Virus matrix protein, VP40, requires phosphatidylinositol 4,5-bisphosphate (PI(4,5)P2) for extensive oligomerization at the plasma membrane and viral egress. Sci Rep 6:19125.
156. Husby ML, Amiar S, Prugar LI, David EA, Plescia CB, Huie KE, Brannan JM, Dye JM, Pienaar E, Stahelin RV. 2022. Phosphatidylserine clustering by the Ebola virus matrix protein is a critical step in viral budding. EMBO Rep 23.
157. Nanbo A, Maruyama J, Imai M, Ujie M, Fujioka Y, Nishide S, Takada A, Ohba Y, Kawaoka Y. 2018. Ebola virus requires a host scramblase for externalization of phosphatidylserine on the surface of viral particles. PLOS Pathog 14:e1006848.
158. Volchkov VE, Feldmann H, Volchkova VA, Klenk H-D. 1998. Processing of the Ebola virus glycoprotein by the proprotein convertase furin. Proc Natl Acad Sci 95:5762–5767.

159. Jeffers SA, Sanders DA, Sanchez A. 2002. Covalent Modifications of the Ebola Virus Glycoprotein. J Virol 76:12463–12472.
160. Sanchez A, Yang Z-Y, Xu L, Nabel GJ, Crews T, Peters CJ. 1998. Biochemical Analysis of the Secreted and Virion Glycoproteins of Ebola Virus. J Virol 72:6442–6447.
161. Jasenosky LD, Neumann G, Lukashevich I, Kawaoka Y. 2001. Ebola Virus VP40-Induced Particle Formation and Association with the Lipid Bilayer. J Virol 75:5205–5214.
162. Noda T, Sagara H, Suzuki E, Takada A, Kida H, Kawaoka Y. 2002. Ebola Virus VP40 Drives the Formation of Virus-Like Filamentous Particles Along with GP. J Virol 76:4855–4865.
163. Gordon TB, Hayward JA, Marsh GA, Baker ML, Tachedjian G. 2019. Host and Viral Proteins Modulating Ebola and Marburg Virus Egress. Viruses 11:25.
164. Lu J, Qu Y, Liu Y, Jambusaria R, Han Z, Ruthel G, Freedman BD, Harty RN. 2013. Host IQGAP1 and Ebola Virus VP40 Interactions Facilitate Virus-Like Particle Egress. J Virol 87:7777–7780.
165. Yasuda J, Nakao M, Kawaoka Y, Shida H. 2003. Nedd4 Regulates Egress of Ebola Virus-Like Particles from Host Cells. J Virol 77:9987–9992.
166. Han Z, Sagum CA, Bedford MT, Sidhu SS, Sudol M, Harty RN. 2016. ITCH E3 Ubiquitin Ligase Interacts with Ebola Virus VP40 To Regulate Budding. J Virol 90:9163–9171.
167. Han Z, Sagum CA, Takizawa F, Ruthel G, Berry CT, Kong J, Sunyer JO, Freedman BD, Bedford MT, Sidhu SS, Sudol M, Harty RN. 2017. Ubiquitin Ligase WWP1 Interacts with Ebola Virus VP40 To Regulate Egress. J Virol 91:e00812-17.
168. Shepley-McTaggart A, Schwoerer MP, Sagum CA, Bedford MT, Jaladanki CK, Fan H, Cassel J, Harty RN. 2021. Ubiquitin Ligase SMURF2 Interacts with Filovirus VP40 and Promotes Egress of VP40 VLPs. Viruses 13:288.
169. Licata JM, Simpson-Holley M, Wright NT, Han Z, Paragas J, Harty RN. 2003. Overlapping Motifs (PTAP and PPEY) within the Ebola Virus VP40 Protein Function Independently as Late Budding Domains: Involvement of Host Proteins TSG101 and VPS-4. J Virol 77:1812–1819.
170. Silvestri LS, Ruthel G, Kallstrom G, Warfield KL, Swenson DL, Nelle T, Iversen PL, Bavari S, Aman MJ. 2007. Involvement of Vacuolar Protein Sorting Pathway in Ebola Virus Release Independent of TSG101 Interaction. J Infect Dis 196:S264–S270.
171. Han Z, Madara JJ, Liu Y, Liu W, Ruthel G, Freedman BD, Harty RN. 2015. ALIX Rescues Budding of a Double PTAP/PPEY L-Domain Deletion Mutant of Ebola VP40: A Role for ALIX in Ebola Virus Egress. J Infect Dis 212:S138–S145.
172. Mori H, Connell JP, Donahue CJ, Boytz R, Nguyen YTK, Leung DW, LaCount DJ, Davey RA. 2022. CAPG Is Required for Ebola Virus Infection by Controlling Virus Egress from Infected Cells. Viruses 14:1903.
173. Han Z, Ruthel G, Dash S, Berry CT, Freedman BD, Harty RN, Shtanko O. 2020. Angiomotin regulates budding and spread of Ebola virus. J Biol Chem 295:8596–8601.
174. Marzi A, Akhavan A, Simmons G, Gramberg T, Hofmann H, Bates P, Lingappa VR, Pöhlmann S. 2006. The Signal Peptide of the Ebolavirus Glycoprotein Influences Interaction with the Cellular Lectins DC-SIGN and DC-SIGNR. J Virol 80:6305–6317.
175. Kuhn JH, Radoshitzky SR, Guth AC, Warfield KL, Li W, Vincent MJ, Towner JS, Nichol ST, Bavari S, Choe H, Aman MJ, Farzan M. 2006. Conserved Receptor-binding Domains of Lake Victoria Marburgvirus and Zaire Ebolavirus Bind a Common Receptor. J Biol Chem 281:15951–15958.
176. Lee JE, Fusco ML, Hessell AJ, Oswald WB, Burton DR, Saphire EO. 2008. Structure of the Ebola virus glycoprotein bound to an antibody from a human survivor. Nature 454:177–182.
177. Tran EEH, Simmons JA, Bartesaghi A, Shoemaker CJ, Nelson E, White JM, Subramaniam S. 2014. Spatial Localization of the Ebola Virus Glycoprotein Mucin-Like Domain Determined by Cryo-Electron Tomography. J Virol 88:10958–10962.
178. Ruiz-Argüello MB, Goñi FM, Pereira FB, Nieva JL. 1998. Phosphatidylinositol-Dependent Membrane Fusion Induced by a Putative Fusogenic Sequence of Ebola Virus. J Virol 72:1775–1781.
179. Ito H, Watanabe S, Sanchez A, Whitt MA, Kawaoka Y. 1999. Mutational Analysis of the Putative Fusion Domain of Ebola Virus Glycoprotein. J Virol 73:8907–8912.

180. Dolnik O, Volchkova V, Garten W, Carbonnelle C, Becker S, Kahnt J, Ströher U, Klenk H-D, Volchkov V. 2004. Ectodomain shedding of the glycoprotein GP of Ebola virus. EMBO J 23:2175–2184.
181. Volchkov VE, Volchkova VA, Slenczka W, Klenk H-D, Feldmann H. 1998. Release of Viral Glycoproteins during Ebola Virus Infection. Virology 245:110–119.
182. Nehls J, Businger R, Hoffmann M, Brinkmann C, Fehrenbacher B, Schaller M, Maurer B, Schönfeld C, Kramer D, Hailfinger S, Pöhlmann S, Schindler M. 2019. Release of Immunomodulatory Ebola Virus Glycoprotein-Containing Microvesicles Is Suppressed by Tetherin in a Species-Specific Manner. Cell Rep 26:1841-1853.e6.
183. Takada A, Watanabe S, Ito H, Okazaki K, Kida H, Kawaoka Y. 2000. Downregulation of β1 Integrins by Ebola Virus Glycoprotein: Implication for Virus Entry. Virology 278:20–26.
184. Simmons G, Wool-Lewis RJ, Baribaud F, Netter RC, Bates P. 2002. Ebola Virus Glycoproteins Induce Global Surface Protein Down-Modulation and Loss of Cell Adherence. J Virol 76:2518–2528.
185. Sullivan NJ, Peterson M, Yang Z, Kong W, Duckers H, Nabel E, Nabel GJ. 2005. Ebola Virus Glycoprotein Toxicity Is Mediated by a Dynamin-Dependent Protein-Trafficking Pathway. J Virol 79:547–553.
186. Zampieri CA, Fortin J-F, Nolan GP, Nabel GJ. 2007. The ERK Mitogen-Activated Protein Kinase Pathway Contributes to Ebola Virus Glycoprotein-Induced Cytotoxicity. J Virol 81:1230–1240.
187. Francica JR, Varela-Rohena A, Medvec A, Plesa G, Riley JL, Bates P. 2010. Steric Shielding of Surface Epitopes and Impaired Immune Recognition Induced by the Ebola Virus Glycoprotein. PLoS Pathog 6:e1001098.
188. Edri A, Shemesh A, Iraqi M, Matalon O, Brusilovsky M, Hadad U, Radinsky O, Gershoni-Yahalom O, Dye JM, Mandelboim O, Barda-Saad M, Lobel L, Porgador A. 2018. The Ebola-Glycoprotein Modulates the Function of Natural Killer Cells. Front Immunol 9:1428.
189. Kaletsky RL, Francica JR, Agrawal-Gamse C, Bates P. 2009. Tetherin-mediated restriction of filovirus budding is antagonized by the Ebola glycoprotein. Proc Natl Acad Sci 106:2886–2891.
190. Kühl A, Banning C, Marzi A, Votteler J, Steffen I, Bertram S, Glowacka I, Konrad A, Stürzl M, Guo J-T, Schubert U, Feldmann H, Behrens G, Schindler M, Pöhlmann S. 2011. The Ebola Virus Glycoprotein and HIV-1 Vpu Employ Different Strategies to Counteract the Antiviral Factor Tetherin. J Infect Dis 204:S850–S860.
191. Gustin JK, Bai Y, Moses AV, Douglas JL. 2015. Ebola Virus Glycoprotein Promotes Enhanced Viral Egress by Preventing Ebola VP40 From Associating With the Host Restriction Factor BST2/Tetherin. J Infect Dis 212:S181–S190.
192. Brinkmann C, Nehlmeier I, Walendy-Gnirß K, Nehls J, González Hernández M, Hoffmann M, Qiu X, Takada A, Schindler M, Pöhlmann S. 2016. The Tetherin Antagonism of the Ebola Virus Glycoprotein Requires an Intact Receptor-Binding Domain and Can Be Blocked by GP1-Specific Antibodies. J Virol 90:11075–11086.
193. Lopez LA, Yang SJ, Hauser H, Exline CM, Haworth KG, Oldenburg J, Cannon PM. 2010. Ebola Virus Glycoprotein Counteracts BST-2/Tetherin Restriction in a Sequence-Independent Manner That Does Not Require Tetherin Surface Removal. J Virol 84:7243–7255.
194. Rizk MG, Basler CF, Guatelli J. 2017. Cooperation of the Ebola Virus Proteins VP40 and $GP_{1,2}$ with BST2 To Activate NF-κB Independently of Virus-Like Particle Trapping. J Virol 91:e01308-17.
195. Escudero-Pérez B, Volchkova VA, Dolnik O, Lawrence P, Volchkov VE. 2014. Shed GP of Ebola Virus Triggers Immune Activation and Increased Vascular Permeability. PLoS Pathog 10:e1004509.
196. GP - Envelope glycoprotein - Zaire ebolavirus (strain Mayinga-76) (ZEBOV) | UniProtKB | UniProt. https://www.uniprot.org/uniprotkb/Q05320/entry. Retrieved 28 May 2023.
197. Manicassamy B, Wang J, Jiang H, Rong L. 2005. Comprehensive Analysis of Ebola Virus GP1 in Viral Entry. J Virol 79:4793–4805.
198. Ito H, Watanabe S, Takada A, Kawaoka Y. 2001. Ebola Virus Glycoprotein: Proteolytic Processing, Acylation, Cell Tropism, and Detection of Neutralizing Antibodies. J Virol 75:1576–1580.

199. Bavari S, Bosio CM, Wiegand E, Ruthel G, Will AB, Geisbert TW, Hevey M, Schmaljohn C, Schmaljohn A, Aman MJ. 2002. Lipid Raft Microdomains : A Gateway for Compartmentalized Trafficking of Ebola and Marburg Viruses✪✪The online version of this article contains supplemental material. J Exp Med 195:593–602.
200. Bornholdt ZA, Noda T, Abelson DM, Halfmann P, Wood MR, Kawaoka Y, Saphire EO. 2013. Structural Rearrangement of Ebola Virus VP40 Begets Multiple Functions in the Virus Life Cycle. Cell 154:763–774.
201. Gomis-Rüth FX, Dessen A, Timmins J, Bracher A, Kolesnikowa L, Becker S, Klenk H-D, Weissenhorn W. 2003. The Matrix Protein VP40 from Ebola Virus Octamerizes into Pore-like Structures with Specific RNA Binding Properties. Structure 11:423–433.
202. Hoenen T, Volchkov V, Kolesnikova L, Mittler E, Timmins J, Ottmann M, Reynard O, Becker S, Weissenhorn W. 2005. VP40 Octamers Are Essential for Ebola Virus Replication. J Virol 79:1898–1905.
203. Dessen A. 2000. Crystal structure of the matrix protein VP40 from Ebola virus. EMBO J 19:4228–4236.
204. Zhang L, Zhou S, Chen M, Yan J, Yang Y, Wu L, Jin D, Yin L, Chen M, Qin Y. 2021. P300-mediated NEDD4 acetylation drives ebolavirus VP40 egress by enhancing NEDD4 ligase activity. PLOS Pathog 17:e1009616.
205. Liang J, Sagum CA, Bedford MT, Sidhu SS, Sudol M, Han Z, Harty RN. 2017. Chaperone-Mediated Autophagy Protein BAG3 Negatively Regulates Ebola and Marburg VP40-Mediated Egress. PLOS Pathog 13:e1006132.
206. Liang J, Djurkovic MA, Shtanko O, Harty RN. 2023. Chaperone-assisted selective autophagy targets filovirus VP40 as a client and restricts egress of virus particles. Proc Natl Acad Sci 120:e2210690120.
207. Liang J, Ruthel G, Sagum CA, Bedford MT, Sidhu SS, Sudol M, Jaladanki CK, Fan H, Freedman BD, Harty RN. 2021. Angiomotin Counteracts the Negative Regulatory Effect of Host WWOX on Viral PPxY-Mediated Egress. J Virol 95:e00121-21.
208. Liang J, Ruthel G, Freedman BD, Harty RN. 2022. WWOX-Mediated Degradation of AMOTp130 Negatively Affects Egress of Filovirus VP40 Virus-Like Particles. J Virol 96:e02026-21.
209. Hoenen T, Biedenkopf N, Zielecki F, Jung S, Groseth A, Feldmann H, Becker S. 2010. Oligomerization of Ebola Virus VP40 Is Essential for Particle Morphogenesis and Regulation of Viral Transcription. J Virol 84:7053–7063.
210. Del Vecchio K, Frick CT, Gc JB, Oda S, Gerstman BS, Saphire EO, Chapagain PP, Stahelin RV. 2018. A cationic, C-terminal patch and structural rearrangements in Ebola virus matrix VP40 protein control its interactions with phosphatidylserine. J Biol Chem 293:3335–3349.
211. McCarthy SE, Johnson RF, Zhang Y-A, Sunyer JO, Harty RN. 2007. Role for Amino Acids $_{212}$ KLR $_{214}$ of Ebola Virus VP40 in Assembly and Budding. J Virol 81:11452–11460.
212. Panchal RG, Ruthel G, Kenny TA, Kallstrom GH, Lane D, Badie SS, Li L, Bavari S, Aman MJ. 2003. *In vivo* oligomerization and raft localization of Ebola virus protein VP40 during vesicular budding. Proc Natl Acad Sci 100:15936–15941.
213. Yamayoshi S, Kawaoka Y. 2007. Mapping of a Region of Ebola Virus VP40 That Is Important in the Production of Virus-Like Particles. J Infect Dis 196:S291–S295.
214. Adu-Gyamfi E, Soni SP, Xue Y, Digman MA, Gratton E, Stahelin RV. 2013. The Ebola Virus Matrix Protein Penetrates into the Plasma Membrane. J Biol Chem 288:5779–5789.
215. Baz-Martínez M, El Motiam A, Ruibal P, Condezo GN, de la Cruz-Herrera CF, Lang V, Collado M, San Martín C, Rodríguez MS, Muñoz-Fontela C, Rivas C. 2016. Regulation of Ebola virus VP40 matrix protein by SUMO. Sci Rep 6:37258.
216. Pleet ML, Mathiesen A, DeMarino C, Akpamagbo YA, Barclay RA, Schwab A, Iordanskiy S, Sampey GC, Lepene B, Ilinykh PA, Bukreyev A, Nekhai S, Aman MJ, Kashanchi F. 2016. Ebola VP40 in Exosomes Can Cause Immune Cell Dysfunction. Front Microbiol 7:1765.
217. Pleet ML, Erickson J, DeMarino C, Barclay RA, Cowen M, Lepene B, Liang J, Kuhn JH, Prugar L, Stonier SW, Dye JM, Zhou W, Liotta LA, Aman MJ, Kashanchi F. 2018. Ebola Virus VP40 Modulates Cell Cycle and Biogenesis of Extracellular Vesicles. J Infect Dis 218:S365–S387.
218. Maecker HT, Todd SC, Levy S. 1997. The tetraspanin superfamily: molecular facilitators. FASEB J 11:428–442.

219. Huang S, Yuan S, Dong M, Su J, Yu C, Shen Y, Xie X, Yu Y, Yu X, Chen S, Zhang S, Pontarotti P, Xu A. 2005. The phylogenetic analysis of tetraspanins projects the evolution of cell–cell interactions from unicellular to multicellular organisms. Genomics 86:674–684.
220. Zimmerman B, Kelly B, McMillan BJ, Seegar TCM, Dror RO, Kruse AC, Blacklow SC. 2016. Crystal Structure of a Full-Length Human Tetraspanin Reveals a Cholesterol-Binding Pocket. Cell 167:1041-1051.e11.
221. Umeda R, Satouh Y, Takemoto M, Nakada-Nakura Y, Liu K, Yokoyama T, Shirouzu M, Iwata S, Nomura N, Sato K, Ikawa M, Nishizawa T, Nureki O. 2020. Structural insights into tetraspanin CD9 function. 1. Nat Commun 11:1606.
222. Yáñez-Mó M, Barreiro O, Gordon-Alonso M, Sala-Valdés M, Sánchez-Madrid F. 2009. Tetraspanin-enriched microdomains: a functional unit in cell plasma membranes. Trends Cell Biol 19:434–446.
223. Radford KJ, Thorne RF, Hersey P. 1996. CD63 Associates with Transmembrane 4 Superfamily Members, CD9 and CD81, and with β1 Integrins in Human Melanoma. Biochem Biophys Res Commun 222:13–18.
224. Oren R, Takahashi S, Doss C, Levy R, Levy S. 1990. TAPA-1, the target of an antiproliferative antibody, defines a new family of transmembrane proteins. Mol Cell Biol 10:4007–4015.
225. Kaji K, Oda S, Miyazaki S, Kudo A. 2002. Infertility of CD9-Deficient Mouse Eggs Is Reversed by Mouse CD9, Human CD9, or Mouse CD81; Polyadenylated mRNA Injection Developed for Molecular Analysis of Sperm–Egg Fusion. Dev Biol 247:327–334.
226. Charrin S, Latil M, Soave S, Polesskaya A, Chrétien F, Boucheix C, Rubinstein E. 2013. Normal muscle regeneration requires tight control of muscle cell fusion by tetraspanins CD9 and CD81. Nat Commun 4:1674.
227. Parthasarathy V, Martin F, Higginbottom A, Murray H, Moseley GW, Read RC, Mal G, Hulme R, Monk PN, Partridge LJ. 2009. Distinct roles for tetraspanins CD9, CD63 and CD81 in the formation of multinucleated giant cells. Immunology 127:237–248.
228. Lagaudrière-Gesbert C, Naour FL, Lebel-Binay S, Billard M, Lemichez E, Boquet P, Boucheix C, Conjeaud H, Rubinstein E. 1997. Functional Analysis of Four Tetraspans, CD9, CD53, CD81, and CD82, Suggests a Common Role in Costimulation, Cell Adhesion, and Migration: Only CD9 Upregulates HB-EGF Activity. Cell Immunol 182:105–112.
229. Feigelson SW, Grabovsky V, Shamri R, Levy S, Alon R. 2003. The CD81 Tetraspanin Facilitates Instantaneous Leukocyte VLA-4 Adhesion Strengthening to Vascular Cell Adhesion Molecule 1 (VCAM-1) under Shear Flow. J Biol Chem 278:51203–51212.
230. Yáñez-Mó M, Alfranca A, Cabañas C, Marazuela M, Tejedor R, Angeles Ursa M, Ashman LK, de Landázuri MO, Sánchez-Madrid F. 1998. Regulation of Endothelial Cell Motility by Complexes of Tetraspan Molecules CD81/TAPA-1 and CD151/PETA-3 with α3β1 Integrin Localized at Endothelial Lateral Junctions. J Cell Biol 141:791–804.
231. Takeda Y, He P, Tachibana I, Zhou B, Miyado K, Kaneko H, Suzuki M, Minami S, Iwasaki T, Goya S, Kijima T, Kumagai T, Yoshida M, Osaki T, Komori T, Mekada E, Kawase I. 2008. Double Deficiency of Tetraspanins CD9 and CD81 Alters Cell Motility and Protease Production of Macrophages and Causes Chronic Obstructive Pulmonary Disease-like Phenotype in Mice. J Biol Chem 283:26089–26097.
232. Tejera E, Rocha-Perugini V, López-Martín S, Pérez-Hernández D, Bachir AI, Horwitz AR, Vázquez J, Sánchez-Madrid F, Yáñez-Mo M. 2013. CD81 regulates cell migration through its association with Rac GTPase. Mol Biol Cell 24:261–273.
233. Hong I-K, Byun H-J, Lee J, Jin Y-J, Wang S-J, Jeoung D-I, Kim Y-M, Lee H. 2014. The Tetraspanin CD81 Protein Increases Melanoma Cell Motility by Up-regulating Metalloproteinase MT1-MMP Expression through the Pro-oncogenic Akt-dependent Sp1 Activation Signaling Pathways. J Biol Chem 289:15691–15704.
234. Witherden DA, Boismenu R, Havran WL. 2000. CD81 and CD28 Costimulate T Cells Through Distinct Pathways. J Immunol 165:1902–1909.
235. Sagi Y, Landrigan A, Levy R, Levy S. 2012. Complementary costimulation of human T-cell subpopulations by cluster of differentiation 28 (CD28) and CD81. Proc Natl Acad Sci 109:1613–1618.
236. Rocha-Perugini V, Zamai M, González-Granado JM, Barreiro O, Tejera E, Yañez-Mó M, Caiolfa VR, Sanchez-Madrid F. 2013. CD81 Controls Sustained T Cell Activation Signaling

and Defines the Maturation Stages of Cognate Immunological Synapses. Mol Cell Biol 33:3644–3658.
237. van Zelm MC, Smet J, Adams B, Mascart F, Schandené L, Janssen F, Ferster A, Kuo C-C, Levy S, van Dongen JJM, van der Burg M. 2010. CD81 gene defect in humans disrupts CD19 complex formation and leads to antibody deficiency. J Clin Invest 120:1265–1274.
238. Oguri Y, Shinoda K, Kim H, Alba DL, Bolus WR, Wang Q, Brown Z, Pradhan RN, Tajima K, Yoneshiro T, Ikeda K, Chen Y, Cheang RT, Tsujino K, Kim CR, Greiner VJ, Datta R, Yang CD, Atabai K, McManus MT, Koliwad SK, Spiegelman BM, Kajimura S. 2020. CD81 Controls Beige Fat Progenitor Cell Growth and Energy Balance via FAK Signaling. Cell 182:563-577.e20.
239. Kummer D, Steinbacher T, Thölmann S, Schwietzer MF, Hartmann C, Horenkamp S, Demuth S, Peddibhotla SSD, Brinkmann F, Kemper B, Schnekenburger J, Brandt M, Betz T, Liashkovich I, Kouzel IU, Shahin V, Corvaia N, Rottner K, Tarbashevich K, Raz E, Greune L, Schmidt MA, Gerke V, Ebnet K. 2022. A JAM-A–tetraspanin–αvβ5 integrin complex regulates contact inhibition of locomotion. J Cell Biol 221:e202105147.
240. Spring FA, Griffiths RE, Mankelow TJ, Agnew C, Parsons SF, Chasis JA, Anstee DJ. 2013. Tetraspanins CD81 and CD82 Facilitate α4β1-Mediated Adhesion of Human Erythroblasts to Vascular Cell Adhesion Molecule-1. PLOS ONE 8:e62654.
241. Chang Y, Finnemann SC. 2007. Tetraspanin CD81 is required for the αvβ5-integrin-dependent particle-binding step of RPE phagocytosis. J Cell Sci 120:3053–3063.
242. Toledo MS, Suzuki E, Handa K, Hakomori S. 2005. Effect of Ganglioside and Tetraspanins in Microdomains on Interaction of Integrins with Fibroblast Growth Factor Receptor*. J Biol Chem 280:16227–16234.
243. Berditchevski F, Zutter MM, Hemler ME. 1996. Characterization of novel complexes on the cell surface between integrins and proteins with 4 transmembrane domains (TM4 proteins). Mol Biol Cell 7:193–207.
244. Domanico SZ, Pelletier AJ, Havran WL, Quaranta V. 1997. Integrin α6Aβ1 Induces CD81-dependent Cell Motility without Engaging the Extracellular Matrix Migration Substrate. Mol Biol Cell 8:2253–2265.
245. Gustafson-Wagner E, Stipp CS. 2013. The CD9/CD81 Tetraspanin Complex and Tetraspanin CD151 Regulate α3β1 Integrin-Dependent Tumor Cell Behaviors by Overlapping but Distinct Mechanisms. PLoS ONE 8:e61834.
246. Stipp CS, Kolesnikova TV, Hemler ME. 2001. EWI-2 Is a Major CD9 and CD81 Partner and Member of a Novel Ig Protein Subfamily. J Biol Chem 276:40545–40554.
247. Stipp CS, Orlicky D, Hemler ME. 2001. FPRP, a Major, Highly Stoichiometric, Highly Specific CD81- and CD9-associated Protein. J Biol Chem 276:4853–4862.
248. Stipp CS, Kolesnikova TV, Hemler ME. 2003. EWI-2 regulates α3β1 integrin–dependent cell functions on laminin-5. J Cell Biol 163:1167–1177.
249. Kolesnikova TV, Stipp CS, Rao RM, Lane WS, Luscinskas FW, Hemler ME. 2004. EWI-2 modulates lymphocyte integrin α4β1 functions. Blood 103:3013–3019.
250. Sala-Valdés M, Ursa Á, Charrin S, Rubinstein E, Hemler ME, Sánchez-Madrid F, Yáñez-Mó M. 2006. EWI-2 and EWI-F Link the Tetraspanin Web to the Actin Cytoskeleton through Their Direct Association with Ezrin-Radixin-Moesin Proteins. J Biol Chem 281:19665–19675.
251. Wang H-X, Sharma C, Knoblich K, Granter SR, Hemler ME. 2015. EWI-2 negatively regulates TGF-β signaling leading to altered melanoma growth and metastasis. Cell Res 25:370–385.
252. Todd SC, Lipps SG, Crisa L, Salomon DR, Tsoukas CD. 1996. CD81 expressed on human thymocytes mediates integrin activation and interleukin 2-dependent proliferation. J Exp Med 184:2055–2060.
253. Bradbury LE, Kansas GS, Levy S, Evans RL, Tedder TF. 1992. The CD19/CD21 signal transducing complex of human B lymphocytes includes the target of antiproliferative antibody-1 and Leu-13 molecules. J Immunol 149:2841–2850.
254. Shoham T, Rajapaksa R, Boucheix C, Rubinstein E, Poe JC, Tedder TF, Levy S. 2003. The Tetraspanin CD81 Regulates the Expression of CD19 During B Cell Development in a Postendoplasmic Reticulum Compartment. J Immunol 171:4062–4072.
255. Susa KJ, Seegar TC, Blacklow SC, Kruse AC. 2020. A dynamic interaction between CD19 and the tetraspanin CD81 controls B cell co-receptor trafficking. eLife 9:e52337.

256. Chen J, Enns CA. 2015. CD81 Promotes Both the Degradation of Transferrin Receptor 2 (TfR2) and the Tfr2-mediated Maintenance of Hepcidin Expression*. J Biol Chem 290:7841–7850.
257. Andreu Z, Yáñez-Mó M. 2014. Tetraspanins in Extracellular Vesicle Formation and Function. Front Immunol 5.
258. Escola J-M, Kleijmeer MJ, Stoorvogel W, Griffith JM, Yoshie O, Geuze HJ. 1998. Selective Enrichment of Tetraspan Proteins on the Internal Vesicles of Multivesicular Endosomes and on Exosomes Secreted by Human B-lymphocytes. J Biol Chem 273:20121–20127.
259. Larios J, Mercier V, Roux A, Gruenberg J. 2020. ALIX- and ESCRT-III–dependent sorting of tetraspanins to exosomes. J Cell Biol 219.
260. Perez-Hernandez D, Gutiérrez-Vázquez C, Jorge I, López-Martín S, Ursa A, Sánchez-Madrid F, Vázquez J, Yáñez-Mó M. 2013. The Intracellular Interactome of Tetraspanin-enriched Microdomains Reveals Their Function as Sorting Machineries toward Exosomes. J Biol Chem 288:11649–11661.
261. Bartosch B, Vitelli A, Granier C, Goujon C, Dubuisson J, Pascale S, Scarselli E, Cortese R, Nicosia A, Cosset F-L. 2003. Cell Entry of Hepatitis C Virus Requires a Set of Co-receptors That Include the CD81 Tetraspanin and the SR-B1 Scavenger Receptor. J Biol Chem 278:41624–41630.
262. Zhang J, Randall G, Higginbottom A, Monk P, Rice CM, McKeating JA. 2004. CD81 Is Required for Hepatitis C Virus Glycoprotein-Mediated Viral Infection. J Virol 78:1448–1455.
263. Viswanathan K, Verweij MC, John N, Malouli D, Früh K. 2017. Quantitative membrane proteomics reveals a role for tetraspanin enriched microdomains during entry of human cytomegalovirus. PLOS ONE 12:e0187899.
264. He J, Sun E, Bujny MV, Kim D, Davidson MW, Zhuang X. 2013. Dual Function of CD81 in Influenza Virus Uncoating and Budding. PLoS Pathog 9:e1003701.
265. Gordón-Alonso M, Yañez-Mó M, Barreiro O, Álvarez S, Muñoz-Fernández MÁ, Valenzuela-Fernández A, Sánchez-Madrid F. 2006. Tetraspanins CD9 and CD81 Modulate HIV-1-Induced Membrane Fusion. J Immunol 177:5129–5137.
266. Mascarau R, Woottum M, Fromont L, Gence R, Cantaloube-Ferrieu V, Vahlas Z, Lévêque K, Bertrand F, Beunon T, Métais A, El Costa H, Jabrane-Ferrat N, Gallois Y, Guibert N, Davignon J-L, Favre G, Maridonneau-Parini I, Poincloux R, Lagane B, Bénichou S, Raynaud-Messina B, Vérollet C. 2023. Productive HIV-1 infection of tissue macrophages by fusion with infected CD4+ T cells. J Cell Biol 222:e202205103.
267. Rocha-Perugini V, Suárez H, Álvarez S, López-Martín S, Lenzi GM, Vences-Catalán F, Levy S, Kim B, Muñoz-Fernández MA, Sánchez-Madrid F, Yáñez-Mó M. 2017. CD81 association with SAMHD1 enhances HIV-1 reverse transcription by increasing dNTP levels. Nat Microbiol 2:1513–1522.
268. Nydegger S, Khurana S, Krementsov DN, Foti M, Thali M. 2006. Mapping of tetraspanin-enriched microdomains that can function as gateways for HIV-1. J Cell Biol 173:795–807.
269. Deneka M, Pelchen-Matthews A, Byland R, Ruiz-Mateos E, Marsh M. 2007. In macrophages, HIV-1 assembles into an intracellular plasma membrane domain containing the tetraspanins CD81, CD9, and CD53. J Cell Biol 177:329–341.
270. Grigorov B, Attuil-Audenis V, Perugi F, Nedelec M, Watson S, Pique C, Darlix J-L, Conjeaud H, Muriaux D. 2009. A role for CD81 on the late steps of HIV-1 replication in a chronically infected T cell line. Retrovirology 6:28.
271. Lambelé M, Koppensteiner H, Symeonides M, Roy NH, Chan J, Schindler M, Thali M. 2015. Vpu Is the Main Determinant for Tetraspanin Downregulation in HIV-1-Infected Cells. J Virol 89:3247–3255.
272. Benayas B, Sastre I, López-Martín S, Oo A, Kim B, Bullido MJ, Aldudo J, Yáñez-Mó M. 2020. Tetraspanin CD81 regulates HSV-1 infection. Med Microbiol Immunol (Berl) 209:489–498.
273. Lasswitz L, Zapatero-Belinchón FJ, Moeller R, Hülskötter K, Laurent T, Carlson L-A, Goffinet C, Simmons G, Baumgärtner W, Gerold G. 2022. The Tetraspanin CD81 Is a Host Factor for Chikungunya Virus Replication. mBio 13:e00731-22.
274. Azorsa D, Hyman J, Hildreth J. 1991. CD63/Pltgp40: a platelet activation antigen identical to the stage- specific, melanoma-associated antigen ME491. Blood 78:280–284.

275. Rossi L, Forte D, Migliardi G, Salvestrini V, Buzzi M, Ricciardi MR, Licchetta R, Tafuri A, Bicciato S, Cavo M, Catani L, Lemoli RM, Curti A. 2015. The tissue inhibitor of metalloproteinases 1 increases the clonogenic efficiency of human hematopoietic progenitor cells through CD63/PI3K/Akt signaling. Exp Hematol 43:974-985.e1.
276. Lee SY, Kim JM, Cho SY, Kim HS, Shin HS, Jeon JY, Kausar R, Jeong SY, Lee YS, Lee MA. 2014. TIMP-1 modulates chemotaxis of human neural stem cells through CD63 and integrin signalling. Biochem J 459:565–576.
277. Jung K-K, Liu X-W, Chirco R, Fridman R, Kim H-RC. 2006. Identification of CD63 as a tissue inhibitor of metalloproteinase-1 interacting cell surface protein. EMBO J 25:3934–3942.
278. Tugues S, Honjo S, König C, Padhan N, Kroon J, Gualandi L, Li X, Barkefors I, Thijssen VL, Griffioen AW, Claesson-Welsh L. 2013. Tetraspanin CD63 Promotes Vascular Endothelial Growth Factor Receptor 2-β1 Integrin Complex Formation, Thereby Regulating Activation and Downstream Signaling in Endothelial Cells in Vitro and in Vivo. J Biol Chem 288:19060–19071.
279. Gräßel L, Fast LA, Scheffer KD, Boukhallouk F, Spoden GA, Tenzer S, Boller K, Bago R, Rajesh S, Overduin M, Berditchevski F, Florin L. 2016. The CD63-Syntenin-1 Complex Controls Post-Endocytic Trafficking of Oncogenic Human Papillomaviruses. 1. Sci Rep 6:32337.
280. Raaben M, Jae LT, Herbert AS, Kuehne AI, Stubbs SH, Chou Y, Blomen VA, Kirchhausen T, Dye JM, Brummelkamp TR, Whelan SP. 2017. NRP2 and CD63 Are Host Factors for Lujo Virus Cell Entry. Cell Host Microbe 22:688-696.e5.
281. Nazli A, Chow R, Zahoor MA, Workenhe ST, Dhawan T, Verschoor C, Kaushic C. 2022. LAMP3/CD63 Expression in Early and Late Endosomes in Human Vaginal Epithelial Cells Is Associated with Enhancement of HSV-2 Infection. J Virol 96:e01553-22.
282. Li G, Endsley MA, Somasunderam A, Gbota SL, Mbaka MI, Murray JL, Ferguson MR. 2014. The dual role of tetraspanin CD63 in HIV-1 replication. Virol J 11:23.
283. Fu E, Pan L, Xie Y, Mu D, Liu W, Jin F, Bai X. 2015. Tetraspanin CD63 is a regulator of HIV-1 replication. Int J Clin Exp Pathol 8:1184–1198.
284. Ivanusic D, Madela K, Bannert N, Denner J. 2021. The large extracellular loop of CD63 interacts with gp41 of HIV-1 and is essential for establishing the virological synapse. 1. Sci Rep 11:10011.
285. Ninomiya M, Inoue J, Krueger EW, Chen J, Cao H, Masamune A, McNiven MA. 2021. The Exosome-Associated Tetraspanin CD63 Contributes to the Efficient Assembly and Infectivity of the Hepatitis B Virus. Hepatol Commun 5:1238.
286. Ikeyama S, Koyama M, Yamaoko M, Sasada R, Miyake M. 1993. Suppression of cell motility and metastasis by transfection with human motility-related protein (MRP-1/CD9) DNA. J Exp Med 177:1231–1237.
287. Miyado K, Yamada G, Yamada S, Hasuwa H, Nakamura Y, Ryu F, Suzuki K, Kosai K, Inoue K, Ogura A, Okabe M, Mekada E. 2000. Requirement of CD9 on the Egg Plasma Membrane for Fertilization. Science 287:321–324.
288. Machado-Pineda Y, Cardeñes B, Reyes R, López-Martín S, Toribio V, Sánchez-Organero P, Suarez H, Grötzinger J, Lorenzen I, Yáñez-Mó M, Cabañas C. 2018. CD9 Controls Integrin α5β1-Mediated Cell Adhesion by Modulating Its Association With the Metalloproteinase ADAM17. Front Immunol 9.
289. Liu J, Zhu G, Jia N, Wang W, Wang Y, Yin M, Jiang X, Huang Y, Zhang J. 2019. CD9 regulates keratinocyte migration by negatively modulating the sheddase activity of ADAM17. Int J Biol Sci 15:493–506.
290. Jiang X, Teng M, Ji R, Zhang D, Zhang Z, Lv Y, Zhang Q, Zhang J, Huang Y. 2020. CD9 regulates keratinocyte differentiation and motility by recruiting E-cadherin to the plasma membrane and activating the PI3K/Akt pathway. Biochim Biophys Acta BBA - Mol Cell Res 1867:118574.
291. Jiang X, Zhang D, Teng M, Zhang Q, Zhang J, Huang Y. 2013. Downregulation of CD9 in Keratinocyte Contributes to Cell Migration via Upregulation of Matrix Metalloproteinase-9. PLOS ONE 8:e77806.
292. Rocha-Perugini V, González-Granado JM, Tejera E, López-Martín S, Yañez-Mó M, Sánchez-Madrid F. 2014. Tetraspanins CD9 and CD151 at the immune synapse support T-cell integrin signaling: Cellular immune response. Eur J Immunol 44:1967–1975.

293. Mikuličić S, Fritzen A, Scheffer K, Strunk J, Cabañas C, Sperrhacke M, Reiss K, Florin L. 2020. Tetraspanin CD9 affects HPV16 infection by modulating ADAM17 activity and the ERK signalling pathway. Med Microbiol Immunol (Berl) 209:461–471.
294. Earnest JT, Hantak MP, Li K, Jr PBM, Perlman S, Gallagher T. 2017. The tetraspanin CD9 facilitates MERS-coronavirus entry by scaffolding host cell receptors and proteases. PLOS Pathog 13:e1006546.
295. Schack VR, Rossen LS, Ekebjærg CC, Thuesen KKH, Bundgaard B, Höllsberg P. 2021. The Tetraspanin Protein CD9 Modulates Infection with Human Herpesvirus 6A and 6B in a CD46-Dependent Manner. J Virol 95:e02259-20.
296. Businger R, Kivimäki S, Simeonov S, Vavouras Syrigos G, Pohlmann J, Bolz M, Müller P, Codrea MC, Templin C, Messerle M, Hamprecht K, Schäffer TE, Nahnsen S, Schindler M. 2021. Comprehensive Analysis of Human Cytomegalovirus- and HIV-Mediated Plasma Membrane Remodeling in Macrophages. mBio 12:10.1128/mbio.01770-21.
297. Schindler M, Würfl S, Benaroch P, Greenough TC, Daniels R, Easterbrook P, Brenner M, Münch J, Kirchhoff F. 2003. Down-Modulation of Mature Major Histocompatibility Complex Class II and Up-Regulation of Invariant Chain Cell Surface Expression Are Well-Conserved Functions of Human and Simian Immunodeficiency Virus nef Alleles. J Virol 77:10548–10556.
298. Pham TNQ, Richard J, Gerard FCA, Power C, Cohen ÉA. 2011. Modulation of NKG2D-Mediated Cytotoxic Functions of Natural Killer Cells by Viral Protein R from HIV-1 Primary Isolates. J Virol 85:12254–12261.
299. Banse P, Moeller R, Bruening J, Lasswitz L, Kahl S, Khan AG, Marcotrigiano J, Pietschmann T, Gerold G. 2018. CD81 Receptor Regions outside the Large Extracellular Loop Determine Hepatitis C Virus Entry into Hepatoma Cells. 4. Viruses 10:207.
300. Businger R, Deutschmann J, Gruska I, Milbradt J, Wiebusch L, Gramberg T, Schindler M. 2019. Human cytomegalovirus overcomes SAMHD1 restriction in macrophages via pUL97. Nat Microbiol 4:2260–2272.
301. Shabman RS, Hoenen T, Groseth A, Jabado O, Binning JM, Amarasinghe GK, Feldmann H, Basler CF. 2013. An Upstream Open Reading Frame Modulates Ebola Virus Polymerase Translation and Virus Replication. PLOS Pathog 9:e1003147.
302. Heckman KL, Pease LR. 2007. Gene splicing and mutagenesis by PCR-driven overlap extension. 4. Nat Protoc 2:924–932.
303. Hilgarth RS, Lanigan TM. 2020. Optimization of overlap extension PCR for efficient transgene construction. MethodsX 7:100759.
304. Gramberg T, Kahle T, Bloch N, Wittmann S, Müllers E, Daddacha W, Hofmann H, Kim B, Lindemann D, Landau NR. 2013. Restriction of diverse retroviruses by SAMHD1. Retrovirology 10:26.
305. Krollmann C, Cieslak K, Koerber R-M, Luksch H, Rösen-Wolff A, Brossart P, Teichmann LL. 2022. Quantification of unperturbed phosphoprotein levels in immune cell subsets with phosphoflow to assess immune signaling in autoimmune disease. STAR Protoc 3:101309.
306. Pfaffl MW. 2001. A new mathematical model for relative quantification in real-time RT–PCR. Nucleic Acids Res 29:e45.
307. Hoffmann M, Crone L, Dietzel E, Paijo J, González-Hernández M, Nehlmeier I, Kalinke U, Becker S, Pöhlmann S. 2017. A Polymorphism within the Internal Fusion Loop of the Ebola Virus Glycoprotein Modulates Host Cell Entry. J Virol 91:10.1128/jvi.00177-17.
308. Abu-Saleh N, Kuo C-C, Jiang W, Levy R, Levy S. 2023. The molecular mechanism of CD81 antibody inhibition of metastasis. Proc Natl Acad Sci 120:e2305042120.
309. Vences-Catalán F, Rajapaksa R, Kuo C-C, Miller CL, Lee A, Ramani VC, Jeffrey SS, Levy R, Levy S. 2021. Targeting the tetraspanin CD81 reduces cancer invasion and metastasis. Proc Natl Acad Sci 118:e2018961118.
310. Meri S, Morgan BP, Davies A, Daniels RH, Olavesen MG, Waldmann H, Lachmann PJ. 1990. Human protectin (CD59), an 18,000-20,000 MW complement lysis restricting factor, inhibits C5b-8 catalysed insertion of C9 into lipid bilayers. Immunology 71:1–9.
311. Saifuddin M, Parker CJ, Peeples ME, Gorny MK, Zolla-Pazner S, Ghassemi M, Rooney IA, Atkinson JP, Spear GT. 1995. Role of virion-associated glycosylphosphatidylinositol-linked proteins CD55 and CD59 in complement resistance of cell line-derived and primary isolates of HIV-1. J Exp Med 182:501–509.

312. Saifuddin M, Hedayati T, Atkinson JP, Holguin MH, Parker CJ, Spear GT. 1997. Human immunodeficiency virus type 1 incorporates both glycosyl phosphatidylinositol-anchored CD55 and CD59 and integral membrane CD46 at levels that protect from complement-mediated destruction. J Gen Virol 78 (Pt 8):1907–1911.
313. Spear GT, Lurain NS, Parker CJ, Ghassemi M, Payne GH, Saifuddin M. 1995. Host cell-derived complement control proteins CD55 and CD59 are incorporated into the virions of two unrelated enveloped viruses. Human T cell leukemia/lymphoma virus type I (HTLV-I) and human cytomegalovirus (HCMV). J Immunol 155:4376–4381.
314. Vanderplasschen A, Mathew E, Hollinshead M, Sim RB, Smith GL. 1998. Extracellular enveloped vaccinia virus is resistant to complement because of incorporation of host complement control proteins into its envelope. Proc Natl Acad Sci 95:7544–7549.
315. Amet T, Ghabril M, Chalasani N, Byrd D, Hu N, Grantham A, Liu Z, Qin X, He JJ, Yu Q. 2012. CD59 incorporation protects hepatitis C virus against complement-mediated destruction. Hepatol Baltim Md 55:354–363.
316. Wei Y, Ji Y, Guo H, Zhi X, Han S, Zhang Y, Gao Y, Chang Y, Yan D, Li K, Liu DX, Sun S. 2017. CD59 association with infectious bronchitis virus particles protects against antibody-dependent complement-mediated lysis. J Gen Virol 98:2725–2730.
317. Qu Z, Liang X, Liu Y, Du J, Liu S, Sun W. 2009. Hepatitis B virus sensitizes hepatocytes to complement-dependent cytotoxicity through downregulating CD59. Mol Immunol 47:283–289.
318. Stearns-Kurosawa DJ, Kurosawa S, Mollica JS, Ferrell GL, Esmon CT. 1996. The endothelial cell protein C receptor augments protein C activation by the thrombin-thrombomodulin complex. Proc Natl Acad Sci 93:10212–10216.
319. Geisbert TW, Young HA, Jahrling PB, Davis KJ, Kagan E, Hensley LE. 2003. Mechanisms Underlying Coagulation Abnormalities in Ebola Hemorrhagic Fever: Overexpression of Tissue Factor in Primate Monocytes/Macrophages Is a Key Event. J Infect Dis 188:1618–1629.
320. Britton C, Poznansky MC, Reeves P. 2021. Polyfunctionality of the CXCR4/CXCL12 axis in health and disease: Implications for therapeutic interventions in cancer and immune-mediated diseases. FASEB J 35:e21260.
321. Bleul CC, Farzan M, Choe H, Parolin C, Clark-Lewis I, Sodroski J, Springer TA. 1996. The lymphocyte chemoattractant SDF-1 is a ligand for LESTR/fusin and blocks HIV-1 entry. Nature 382:829–833.
322. Bernhagen J, Krohn R, Lue H, Gregory JL, Zernecke A, Koenen RR, Dewor M, Georgiev I, Schober A, Leng L, Kooistra T, Fingerle-Rowson G, Ghezzi P, Kleemann R, McColl SR, Bucala R, Hickey MJ, Weber C. 2007. MIF is a noncognate ligand of CXC chemokine receptors in inflammatory and atherogenic cell recruitment. Nat Med 13:587–596.
323. Saini V, Staren DM, Ziarek JJ, Nashaat ZN, Campbell EM, Volkman BF, Marchese A, Majetschak M. 2011. The CXC chemokine receptor 4 ligands ubiquitin and stromal cell-derived factor-1α function through distinct receptor interactions. J Biol Chem 286:33466–33477.
324. Feng Z, Dubyak GR, Lederman MM, Weinberg A. 2006. Cutting Edge: Human β Defensin 3—A Novel Antagonist of the HIV-1 Coreceptor CXCR4[1]. J Immunol 177:782–786.
325. Feng Y, Broder CC, Kennedy PE, Berger EA. 1996. HIV-1 Entry Cofactor: Functional cDNA Cloning of a Seven-Transmembrane, G Protein-Coupled Receptor. Science 272:872–877.
326. Dolnik O, Volchkova VA, Escudero-Perez B, Lawrence P, Klenk H-D, Volchkov VE. 2015. Shedding of Ebola Virus Surface Glycoprotein Is a Mechanism of Self-regulation of Cellular Cytotoxicity and Has a Direct Effect on Virus Infectivity. J Infect Dis 212:S322–S328.
327. Théry C, Amigorena S, Raposo G, Clayton A. 2006. Isolation and Characterization of Exosomes from Cell Culture Supernatants and Biological Fluids. Curr Protoc Cell Biol 30:3.22.1-3.22.29.
328. Raposo G, Nijman HW, Stoorvogel W, Liejendekker R, Harding CV, Melief CJ, Geuze HJ. 1996. B lymphocytes secrete antigen-presenting vesicles. J Exp Med 183:1161–1172.
329. Nelson EV, Pacheco JR, Hume A, Cressey TN, Deflubé LR, Ruedas JB, Connor JH, Ebihara H, Mühlberger E. 2017. An RNA polymerase II-driven Ebola virus minigenome system as an advanced tool for antiviral drug screening. Antiviral Res 146:21–27.

330. Zinzula L, Nagy I, Orsini M, Weyher-Stingl E, Bracher A, Baumeister W. 2019. Structures of Ebola and Reston Virus VP35 Oligomerization Domains and Comparative Biophysical Characterization in All Ebolavirus Species. Structure 27:39-54.e6.
331. Lee JE, Cathey PI, Wu H, Parker R, Voeltz GK. 2020. Endoplasmic reticulum contact sites regulate the dynamics of membraneless organelles. Science 367:eaay7108.
332. Dolnik O, Stevermann L, Kolesnikova L, Becker S. 2015. Marburg virus inclusions: A virus-induced microcompartment and interface to multivesicular bodies and the late endosomal compartment. Eur J Cell Biol 94:323–331.
333. Fang J, Castillon G, Phan S, McArdle S, Hariharan C, Adams A, Ellisman MH, Deniz AA, Saphire EO. 2023. Spatial and functional arrangement of Ebola virus polymerase inside phase-separated viral factories. 1. Nat Commun 14:4159.
334. Stupack DG, Cheresh DA. 2002. Get a ligand, get a life: integrins, signaling and cell survival. J Cell Sci 115:3729–3738.
335. Yatim N, Albert ML. 2011. Dying to Replicate: The Orchestration of the Viral Life Cycle, Cell Death Pathways, and Immunity. Immunity 35:478–490.
336. Schornberg KL, Shoemaker CJ, Dube D, Abshire MY, Delos SE, Bouton AH, White JM. 2009. α5β1-Integrin controls ebolavirus entry by regulating endosomal cathepsins. Proc Natl Acad Sci 106:8003–8008.
337. Allen JR, Ge L, Huang Y, Brauer R, Parimon T, Cassel SL, Sutterwala FS, Chen P. 2018. TIMP-1 Promotes the Immune Response in Influenza-Induced Acute Lung Injury. Lung 196:737–743.
338. Fujii M, Kawai K, Egami Y, Araki N. 2013. Dissecting the roles of Rac1 activation and deactivation in macropinocytosis using microscopic photo-manipulation. Sci Rep 3:2385.
339. Moller-Tank S, Kondratowicz AS, Davey RA, Rennert PD, Maury W. 2013. Role of the Phosphatidylserine Receptor TIM-1 in Enveloped-Virus Entry. J Virol 87:8327–8341.
340. Jemielity S, Wang JJ, Chan YK, Ahmed AA, Li W, Monahan S, Bu X, Farzan M, Freeman GJ, Umetsu DT, DeKruyff RH, Choe H. 2013. TIM-family Proteins Promote Infection of Multiple Enveloped Viruses through Virion-associated Phosphatidylserine. PLoS Pathog 9:e1003232.
341. Yoshida S, Gaeta I, Pacitto R, Krienke L, Alge O, Gregorka B, Swanson JA. 2015. Differential signaling during macropinocytosis in response to M-CSF and PMA in macrophages. Front Physiol 6.
342. Bhattacharyya S, Warfield KL, Ruthel G, Bavari S, Aman MJ, Hope TJ. 2010. Ebola virus uses clathrin-mediated endocytosis as an entry pathway. Virology 401:18–28.
343. Lineberry N, Su L, Soares L, Fathman CG. 2008. The Single Subunit Transmembrane E3 Ligase Gene Related to Anergy in Lymphocytes (GRAIL) Captures and Then Ubiquitinates Transmembrane Proteins across the Cell Membrane*. J Biol Chem 283:28497–28505.
344. Hosokawa K, Ishimaru H, Watanabe T, Fujimuro M. 2020. The Lysosome Pathway Degrades CD81 on the Cell Surface by Poly-ubiquitination and Clathrin-Mediated Endocytosis. Biol Pharm Bull 43:540–545.
345. Bartee E, Eyster CA, Viswanathan K, Mansouri M, Donaldson JG, Früh K. 2010. Membrane-Associated RING-CH Proteins Associate with Bap31 and Target CD81 and CD44 to Lysosomes. PLoS ONE 5:e15132.
346. Yu C, Li S, Zhang X, Khan I, Ahmad I, Zhou Y, Li S, Shi J, Wang Y, Zheng Y-H. 2020. MARCH8 Inhibits Ebola Virus Glycoprotein, Human Immunodeficiency Virus Type 1 Envelope Glycoprotein, and Avian Influenza Virus H5N1 Hemagglutinin Maturation. mBio 11:e01882-20.
347. Tada T, Zhang Y, Koyama T, Tobiume M, Tsunetsugu-Yokota Y, Yamaoka S, Fujita H, Tokunaga K. 2015. MARCH8 inhibits HIV-1 infection by reducing virion incorporation of envelope glycoproteins. 12. Nat Med 21:1502–1507.
348. Flint M, Maidens C, Loomis-Price LD, Shotton C, Dubuisson J, Monk P, Higginbottom A, Levy S, McKeating JA. 1999. Characterization of Hepatitis C Virus E2 Glycoprotein Interaction with a Putative Cellular Receptor, CD81. J Virol 73:6235–6244.
349. Vences-Catalán F, Kuo C-C, Rajapaksa R, Duault C, Andor N, Czerwinski DK, Levy R, Levy S. 2019. CD81 is a novel immunotherapeutic target for B cell lymphoma. J Exp Med 216:1497–1508.

9. Declaration of contribution

The dissertation work was carried out at the Institut für Medizinische Virologie und Epidemiologie der Viruskrankheiten under the supervision of Prof. Dr. Michael Schindler. The study was designed by Prof. Dr. Michael Schindler and the candidate. The initial lab training was done by Dr. Ramona Businger and Maximilian Bunz (AG Schindler).

The following work were contributed by others.

Dr. Thomas Hoenen and Dr. Lisa Wendt from Friedrich-Loeffler-Institut did the authentic recombinant EBOV infection experiments, including rgEBOV-ilu2 and rgEBOV-eGFP infection.

Georgios Vavouras Syrigos (AG Schindler) prepared Human primary macrophages.

Prof. Dr. Daniel Sauter suggested the BiFC experiment.

I confirm that I wrote the manuscript myself and that any additional sources of information have been duly cited.

Signed_____

on [date] _____ in Tübingen

10. Acknowledgements

Firstly, I would like to thank Prof. Dr. Michael Schindler for offering this project and giving me opportunity to work in his lab. I really appreciate his constant supports and excellent supervision. I would also like to thank Prof. Dr. Julia Skokowa and Apl.Prof. Dr. Frank Stubenrauch for being my doctoral committee members.

Thanks to Dr. Thomas Hoenen and Dr. Lisa Wendt for doing the EBOV infection experiment, discussing the results and frequent share of plasmids and protocols. Thanks to former PhD student Julia Nehls to do the screen, so there is this project.

Thanks to all members in the group and the institute always being helpful. In particular, I would like to thank Ramona and Max for showing me the lab work, sharing protocols/techniques and discussing results. Thanks to George for preparing the macrophages and discussing results and analysis. Thanks to Daniel for sharing methods. Thanks to Raphael for discussing my project, reading my thesis and giving suggestions. Thanks to George, Justus, Jasmin, Max, Raphael and Elena for the fun time in the office.

I would like to thank Chinese Scholarship Council for giving me the opportunity to study in Tübingen university. Thanks to my families for understanding and supporting. Thanks to my friends for the accompany and positive thoughts of life.